


Summer 8-2016

RELATIONSHIP BETWEEN
MORPHOGENESIS AND SECRETION IN
THE FILAMENTOUS FUNGUS
ASPERGILLUS NIDULANS

Lakshmi Preethi Yerra

University of Nebraska-Lincoln, neha0025@hotmail.com

Follow this and additional works at: <http://digitalcommons.unl.edu/bioscidiss>

 Part of the [Genetics Commons](#), [Laboratory and Basic Science Research Commons](#), [Molecular Genetics Commons](#), and the [Other Microbiology Commons](#)

Yerra, Lakshmi Preethi, "RELATIONSHIP BETWEEN MORPHOGENESIS AND SECRETION IN THE FILAMENTOUS FUNGUS *ASPERGILLUS NIDULANS*" (2016). *Dissertations and Theses in Biological Sciences*. 85.
<http://digitalcommons.unl.edu/bioscidiss/85>

This Article is brought to you for free and open access by the Biological Sciences, School of at DigitalCommons@University of Nebraska - Lincoln. It has been accepted for inclusion in Dissertations and Theses in Biological Sciences by an authorized administrator of DigitalCommons@University of Nebraska - Lincoln.

RELATIONSHIP BETWEEN MORPHOGENESIS AND SECRETION IN THE
FILAMENTOUS FUNGUS *ASPERGILLUS NIDULANS*

By

Lakshmi Preethi Yerra

A Thesis

Presented to the Faculty of
The Graduate College at the University of Nebraska
In Partial Fulfilment of Requirements
For the Degree of Master in Science

Major: Biological Sciences

Under the Supervision of Professor Steven D. Harris

Lincoln, Nebraska

August 2016

RELATIONSHIP BETWEEN MORPHOGENESIS AND SECRETION IN THE
FILAMENTOUS FUNGUS *ASPERGILLUS NIDULANS*

Lakshmi Preethi Yerra, MS

University of Nebraska, 2016

Advisor: Steven D. Harris

Filamentous fungi have a long history in biotechnology for the production of food ingredients, pharmaceuticals and enzymes. The advancements made in recent years have earned filamentous fungi such as *Aspergillus* species a dominant place among microbial cell factories. Although the model fungus *A. nidulans* has been extensively studied, the genetic and regulatory networks that underlie morphogenesis and development have yet to be fully characterized. The Rho GTPases (Cdc42 and RacA) are one of the most important regulators of the morphogenetic processes among diverse eukaryotic organisms. Although the functions of these GTPases are relatively well-characterized, little is known about their downstream effectors. One likely effector is the formin SepA, which also belongs to a complex known as the polarisome that helps to stabilize and support hyphal growth. The uncharacterized gene *ANID_05595.1 (ModB)* possesses sequence features that suggest it also belongs to the polarisome. My genetic and functional characterization of ModB reveals some overlap with SepA, but also shows that ModB possesses distinct roles in the maintenance of hyphal polarity.

In filamentous fungi, hyphal morphology requires the localized delivery of exocytic vesicles to the hyphal tip as well as to septation sites. The mechanisms that regulate vesicle trafficking to these locations are not yet well understood. In addition, because fungal hyphae presumably extend through a nutritionally variable environment, these mechanisms must be extremely sensitive to growth conditions. To begin to address these issues, I have investigated the effects of nutrient

conditions on localization patterns of two different proteins that are trafficked to the cell surface; a glucose transporter (HxtB) and the enzyme β -glucosidase (BglA). Although the final localization of each protein differs, they display similar localization dynamics upon release from glucose repression. In parallel, I also used fluorescence microscopy to determine how shifts from glucose to a non-preferred carbon source (e.g., cellulose) affect hyphal extension and morphology. My results suggest that relief from glucose repression leads to the production of thinner hyphae after a transient delay in hyphal extension. Use of variety of signaling mutants further demonstrates that this response requires a functional protein kinase A (PKA) as well as proper down-regulation of heterotrimeric G protein signals. Collectively, these observations provide valuable new insight into how vesicle trafficking responds to variable growth conditions.

TABLE OF CONTENTS

OVERVIEW	1
GERMINATION	2
ESTABLISHMENT OF POLARITY	3
MAINTENANCE OF POLARITY	6
RHO-LIKE GTPASE	8
ACTIVATION AND LOCALIZATION OF Cdc42	12
CDC42 AND RAC1	14
POLARISOME IN <i>A. nidulans</i>	14
CARBON METABOLISM	15
INTERCELLULAR SIGNALING	16
EXTRACELLULAR SIGNALING	17
SECRETION PATHWAY	18
FIGURES	20
CHAPTER 1	25
INTRODUCTION	25
MATERIAL AND METHODS	28
RESULTS	35
DISCUSSIONS	39
FUTURE DIRECTIONS.....	41
TABLE & FIGURES	43
CHAPTER 2	51
INTRODUCTION	51
MATERIAL AND METHODS	54
RESULTS	57
DISCUSSIONS	59
FUTURE DIRECTIONS	61
TABLE & FIGURES	63

CHAPTER 3	75
INTRODUCTION	75
MATERIAL AND METHODS	77
RESULTS	80
DISCUSSIONS	82
FUTURE DIRECTIONS	84
FIGURES	86
REFERENCES	94

Overview

Filamentous fungi are a diverse group of heterotrophic microorganisms that are medically and agriculturally important and are also widely used in production of food, beverages, antibiotics, enzymes, organic acids and in biomass conversion. They are also serious human pathogens, especially to immuno-compromised patients and have been reported to account for up to 40% of deaths from hospital acquired infections (Muthuvijayan et al. 2004).

Aspergillus is a ubiquitous filamentous fungus found in nature. It is commonly found in soil, plant debris and indoor air environment. The genus *Aspergillus* includes over 185 species out of which about 20 are identified as opportunistic pathogens. *Aspergillus nidulans* is commonly used as model filamentous fungus because it is closely related to a large number of other *Aspergillus* species of industrial (e.g., *A. niger*, *A. oryzae*) and medical (e.g., *A. flavus* and *A. fumigatus*) significance. Hence a better understanding in *A. nidulans* molecular mechanisms and physiology will yield information on improving our knowledge in other industrially and medically significant filamentous fungi (Muthuvijayan et al. 2004). Although, *A. nidulans* has been researched for decades many molecular and metabolic mechanisms are poorly understood. *Saccharomyces cerevisiae*, a yeast, shares the same phylum: Ascomycota as *A. nidulans*. *S. cerevisiae* has been well studied and its genetic and metabolic pathways were used as a template during this study (Downs. 2012).

Fungi exhibit two forms of cellular morphogenesis: hyphal growth and yeast growth. Hyphae are long tubular structures that extend solely at the tips and are partitioned into cellular compartments by forming septa (Figure 1b). Yeast are unicellular fungi that exhibit diverse morphology ranging from ovals to elongated rods (Figure 1a). Both yeast and

hyphal cells grow by cell surface expansion at specific cortical sites. Two key features that differentiate yeast and hyphal modes of growth are: yeast cells do not undergo sustained polarized growth and yeast cells separate by budding or fission whereas hyphae remain attached (Harris et al., 2009).

Hyphae are populated by multiple nuclei due to a series of parasynchronous nuclear divisions (conidia (asexual spore) are uninucleated and ascospores are binucleated). Nuclear division is coordinated with growth such that each division is coupled to doubling of cell mass and the entire process is referred as the duplication cycle. Once hyphae reaches a certain volume, depending on growth conditions, they are then partitioned by forming the first septum. Following the first septation event, each duplication cycle is terminated by forming a septa in the hyphae. Sub-apical compartments enter a period of mitotic quiescence that is eventually broken by the formation of a branch that generates a new hypha. Branch formation requires the establishment and maintenance of a new polarity axis, likely a repetition many of the events in germination. (Trinci; Harris. 1997 and Si. 2010). *S. cerevisiae* and *A. nidulans* also share the similar growth pattern: germination, polarity establishment and polarity maintenance (Figure 2). Both use the same key proteins that play a similar role in germination and polarity establishment. However, different patterns are used during polarity maintenance, i.e. hyphal elongation (Downs, 2012).

Germination

Germination of conidia in *A. nidulans* is when a dormant conidia breaks dormancy by first growing isotropically adding new cell wall material uniformly in every direction. This leads to the swelling of the conidia as it rehydrates by uptake of water, initiation of

translation (mainly genes encoding osmolytes and *prnB* (proline transporter)) and recommencement of metabolic activity (maintain levels of intracellular glycerol) within the conidia (d'Enfert and Fontaine.1997, d'Enfert et al.1999, Fillinger et al. 2001, de Vries et al. 2003, Tazebay, Sophianopoulou et al.1995 and Tazebay, Sophionopoulou et al.1997). The primary trigger for germination appeared to be glucose, whereas nitrogen or phosphorus also seem to trigger germination. The presence of glucose is sensed by a G protein-coupled receptor (GPCR), and because G protein (*GanB*) is constitutively active (GTP bound state) leads to germination in the absence of a carbon source. One of the downstream effectors of *GanB* could be *CynA*, an adenylate cyclase required for cyclic AMP (cAMP) production. cAMP acts as a secondary messenger that binds to the regulatory subunit of protein kinase A (PKA) which then activates the catalytic subunit. In *A. nidulans* both *CyaA* and PKA are needed for efficient conidial germination (Figure 3) (Fillinger et al. 2002 and Si. 2012).

Establishment of polarity

The establishment of a polarity is the successful emergence of a germ tube from a swollen conidia. Polarity establishment includes processes of a new polarity axis and the use of the resulting positional information to spatially organize the morphogenetic machinery. This terminates the isotropic expansion of the conidia and results in the cell wall deposition to a specific site that will eventually become the hyphal tip. Despite considerable interest in the mechanisms in polarity establishment in *A.nidulans*, the mechanisms remains poorly defined. However, genetic analysis has provided some insight into how new polarity axes are specified and also implicate several cellular functions in the establishment of polarity (Si. 2010).

In *S. cerevisiae*, the bud site selection system is well understood and is used as a model for the establishment of a polarization site in fungi. This system is based on the use of distinct cortical markers that specify one of the two possible budding patterns (axial and bipolar). The axial (Bud3, Bud4, and Bud10) and bipolar (Bud8, Bud9, Rax1, and Rax2) landmark proteins generate positional information that is relayed to GTPase Cdc42 via a Ras-related GTPase Rsr1/Bud1 and its associated regulators Bud2 and Bud5. Locally active Cdc42 then triggers the assembly polarity establishment machinery to the presumptive bud site. The *A.nidulans* genome shows axial landmark proteins are poorly conserved but the bipolar landmark proteins are absent. Also, the functional characterization of poorly conserved homologues show they have no obvious role in the establishment or maintenance of hyphal polarity. However, studies using *A. fumigatus* indicate a Ras GTPase, RasB in the spatial regulation of polarized hyphal growth, and cortical markers that generate positional information in *A.nidulans* have also been identified. The proper localization of cortical marker TeaR, a putative prenylated membrane protein, interacts with TeaA, a cell-end-marker protein important for localizing the growth machinery at the hyphal tips. These cortical markers are important for microtubule growth at the hyphal tips (Takeshita, Higashitsuji et al. 2008 and Si. 2010).

An alternative model for establishing polarity is available in *S. cerevisiae* as the mating pheromone response. Binding of mating pheromone to its cognate GPCR leads to activation of an associated heterotrimeric G protein, which is able to serve as a positional marker that locally recruits components of the Cdc42 GTPase module. Local activation of Cdc42 then reorganizes the morphogenetic machinery in a manner that overrides existing bud site selection signals. Most components of the pheromone response pathway are

conserved in *A. nidulans*, at least one GPCR and a heterotrimeric G protein have been implicated in regulation of conidial germination. Heterotrimeric G proteins also regulate the orientation of hyphal growth and control lateral branch formation in other filamentous fungi (Si. 2010).

Studies on polarity establishment in *S.cerevisiae* suggest that these cortical markers are not needed and in the absence of all known landmark proteins, polarity establishment becomes reliant upon a set of positive and negative feedback loops in local Cdc42 levels until they exceed a given threshold at a random site. Key elements in this feedback loop includes filamentous actin and the modular scaffold protein Bem1, which promotes localized vesicle exocytosis toward the presumptive polarized site where endocytosis retrieves polarity factors from other sites. A similar mechanisms could be in use in *A. nidulans* germination and/ or branch formation as the current research implies that the polarity axis to form the first germ tube is randomly selected in a swollen spore (Si. 2010).

A. nidulans also seems to require fewer but crucial functions for polarity establishment some of which are the proper function of actin cytoskeleton, vesicle trafficking machinery and also the proper organization of the Golgi apparatus. The disruption of actin filaments (mutations affecting the formin SepA) only delay the polarity establishment but dramatically affect polarity maintenance. But the deletion of genes that encode actin and key regulators such as α -actinin and Bud6 are lethal. Several studies have shown that a functional actin cytoskeleton is required for localized cell surface expansion and cell wall deposition in filamentous fungi. Exposure to depolymerizing agents have shown that there was no hyphal extension and this also triggered randomized swelling of the tip. Further studies done to disrupt cytoplasmic microtubules show they play a similar role as the actin

cytoskeleton in the hyphal polarity as they display a swollen spore but can maintain a hyphal growth and their hyphal tips show morphological defects. These studies also seem to reflect the role of microtubules is downstream of actin filaments, as they control the position of the apical vesicle cluster known as Spitzenkorper (SPK). Recent studies also show that microtubules are needed to achieve maximal rates of hyphal tip extension because they play a role in transporting vesicles to the tip. The Golgi apparatus plays an important role in the sorting and processing of proteins destined for secretion in eukaryotic cells. In *A. nidulans*, organization of the Golgi apparatus are spatially segregated within the hyphal tip and depend on the integrity of the cytoskeleton. Loss of normal Golgi organization stops polarized hyphal extension and triggers de-polymerization of the hyphal tips (Harris. 2013 and Si. 2010).

Maintenance of Polarity

Once the polarity axis is established, it must be stabilized for a germ tube or branch and to form a mature hyphae that grows by apical extension. This ability to maintain polarity axis for long distances defines filamentous fungi such as *A. nidulans*. The functions and components important in maintenance of polarity include: O-glycosylation, sphingolipid biosynthesis and organization, the Spitzenkorper and vesicle trafficking (Si. 2010, Goto.2007, Taheri-Talesh et al. 2008, and Rittenour et al.2011).

Glycosylation is a conserved post translational modification which helps to generate proteins with multiple functions and is found in all eukaryotes, Glycosylation is also important for protein stability, secretion and localization. O-linked glycosylation occurs in Golgi apparatus and is attached to protein residues of either serine or threonine. The sugars

that are attached to the O-linked structure vary among different fungi (Goto. 2007). In the course of secretion the proteins undergo glycosylation where they provide enzyme stability and protection from degradation. Post translational modification is also shown to be important to polarity maintenance as many temperature sensitive (Ts) mutants generated have shown their ability to establish polarity but when grown in restrictive temperature were unable to maintain polarity(Si. 2010). The Ts strains used in this study were deletion of Δ sepA and Δ mesA.

Serine palmitoyltransferase (SPT) is a sphingolipid that is important in polarity maintenance. SPT catalyzes the first committed step in sphingolipid biosynthesis and is required for formation of all sphingolipid derivatives (sphingoid bases, ceramides, etc.). Inactivation of SPT prevents polarity establishment without affecting growth or nuclear division. It was also found in absence of sphingolipids existing polarity axes are terminated and leads to profuse branching of the hyphal tip. BarA, ceramide synthase, generates a pool of glucosylceramides that promote localization of SepA to the hyphal tips. Sphingoid bases may have an additional set of functions that may involve lipid signaling, that separately promotes polarity establishment (Si. 2010, Rittenour et al.2011)

The Spitzenkorper (SPK) is phase dark structure that is present at the extreme apex of the fungal hyphae and is shown to have an intimate role in promoting polar growth. SPK can be assumed to function as the vesicle trafficking center (Figure 4). The polarisome (components of the yeast polarisome: Spa2, Pea2, Bud6 and Bni1), a protein complex that plays a role in determining cell polarity by directing the localized assembly of actin filaments to polarization sites. In *A. nidulans*, localization of SepA (homologue of Bni1) implied that polarisome exists as surface crescent at the hyphal tip, whereas SPK sits just

behind the tip and appears as a spot (Taheri-Talesh et al. 2008, Pearson et al. 2004 and Si. 2010).

Research also indicates that SPK and the polarisome are part of a complex which helps mediate delivery of exocytic vesicles to the apex. This cluster of vesicles delivered by kinesin-dependent transport on cytoplasmic microtubules which could later be transferred to actin filaments that are nucleated by SepA and transported to exocytic zone at the extreme apex and it could be possible that the polarisome might play a role in the formation of SPK. Recent research also shows the importance of endocytosis in the polarity maintenance. As exocytosis relies on filamentous actin for transport of vesicles to the apex, endocytosis rely on branched actin patches for moving vesicles into the cell from actin patch region behind the apex. A number of endocytic proteins (AbpA, SlaB, FimA) have been shown to interact and stabilize these actin patches and mutations in these proteins causes severe defects in polarity maintenance and in polarity establishment. MesA is a predicted cell surface protein known to promote localized assembly of actin cables at polarized sites and aids in recruitment of SepA. Δ mesA mutants displays dramatic defects in the maintenance of hyphal polarity including an aberrant pattern of cell wall deposition and delocalization of sterol-rich membrane domains. MesA is also not required for the initial recruitment of SepA to polarized sites but is required for retention of SepA (Pearson et al. 2004, Araujo-Bazan et al.2008, Taheri-Talesh et al.2008, Upadhyay et al.2008, Takeshita et al. 2008, Harris. 1997 and Si. 2010).

Rho-like GTPases

While studying the complexes that are important in polarity established and polarity maintenance it is important to look at GTPases that regulate the actin cytoskeleton dynamic and their implications in cell polarization. Small GTPases of Ras superfamily function as molecular switches in many signaling pathways have a crucial role in cell polarization. The Rho (Ras homologous) family proteins of the Ras superfamily comprise of upto 20 members which also include Cdc42, Rac1 and RhoA. Rho GTPases regulate and coordinate signaling pathways of both extracellular and intracellular signals of diverse cellular functions including cell cycle progression, migration, endocytosis, and cell morphology. These signaling pathways also function to assemble and organize the actin cytoskeleton. Cdc42 and Rac1 are both Rho-like GTPases, their importance and function differs in a variety of fungi (Iden et al.2008, Johnson and Pringle.1990, Ziman et al.1993, Schmidt and Hall.1998 and Downs. 2012).

The Rho-like GTPases cycle between active state (GTP-bound) and inactive (GDP-bound) state with the aid of guanine nucleotide exchange factor (GEF), the other regulators also include GTPase- activating proteins (GAPs) and guanine nucleotide dissociation inhibitors (GDI). GAPs convert GTP-bound form of Cdc42/Rac1 to GDP-bound form. GAP might also function as effectors to different Rho proteins. The two main GAPs found in fungi are Rga1 and Bem3. The GDI are proteins that are capable of inhibiting the dissociation of GDP from Rho-like GTPases, suggesting that GDIs function is to inhibit GEFs and GAPs. GDIs can interact with both GTP- bound and GDP-bound Cdc42 but prefers the GDP-bound state. GDI are also capable of solubilizing both GTP and GDP bond Cdc42 from the cell membrane (Iden et al. 2008, Quilliam et al.1995, Cerione and Zheng.1996, Whitehead et al.1997, Schmidt et al.1998 and Downs. 2012).

A class of proteins known as effectors interact directly with the Rho-like GTPases to activate or maintain cellular function in the cell. Only a small number of effectors are known and they fall into three classes: the p-21 activated kinases (PAKs), Cla4 and Ste20, the CRIB-domain proteins Gic1 and Gic2, and the formins. While the PAKs and formins are conserved in eukaryotes, Gic proteins and CRIB domains are not detected in the genome annotation. (Virag et al. 2007 and Downs. 2012).

The activity of PAK proteins is regulated by Cdc42 and Rac1 through the control of the autoinhibitory mechanism and cellular localization of PAK. After the PAK and CRIB domain binds to Cdc42 or Rac1, the PAK kinase domain is allowed to be autophosphorylated. A Ste20 protein with a mutation in its autoinhibitory mechanism causes a decrease interaction with Cdc42, which reduction of mating signals, loss of filamentous growth and loss of localization to the site of polarized growth. The deletion of the CRIB domain shows Ste20 independent of Cdc42. The Cla4 protein might not be conserved in all Cla4 homologs as the Δ cla4 can be restored by causing a disruption in the autoinhibition (Downs, 2012). The function of PAK kinase in filamentous fungi varies. In *Magnaporthe grisea*, neither Ste20 nor Cla4 is required for polarized hyphal growth whereas in *C. albicans* and *A. gossypii*, both Ste20 and Cla4 are involved in polarized growth. Ste20 and Cla4 may have overlapping functions as only a double mutant shows an altered phenotype. Ste20p and Cla4p may control actin cytoskeletal organization by regulating the polarisome (Cvrckova et al.1995, Brown et al. 1997, Chen et al.1997, Evangelista et al. 1997, Schmidt and Hall. 1998, Lamson et al.2002, Boyce et al.2009 and Downs. 2012).

Formins are multidomain proteins that interact with diverse signaling molecules and cytoskeletal proteins, although some formins have been assigned to function within the nucleus. Formins are characterized by the presence of two FH domains (FH1 and FH2). The proline-rich FH1 domain mediates interactions with a variety of proteins, including the actin-binding protein profilin, SH3 (Src homology 3) domain proteins, and WW domain proteins. The FH2 domain is required for the self-association of formin proteins through the ability of FH2 domains to directly bind each other, and may also act to inhibit actin polymerization. In addition, some formins can contain a GTPase-binding domain (GBD) required for binding to Rho small GTPases, and a C-terminal conserved Diaautoregulatory domain (DAD) which can interact intramolecularly and modulate activity and/or localization. The FH1 and FH2 domains appear to be separable and vary among species (Tanaka. 2000, Shimada et al. 2004 and Takeya et al. 2003).

Using florescent fusion proteins in *A. nidulans* SepA::GFP, a formin protein, localizes at the crescent of the hyphal tip and septation sites interacting with the actin ring. The lack of both the FH1 and FH2 domains in SepA shows it can still localizes as a broad crescent at hyphal tip but is no longer localized at the septa. Also recent studies show cells lacking the complete FH1 and FH2 domains of SepA have an increase in dichotomous branching and abnormally wide hyphae. Notably, these cells lacked actin rings at septation sites, but some disorganized actin structures were still found at tips, presumably supporting the aberrant hyphal growth (Gladfelter. 2006). Cdc42 is known to interact with putative polarisome components and regulate their localization. In *A. nidulans*, the observations suggest that polarisome recruitment to hyphal tips is not strictly dependent on Cdc42. In the absence of $\Delta cdc42 \Delta sepA$ the growth of the colonies were restricted but were still able establish

polarity with significant amount of time suggesting that Cdc42 may not activate SepA but is required to maintain polarity (Virag et al. 2007).

Activation and localization Cdc42

In *S. cerevisiae*, newly synthesized Cdc42 is geranylgeranylated by Cdc43-Ram2 and interacts with the Rdi1 (Rho GDP-dissociation inhibitor) protein within the cytosol. The Cdc42 GDP-Rdi1 complex then interacts with Cdc24-Bem1 in the plasma membrane. This Cdc24-Bem1 complex is bound to the plasma membrane either through an interaction between Cdc24 and the GTP-bound Rsr1 (Ras-Related Protein) GTPase, or through the Cdc24 PH domain. The Cdc24 then catalyzes the dissociation of GDP from Cdc42 and is activated with GTP. This leads to Cdc24 dissociation from both Cdc42 and Bem1, and interaction with the GDP bound Rsr1 through the interaction with Bud2 (an inhibitory regulator protein), GAP and Bud5 (Bud Site Selection protein). The now released Cdc24 is free to recycle to the bud site or become available for nucleotide exchange later in the cell cycle (Moskow et al.2000, Gladfelter et al.2002 and Down. 2012).

The selection of the bud site and the orientation of the actin cytoskeleton is controlled by the cell polarity establishment proteins, which include Cdc42, Cdc24 and Bem1, a SH3 domain-containing protein. It has been shown that cells lacking Cdc42, Cdc24, Cdc43 or Bem1 are unable to form a bud, have a randomized actin cytoskeleton and have large unbudded multinucleate cells. After Cdc42 and Bem1 localize to the plasma membrane at the incipient bud site, Bud1 binds to the activated Cdc42, which causes the Bud gene products to select a bud site and guides in cell polarity establishment proteins. Then, the cell can organize the cytoskeleton and initiate bud growth (Sloat et al.1981, Schmidt and Hall.1998,

Bender and Pringle.1989 Ziman et al.1993, Chenevert.1994, Chant and Herskowitz.1991, Zheng et al.1995 and Downs. 2012).

Once the cell reaches resting phase, Cdc42 is released from the Bem1-Bud1 complex and binds to a GDI in the cytoplasm. However, when the cell is activated, the Cdc42 is released from the GDI and can now be translocated to the cell's membrane. Cdc42 is targeted to the membrane because of its post-translational attachment of prenyl groups. The C-terminal of the Cdc42 consists of the sequence Cys-X-X-Leu, where X can be any amino acid. C20 geranylgeranyl isoprenoid can modify this terminal at the Cys residue, causing the covalent thioether linkage of geranylgeranyl groups to the Cys residue in the CAAX-box of the GTPase. This is followed by the removal of the -AAX and methylation of the exposed Cys residue. It is the geranylgeranyl group that anchors the Cdc42 protein to the cellular membrane (Takai et al.1995, Schmidt and Hall.1998, Katayama et al.1991, Adamson et al.1992 and Down. 2012).

In *A. nidulans*, Swof is needed for the modification of Cdc42 and this modification allows Cdc42 to attach to the plasma membrane. Swof gene, is an N-myristoyl transferase, increases the affinity of its target to the plasma membrane. This modification is similar to the lipid modification, geranylgeranylation, in yeast. It also seems that inositol phosphorylceramide (IPC), a sphingolipid, is needed for the attachment of Cdc42 to the plasma membranes in filamentous fungi. The IPC synthesis is important for forming lipid rafts, which are thought to act by selective inclusion of specific membrane-bound proteins. These rafts are also known to sequester polarity proteins. If there is a disruption of the IPC synthase after polarization has established, the apical cap becomes disorganized, resulting

in dichotomous branching and splitting of the apical hyphae (Shaw et al.2002, Cheng et al.2001 and Down. 2012).

Cdc42 and Rac1

In most fungi, Rac1 is more important than Cdc42 for the establishment of hyphal polarity but in *A. nidulans*, Cdc42 has a pivotal role in polarization of hyphal growth, whereas RacA is mostly dispensable. In the absence of Cdc42 delay in the formation of lateral branches and secondary germ tubes but initial germination, polarity establishment and polarity maintenance is not affected (Virag *et al.* 2007). In $\Delta cdc42$ strains, the formin SepA seems to lose specificity for the hyphal tip, suggesting that the polarity axis is altered. Finally, $\Delta cdc42$ strains have strongly altered conidiophores that support a more complex role than just regulation of budding morphogenesis during conidiation (Sharpless and Harris.2002, Timberlake.1990 and Downs. 2012)

Cdc42 and Rac1 have overlapping functions as $\Delta rac1$ in *A. nidulans* has no obvious phenotype. An overexpressed Rac1 has been shown to restore a $\Delta cdc42$ to a near wild-type phenotype. It has also been proposed that Cdc42 has an equal role in primary polarity axis during conidiophore germination. However, Cdc42 does seem to be the pivotal GTPase after the primary polar axis is established (Virag et al. 2007 and Down. 2012).

Polarisome in *A.nidulans*

The homologues of the polarisome in *A.nidulans* were recently found and characterized, the homologous for Spa2, Bud6 and formin Bni1 are SpaA, BudA and formin SepA but none were found for Pea2. Comparison between the Spa2 and SpaA revealed that SpaA

lacked domain II but has three additional domains which are conserved in filamentous fungi and localization studies show that SpaA functions exclusively at the hyphal tip. The deletion of the *spaA* gene however showed more dichotomous branching, where two hyphal tips are formed by splitting from an existing tip, than compared to wild type (Figure 5). The comparison between Bud6 and BudA showed that BudA shares the AIP3 domain at the carboxy terminus that is important for interaction with actin and another highly homologous domain at the amino terminus. The deletion of BudA has been shown to be lethal in *A. nidulans* and the localization studies show that BudA::GFP is visible only at sites of septum formation not at hyphal tips. SepA localizes at the hyphal tip primarily at the surface crescent which suggest that the polarisome also exists at the surface crescent as SepA. In yeast the Bni1 formin forms a complex and is necessary for normal cell morphogenesis. In *A.nidulans* however SepA is not required for the localization of SpaA leading to believe the polarisome components in *A.nidulans* might not work as a complex (Virag et al. 2006). We further screened several genes to find genetic similarity to the polarisome components and found ANID_05595.1 (ModB) is located on chromosome 5, contig 96 and encodes 946 amino acid hypothetical involucrin repeat protein and when compared to the components of the polarisome shared some genomic similarity to SepA (shown in Figure 6 after performing multiple alignment of the DNA sequences).

1. The first objective in this study is to explore the role of ModB during hyphal morphogenesis and its possible role in the polarisome along with SepA.

Carbon Metabolism

Many filamentous fungi find the primary source of nutrients in the natural environment is dead and decaying plant matter. Plant cell wall consist of cellulose, hemicellulose and pectin, which is broken down to glucose by cellulolytic enzymes secreted by fungi to obtain glucose. Glucose represents the most preferred carbon source for majority of microbes and also acts as trigger in *A. nidulans* to start germination of conidia. The ability to sense intracellular and extracellular nutrient source helps the cells to coordinate cellular metabolism and use the preferred carbon source prior to the use of alternate carbon sources. This ability is known as the carbon catabolite repression (CCR). CreA is a transcriptional repressor in *A. nidulans* that is central to CCR. Nutrient sensing and the downstream signaling cascades control the regulation of biochemical metabolic pathways, biosynthetic processes and developmental changes. Previously described the glucose sensing in germination, G-protein-coupled receptor-mediated and Ras-mediated cAMP-PKA pathways regulate germination and trehalose metabolism, whereas SchA kinase performs parallel functions. Despite recent advancements, the understanding of how carbon metabolism occurs during germination, polarity establishment and polarity maintenance is scarce. The importance of this knowledge is immense as the extensive use of filamentous fungi in bioprocess industry where it most likely encounters nutrient limitation and starvation conditions affects production of valuable products (Assis, 2015, Bhargava et al.2003 and Li et al.2000).

Intercellular Signaling

Fungi are equipped with many receptors that sense both abiotic and biotic stimuli. These receptors facilitate the coordinate mechanisms of: fungal development, morphogenesis and metabolism in accordance with the environment. G-protein coupled receptors (GPCRs) are

a large family of transmembrane receptors, which detect mostly unknown extracellular signals and initiate intracellular signaling cascades. GPCRs sense a wide range of stimuli including light, sugars, amino acids and pheromones. GPCRs possess seven transmembrane domains and initiates downstream signaling through the associated heterotrimeric G-proteins. Sensitization of a GPCR by a ligand results in the activation of (exchange of GTP for GDP) $G\alpha$ subunit, leading to its dissociation from the $G\beta\gamma$ subunits. This allows in both $G\alpha$ subunit and $G\beta\gamma$ subunits to interact with effector proteins that regulate downstream signaling. In fungi, GPCR-regulated signaling pathways includes the cAMP-dependent protein kinase (PKA) pathway and the mitogen-activated protein kinase (MAPK) cascades, which regulate metabolism, growth, morphogenesis, mating, stress responses and virulence (Brown et al. 2015 and Fernanda dos Reis.2013).

Heterotrimeric G-proteins are conserved in all eukaryotes and are essential components for transmitting external signals into the cells. The sequential sensitization and activation of G-proteins then translates these signals into the proper transcriptional, biochemical and behavioral alterations. Regulators of G-protein signaling (RGSs) control the intensity and duration of the G-protein. In *A. nidulans*, the activated $G\alpha$ subunit, FadA, promotes vegetative growth and inhibits both asexual and sexual development. The RGS, FlbA, inhibits FadA and is required to control vegetative growth and also to allow asexual development (Figure 8) (Brown et al. 2015).

Extracellular Signaling

Due to filamentous fungi role in biotechnology the need to identify and specify different transport systems has become increasing important. The transport system for the sugar

uptake is well characterized in *S. cerevisiae* has shown to be able to transport and metabolize glucose, fructose, mannose and galactose. Transport of simple sugars is mediated by facilitated diffusion by the Hxt (Hexose transporter) family, which is the largest subfamily of major facilitator superfamily (MFS). In *S. cerevisiae* about 20 proteins have been classified as Hxt proteins with different Hxt proteins being induced depending on the concentration of glucose available. These sugar transporters can be characterized as high affinity and moderate to low affinity based on their different substrate affinities or specificities. In *A. nidulans* an attempt to characterize the genes in the Hxt family was made and found four putative glucose transporters homologues. One of homologues HxtB, a high affinity glucose transporter was tagged to GFP to understand the localization and the mechanism used for transport (Fernanda dos Reis et al. 2013).

Secretory Pathway

Filamentous fungi have naturally high capacity to secrete proteins. However, the producing of non-fungal proteins has been low. Many studies have attempted to understand the secretory capacity of filamentous fungi at the transcriptome level and to better understand the limitation of the secretory pathway. These studies identified genes that play a major part in the different stages of protein secretion such as translocation, folding, cargo transport and exocytosis (Schalen et al. 2016).

The transport in the secretory pathway begins with translocation of protein to the ER, where the protein glycosylation, phosphorylation occurs and disulfide bridges are formed. After passing through the quality control mechanism, the cargo is transported in vesicles from the ER to the Golgi apparatus. The vesicles bud off from the ER membrane and attach to

the Golgi with the aid of soluble N-ethylmaleimide-sensitive (NSF) factor receptor (SNARE) that mediates vesicle docking and fusion. After further modifications in the Golgi apparatus, such as glycosylation and peptide processing, the secretory cargo leaves the Golgi in vesicles bound for the plasma membrane, where exocytosis occurs (Schalen et al. 2016). One of the common techniques used to study the secretory pathway in more detail is used gene deletion or genes attached to fluorescent proteins to visualize the protein secretion (Schalen et al. 2016).

A high secreting fungal enzyme (β -glucosidase) was tagged to GFP to characterize the localization pattern and visualize its response to various conditions that mimic the conditions they may face during production (Ishitsuka et al 2015).

2. The second objective in this study is to visualize and characterize the functions of genes (gene deletion) that play a role as a role in carbon metabolism and control the metabolic and growth regulation in a hyphae. We also used the same system to characterize the localization of glucose transporter (HxtB) and enzyme (β -glucosidase) and its response to various nutrient conditions.

Figures

Figure 1: Fungal morphogenesis: a) yeast growth by budding b) hyphal growth with red arrows showing septa and green arrows showing secondary and tertiary branches of hyphae, c) Asexual reproduction of *A. nidulans* and shows the characteristics of hyphal growth and yeast growth when rows of conidia are formed by budding, and d) signaling pathway to the conidiation in *A. fumigatus* (Thompson et al. 2011 and Etxebeste et al. 2010).

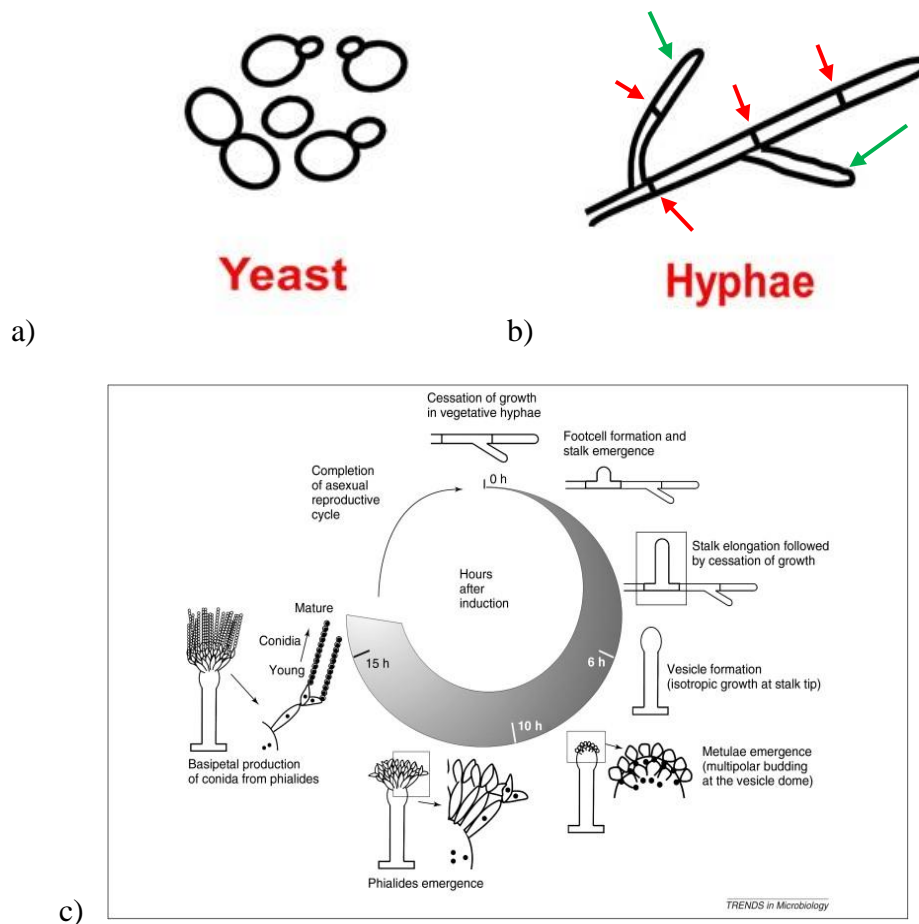


Figure 2. Growth from spore to hypha. Shows the isotropic growth (germination) to polarity establishment and to the polarity maintenance (Si. 2010).

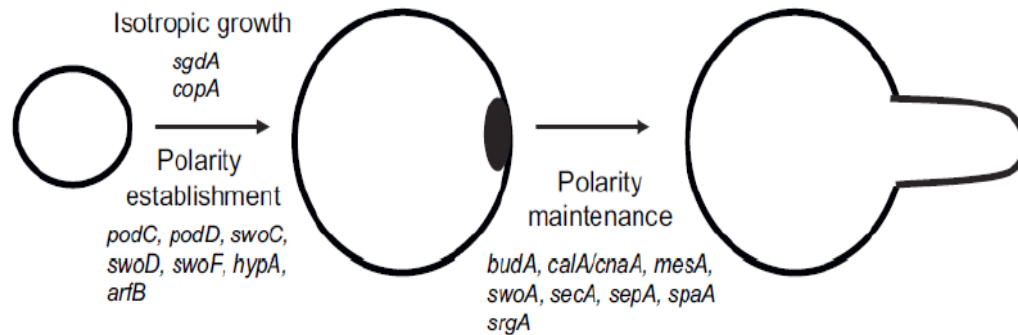


Figure 3: Show the activation of the cAMP-PKA pathway in *S. pombe* and in *A. nidulans*. The *A. nidulans* sequence homologs of *S. pombe* are listed in square brackets (Muthuvijayan et al. 2004).

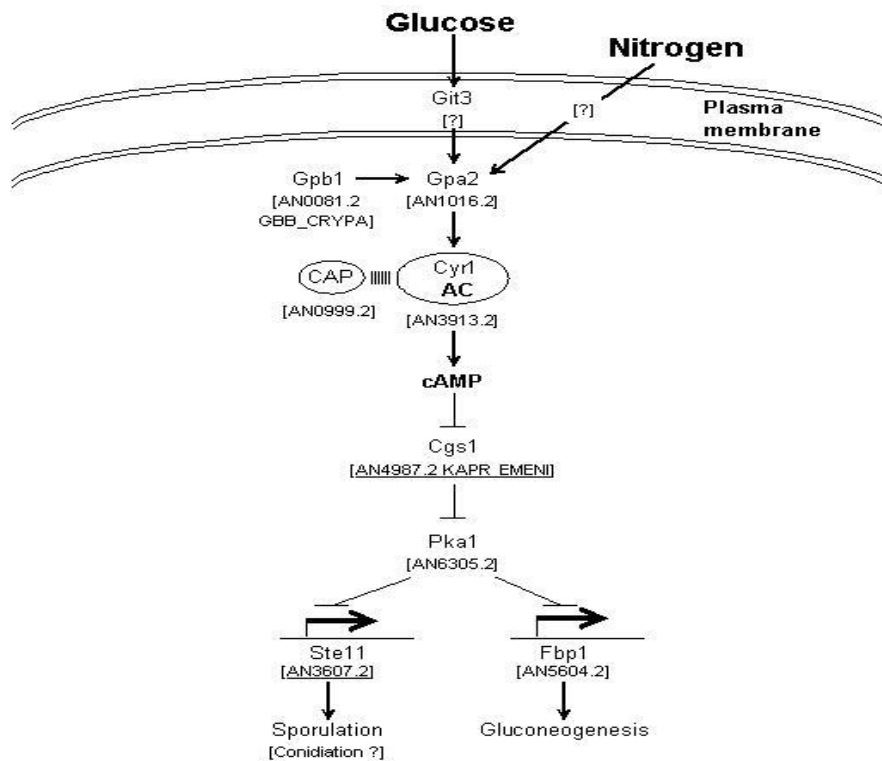


Figure 4. Morphological form of a filamentous hyphae along with the locations of actin cables and the Spitzenkörper (SPK) and also shows the interactions of Cdc42 with the exocyst and polarisome (Sudbery. 2011)

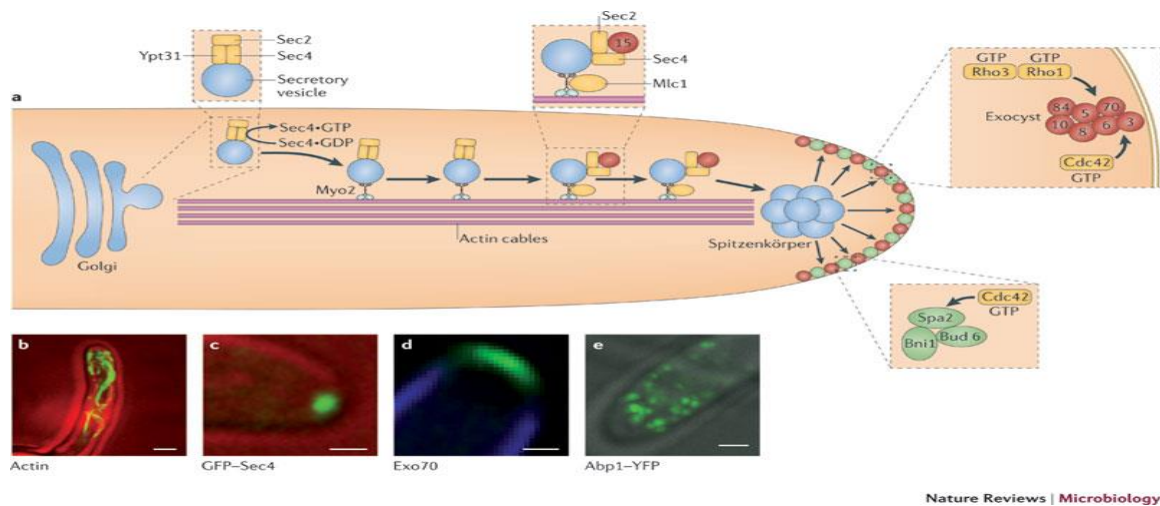


Figure 5: Polarity in *A. nidulans*. (a) Germ tube elongation. (b) Subapical branching. (c) Tip splitting (dichotomous branch) showed by red arrows (Momany. 2002).

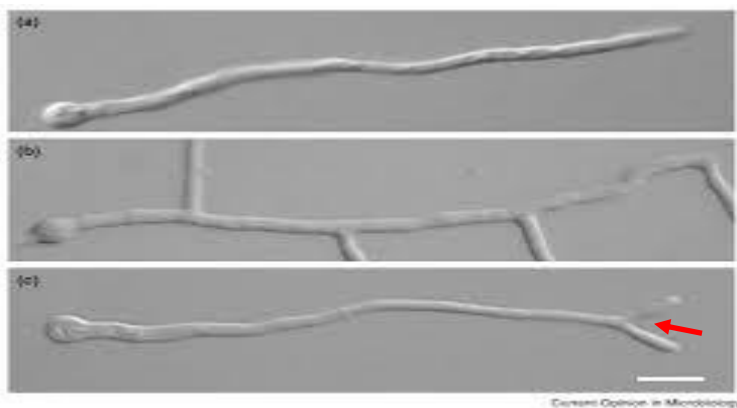


Figure 6: Phylogenetic tree of showing genetic similarity to components of the polarisome in yeast and *A. nidulans*.

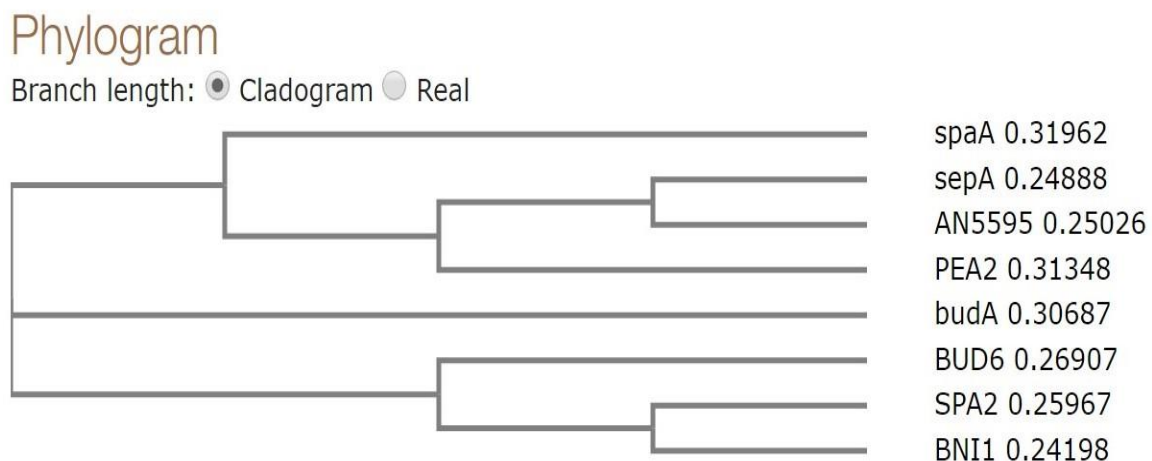


Figure 7: A4 (wildtype) in the derepression system was moved from YGV (yeast extract, glucose media) to CMC media and measured for 4 hours. The red arrows point to change in hyphal morphology.

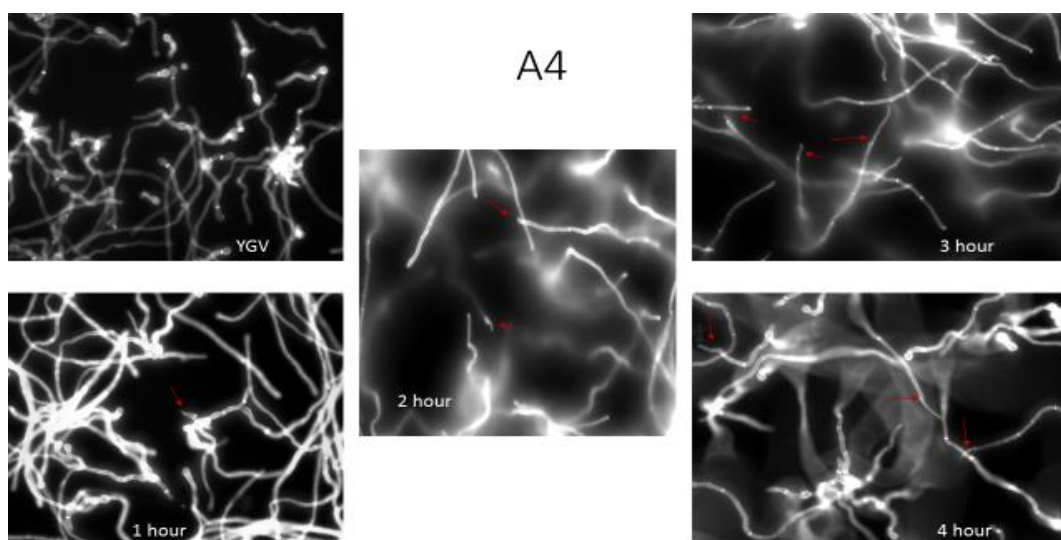


Figure 8: FlbA, a GTPase- activating protein negatively regulates FadA (α -subunit of heterotrimeric G protein) by forming a $G\alpha$ - $G\beta$ - $G\gamma$ complex. Active FadA positively regulates PkaA inducing vegetative growth and inhibiting conidiation and secondary metabolism (Kato et al. 2003).

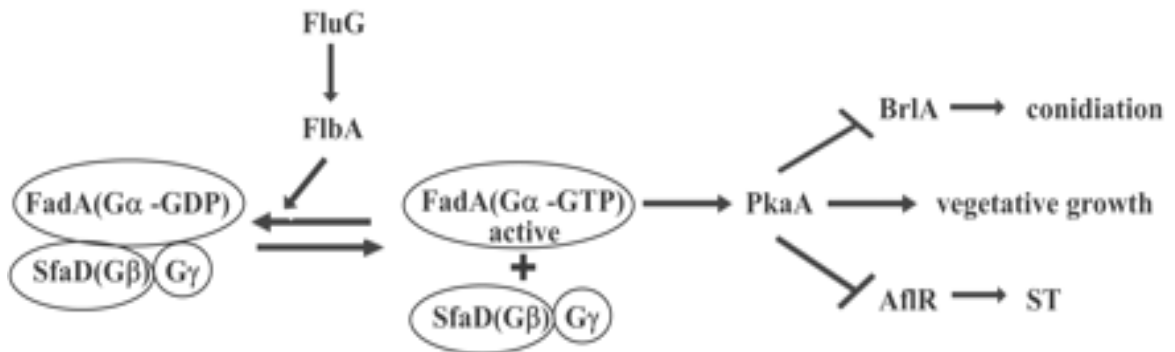
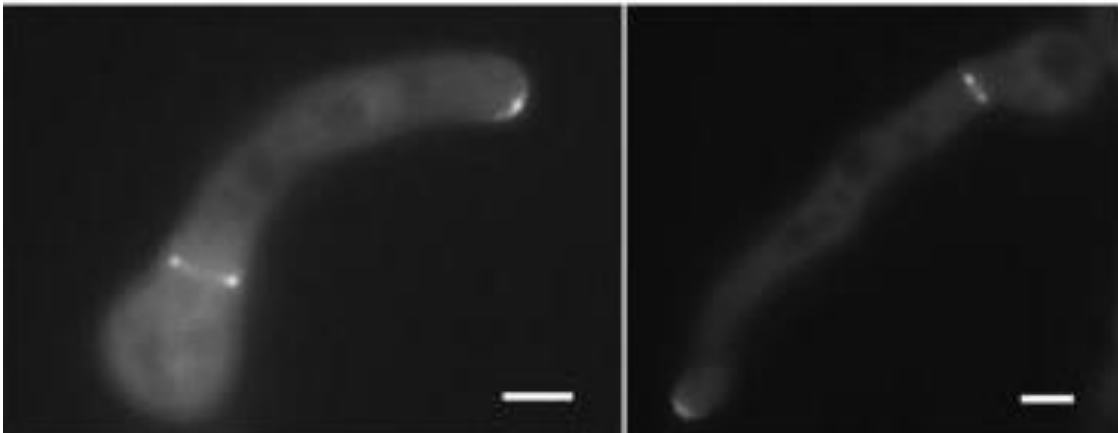


Figure 9: SepA::GFP localization in *A. nidulans* is at the septa and at the hyphal tips (Sharpless and Harris.2002)



Chapter 1

Introduction

Polarized hyphal growth is a defining feature of filamentous fungi where most of the growth occurs at hyphal tips. Hyphae are organized so that the cell surface expansion and cell wall deposition are restrained to discrete sites at the hyphal tip. This method of growth is supported by extreme polarization of the cytoskeleton and the vesicle-trafficking machinery, which delivers exocytic vesicles from the interior of the tip along with endocytic mechanisms that remove materials as they are displaced from the tip. Due to the attention given on understanding polarized growth has resulted in identification and characterizing gene products that are required for the establishment and maintenance of hyphal polarity (Si et al. 2016, Horio et al. 2005). Although the process for understanding the hyphal morphogenesis is well studied the genes involved in the molecular mechanisms are still poorly understood. The general model for these mechanisms had emerged from the study of polarity establishment in yeast cells (Pearson et al. 2004).

The genes that have been of most interest in the establishment of polarity are the Rho-related GTPases (Cdc42, Rac, Rho). These GTPases are molecular controls that control many aspects of the hyphal morphogenesis and in other eukaryotic cells. In *Saccharomyces cerevisiae* Cdc42 acts as control center for the different regulatory networks that relay the spatial and temporal information to recruit the cytoskeleton and vesicle trafficking machinery to polarized growth sites. In absence of Cdc42 in yeast cells, they are unable form budding or mating polarity axis. The importance of Cdc42 led to identification and characterization of Cdc42 and Rac1 homologous in any filamentous fungi (Si et al. 2016). In *Aspergillus nidulans* Cdc42 is not required for polarity establishment or polarity

maintenance, instead RacA can control these functions as the deletion of *Δcdc42* can germinate and can establish hyphal polarity but the hyphae are atypically straight and exhibit delay in the formation of lateral branches. This suggests that Cdc42 is required for polarity establishment of secondary hyphal growth. The essential role of RacA in polarity establishment of hyphae was demonstrated when extra copies of RacA was provided on a high-copy plasmid in absence *Δcdc42* and this suppressed the *Δcdc42* mutant phenotype and the *Δcdc42 ΔracA* double mutant are inviable. Therefore neither Cdc42 nor RacA are absolutely required for polarity establishment and act redundantly at some level for normal polarized hyphal growth. Cdc42 and RacA also have individual important roles in hyphal morphogenesis as RacA is an activator of fungal NADPH oxidases and Cdc42 is a regulator for MAP kinase signaling pathway (Virag et al. 2007, Si et al. 2016).

In yeast Cdc42 activates three distinct classes: p21- activates kinases (PAKs), the CRIB-domain proteins Gic1 and Gic2, and the formins. In filamentous fungi relatively little is known about the Cdc42 effectors. Although PAKs and formins are conserved in filamentous fungi, the homologues of Gic proteins or other proteins with a CRIB domain are absent (Virag et al. 2007).

Formins are multidomain scaffold proteins involved in actin-dependent morphogenetic events. As the sole member of the formin family in *A. nidulans* proteome, SepA is required for septum formation and polarized growth. SepA is also suggested to function within a complex (the polarisome) that is regulated by Cdc42. The disruption of actin filaments (mutations affecting the formin SepA) only delay the polarity establishment but dramatically affect polarity maintenance. But the deletion of genes that encode actin SepA and key regulators such as α -actinin and Bud6 are lethal. Several studies have shown that

a functional actin cytoskeleton is required for localized cell surface expansion and cell wall deposition in filamentous fungi. MesA a fungal protein that stabilizes the polarity axis in *A. nidulans* by regulating the localization of SepA directed to hyphal tips. Although MesA is not required for initial recruitment of SepA to polarized sites, it is required for retaining the polarity during hyphal growth (Sharpless et al. 2002, Virag et al. 2006, Virag et al. 2007, Taheri-Talesh et al. 2008, Harris et al. 2005).

The establishment and maintenance of the hyphal tip can be attributed to formation of several complexes that seem to work synchronously and can be termed as the “tip growth apparatus”. The tip growth apparatus contains the Spitzenkorper, polarisome and the exocyst complex helped by the actin cytoskeleton and microtubules. Ultrastructural analysis and live cell imaging have shown the importance of the Spitzenkorper as it mainly consists of the aggregated vesicles located at the extreme apex of a growing hyphal tip. The homologues of the polarisome in *A. nidulans* of Spa2, Bud6 and formin Bni1 are SpaA, BudA and formin SepA but none were found for Pea2 (Pearson et al. 2004, Virag et al. 2006, Taheri-Talesh et al. 2008, Sharpless et al. 2002). However, scanning the genome of *A. nidulans* for genes that carry similar characteristic for SpaA, BudA or SepA we came across ANID_05595.1 (ModB). ModB showed some genetic similarity to SepA by sharing some sequence similarity in coiled coil domain (Harris unpublished). (Taheri-Talesh et al. 2008, Virag et al. 2006, Gross et al. 2013).

ANID_05595.1 (ModB) is located on chromosome 5, contig 96 and encodes 946 amino acid hypothetical involucrin repeat protein. While characterizing the function of ModB, the deletion of *ΔmodB*, resulted in restricted colony growth, increased hyphal diameter and dichotomous hyphal branching patterns (the hyphal tip splits into two branches instead of

continuing as a single tip). The phenotype was similar to phenotype found in *ΔspaA* and *ΔsepA* deletion (The *ΔsepA* strain in this study has a point mutation, an L1369S substitution in the FH2 domain, that causes substitution of hydrophilic amino acid for a hydrophobic amino acid) (Sharpless et al. 2002). The ModB hypothetical protein shows some structural similarities to the SepA protein. This suggests that ModB may have some similar mechanistic function to SepA. Further characterization of ModB::GFP also shows localization initially at the septa and at the hyphal tip but overtime the localization is maintained only at the hyphal tips which was similar pattern to SepA::GFP (Virag et al. 2006, Sharpless et al. 2002, Gross et al. 2013). Here we present how SepA and ModB are different in their interactions and show that they may use different pathways for polarized hyphal growth.

Material and Methods

Strains, Media and Growth Conditions

Strains used in this study are shown in Table 1. The glucose rich media and supplements was prepared as previously described in Harris et al.1994. The minimal media was prepared as previously described in Kafer.1997. The study used both solid (with ~2% agar) and liquid media (without agar). MAG (2% Malt extract, 2% dextrose with vitamin), MAGUU (MAG with uridine and uracil), MN (1% dextrose and nitrate salts), MNV (MN with vitamins) and water agar were used as solid media. YGV (0.5% yeast extract, 1% dextrose and vitamins) and YGVUU (YGV with uridine and uracil) were used as liquid media. All the strains were grown in 28°C unless indicated otherwise.

modB gene replacement

The $\Delta modB$ gene replacement was constructed by fusion PCR and then transformed into the *A. nidulans* genome (Fig A). The plasmid pFNO3 was used as the source of the auxotrophic marker *pyrG* that replaced *modB*. The AspGD database (<http://www.aspergillusgenome.org>) was used to retrieve ~1000 nucleotides of sequence upstream and downstream of *modB* which was then fused with *pyrG* through PCR. The MacVector software was used to construct primers for different fragments of the DNA construct. Each fragments was generated through PCR using the Expand High Fidelity PCR kit (Roche). Expand Long Template PCR kit (Roche) was used for fusion PCR of the fragments. The fragments were purified after amplification in the PCR by using PCR Purification kit (Qiagen). The *modB* gene replaced construct was purified using Gel Extraction kit (Qiagen) after PCR fusion. All fragments and the fused construct were verified after each amplification by gel electrophoresis to confirm the correct product size. The construct was transformed into *A. nidulans* wild-type strain TN02A3 using a standard lab protocol (Downs. 2012). All work in knockout, transformation and verification was performed by a pervious graduate student, Bradley Downs.

Construction of ModB::GFP

The Aspergillus Genome Database was used to identify the location of the gene and retrieve the sequence of *modB* (ANID_05595.1 nucleotides 2288415 to 2291359 on chromosome V). To build ModB::GFP the DNA construct and primer design was done using the Macvector software. The plasmid pFNO3 was used for retrieving the C-terminal GFP and *pyrG* (auxotrophic marker). pFNO3 was acquired from the Fungal Genetic Stock Center. Oligonucleotide primers were purchased from IDT, Inc. The construction of ModB::GFP used PCR to amplify fragments of the ModB::GFP construct and PCR fusion

for amplifying the whole fragment (upstream (5199 base pair), downstream (3858 base pair), *GFP-pyrG* (2642 base pair) and the fusion (8313 base pair)). The Expand High Fidelity PCR kit (Roche) was used to amplify each fragment. Expand Long Template PCR kit (Roche) was used for the fusion and amplification of all fragments. We used PCR Purification (Qiagen) for purifying fragments after amplification through PCR and Gel Extraction Kit (Qiagen). After each PCR amplification the product was verified using gel electrophoresis. After the generating ModB::GFP DNA construct, it was transformed into *A. nidulans* wild-type strain TN02A3 using a standard lab protocol (Downs. 2012).

Transformation of A. nidulans with Mod::GFP

Transformation in this study was done by growing fresh TN02A3 spores (10^7 /mL) in YGV+UU at 28°C, 200 rpm for 12-14 hours. The protoplast solution consisted of: 20mL of Solution 1 (0.8M ammonium and 100mM citric acid in ddH₂O), 20mL of Solution 2 (1% yeast extract and 2% sucrose dissolved in sterile ddH₂O), 7mL of 1M Magnesium Sulfate, 200mg of Driselase, 250mg of Glucanex, 250mg of Vinoflow, 100mg of Lysing Enzyme, and 500mg of BSA (Bovine Serum Albumin). The protoplast solution was incubated at 30°C, 100 rpm for 15 minutes, to dissolve the solutes into solution. The solution was filter sterilized.

The mycelium was collected by making a pellet of mycelia from centrifuging the solution at 3500 rpm, for 5 minutes, at room temperature. The YGV+UU was discarded and the sterilized protoplast solution was added to the pellet. The solution was incubated at 30°C (at 100rpm) for 4hours. The solution was checked for protoplast formation at hour 3. After 4 hours, the protoplast was filtered through a Miracloth and into a 50mL falcon tube (to collect all of the

hyphae that did not grow protoplast). The falcon tube was centrifuged for 5 minutes, at 3000rpm, to collect the protoplast.

After protoplasts were collected, the supernatant was discarded. The protoplast pellet was washed with 20-30mL of Solution 3 (0.4M ammonium sulfate, 1% sucrose and 50mM citric acid in ddH₂O) on ice until the entire pellet was resuspended. The solution was centrifuged for 5 minutes, at 3000 rpm, to collect the protoplast pellet. This wash was repeated twice. Protoplast were resuspended in 100 μ L/reaction of Solution 5 (0.6M KCl, 50mM CaCl₂ and 10mM MES in ddH₂O) and incubated on ice for 10 minutes. After incubation, 50 μ L of protoplasts were removed twice and placed separately into two 1.5mL tubes, one for positive and one for negative control. Typically, 10 reactions are required per DNA construct. Nine of the reactions are designated for the DNA construct and 1 reaction was designated for the positive and negative control. Each reaction was equivalent to two plates.

4 μ L of pFNO3 plasmid was added to the positive control. 50 μ L of Solution 4 per reaction was added and incubated on ice for 20 minutes. 1mL of Solution 4 (25% Polyethylene Glycol 8000, 100mM CaCl₂, 0.6 KCl and 10mM Tris HCl (pH=7.5) in ddH₂O) per reaction was added to each tube and incubated at room temperature for another 20 minutes.

The top agar was equilibrated in a 60°C water bath and was removed 5 minutes before the last incubation time. This allowed the agar to cool down so that the heat would not affect the protoplast. 2.3mL (766.66 μ L, 3 times) of protoplasts were transferred to 40mL of top agar and mixed gently. 10mL of top agar mixture was added per plate. The plates were left at room temperature overnight and transferred to 28°C incubator.

The transformation colonies were grown for 5 days and checked for growth, if a knockout mutant has been used the colonies could take longer to grow due to diminished growth phenotype. After the colonies were ready, a toothpick was used to transfer the colonies to a MAG plates to revive sick colonies. After a sampling of phenotypes are picked. DNA was extracted and PCR verified, once the colonies were verified they were plated out on fresh MAG plates. The spores were then stored at -80°C (Downs. 2012).

DNA Extraction

DNA was extracted using the Mo Bio Powersoil DNA isolation kit (Catalog No. 12888-100). The protocol followed instructions provided by the vendor. This kit has been used in many studies and has been used to extract DNA from a variety of yeast, bacterial and filamentous fungi.

PCR

After DNA extraction, sequences were amplified by PCR. There were three types of PCR reactions used in this study (based on the polymerase employed): native polymerase (Invitrogen, Carlsbad, CA), High fidelity polymerase (Roche) and Long template polymerase (Roche). The native Taq polymerase was used for PCR verification on all sequences that were not used in transformations. The High fidelity polymerase and Long template polymerase was used for sequences used in transformation. PCR reactions were set up follows:

- (i) PCR verification reaction (Invitrogen, Carlsbad, CA): $5\mu\text{L}$ of buffer, 2.5 mM MgCl_2 , $200\mu\text{M}$ dNTP, 100ng of DNA template, 400nM of downstream and

upstream primers (each), 0.5 units of Taq polymerase and double distilled water to bring the final solution to 50 μ L.

- (ii) Expand High Fidelity PCR System (Roche, Mannheim, Germany): 5 μ L of buffer, 2.5 mM MgCl₂, 200 μ M dNTP, 100ng of DNA template, 400nM of downstream and upstream primers, 0.75 units of Expand High Fidelity Enzyme mix and double distilled water to bring the final solution to 50 μ L.
- (iii) Expand Long Template PCR System used for PCR fusion (Roche, Mannheim, Germany): 5 μ L of buffer (with a final concentration of 2.75 mM MgCl₂), 500 μ M dNTP, 100ng of DNA template, 400nM of downstream and upstream primers, 0.75 units of Expand Long Template Enzyme mix and double distilled water to bring the final solution to 50 μ L (Downs. 2012).

The PCR Conditions

The simplest protocol was PCR verification, where the thermocycler, (Biorad MJ mini gradient thermocycler) lid was set for 105°C and the block was set to reach 94°C (the DNA denaturing temperature). The block was then held 94°C and polymerase was added to each reaction. After polymerase was added, there was a 90 second 94°C denaturing step. The annealing temperature was specific for each primer set, usually 50-60°C, for 30 seconds. The elongation temperature was 72°C with the time dependent on the length of the product. In this study, for every 1kb, 1 minute was added to the elongation time. This cycle was repeated 30 times. The final step was 72°C for 7 minutes to finish up all of the elongations. The PCR reaction was then held at 4°C to stabilize the sequence after the run.

While using the High fidelity PCR system, there were two different denaturing, annealing and elongation cycles. The first 10 cycles were the same as stated above but, the next 20 cycles required an additional 5 seconds added to each elongation cycle.

While using Expand Long Template PCR System, the elongation temperature was set at 68°C and the last 20 cycles were increased by 20 seconds per cycle.

Electrophoresis

The gels used for electrophoresis in this study was made of 0.8% purified agar in 1xTAE and 1µL of ethidium bromide. To determine the size of the band, 1+KB ladder (Invitrogen) was used. To determine the mass of the bands, the High Mass Ladder (Invitrogen) was added to the gel in two different quantities of 2µL and 4µL.

Microscopy

Microscopy images were captured and processed using Metamorph software. Brightfield and fluorescence microscopy was performed using an Olympus BX- microscope housed in the Harris lab. (All of the Brightfield (40X magnifications was used for all images except for GFP images. 100X magnification was used for GFP images). Confocal microscope at the Microscopy Core Facility was used for GFP images. Calcofluor (a non-specific fluorochrome that binds with cellulose and chitin which is contained in the cell walls of fungi) staining was used to visualized hyphal tips and septa.

Bright Field (BF)

The spores of strains were collected from fresh plates. 15mL and/or 50 mL YGV was added into falcon tubes depending on the number of coverslips being used. Sterile glass coverslips (22X22mm) were flamed to remove lint and laid on the bottom of a clean Petri dish. For

small Petri dish (60 cm) use 10mL of media and 10 μ L of spores were used. For large Petri dish (100 cm) 20mL of media and 20 μ L of spores were used. Media and spores were mixed in the Falcon tube then poured into the Petri dish with coverslips. Gentle tapping was used to eliminate air bubbles between the coverslips and the bottom of the Petri dishes, which were then put in the incubator 28°C or 42°C (when ts strains were used) for 12- 14 hours.

Calcofluor

The samples were set up as it was done in BF. After the 12-14 hour incubation time the coverslips were fixed with ethanol for 2 min. They were then treated with Calcofluor (in 50mL falcon tube add 40mL of water and add 17 μ L Calcofluor (10mg/mL) and mixed well) for 5 min. The final wash was with sterile water. Then mount solution was added onto the slide and the stained coverslip was added to the slide and finally analyzed on the microscope.

Characterization of $\Delta modB$ crossed with $\Delta sepA$, $\Delta mesA$, $\Delta cdc42$ and $\Delta racA$

The parent strains were streaked on MAGUU plates and then crossed sections were plated on MN plates. Once the cleistothecia had matured, they were dissected on water agar plates. The dissected spores were diluted with water and spread on MN plates. Selected outcrosses segregants were then plated on MAG plates to perform DNA extraction (Mio-Bio Powersoil kit) and then PCR verified (Invitrogen, native/ recombinant Taq polymerase). Once the outcrosses were verified the spores were stored at -80°C and imaged using both BF and Calcofluor microscopy.

Results

Phenotypic characterization of $\Delta modB$

The gene replacement of $\Delta modB$ showed restrictive growth on MAG plates. The hyphal growth was analyzed by BF and Calcofluor microscopy and noted the phenotype of dichotomous branching compared to the A4 (wildtype) which only formed a single hyphal tip (Fig 1). However, the dichotomous branching in $\Delta modB$ did not occur in all hyphae, as displayed in the $\Delta sepA$ mutant, but only in about 40% of the hyphae. (Fig 1) (Sharpless and Harris. 2002). The $\Delta sepA$ mutant also showed that they cannot produce septa or there is a delay in septum formation in some deletion strains of $\Delta sepA$, while $\Delta modB$ can form a septa similar to wildtype.

ModB::GFP localizes at the hyphal tips and initially at the septa

To further explore the role of ModB we first generated ModB::GFP strain. After 12 hours of growth in YGV media, the GFP localization was displayed at the septa and at the crescent of the hyphal tips (Fig: 2a). We also noted that the localization is constant at the hyphal tips whereas the localization at the septa disappears after 14 hours of growth (Fig: 2d&e). During the time course of 12-16 hours we noted the changes in localization from the septa and at the crescent of the hyphal tips to localization only at the hyphal tips (Fig: 2a-e). Similar to the $\Delta modB$'s phenotype of dichotomous branching, the localization of GFP was not seen in all hyphal tips and septa but only in ~40% of the hyphae that were wider compared to the wildtype.

SepA::GFP has shown the similar pattern of localizing at the septa and at the hyphal tips (Overview Fig 9) (Virag et al. 2007). Unlike ModB::GFP the SepA::GFP localized at all hyphal tips and septa. This shows that ModB may function along with or may have similar functions as SepA.

The $\Delta sepA \Delta modB$ double mutant shares the same phenotype as $\Delta sepA$: of restricted growth, form dichotomous branching and unable to form septa.

To further explore the functions of SepA and ModB, a double mutant was generated by crossing $\Delta modB$ and $\Delta sepA$. The PCR verification showed no presence of $\Delta modB$ (Figure 3A). The mutants were then analyzed microscopically and stained with Calcofluor while growing them in YGVUU at 42°C. The double mutant strains showed the same phenotype as $\Delta sepA$ where they formed dichotomous branching and couldn't form a septin ring. The $\Delta modB$ displayed the same phenotype of dichotomous branching but could form a septa in 42°C. The colonies were also grown in MAGUU plates in 42°C and the colonies showed the same restricted phenotype as $\Delta sepA$ (Figure 3B). As previously described the phenotype of double mutants as $\Delta sepA \Delta modB$ exhibit the same phenotype as $\Delta sepA$ where they showed the same dichotomous branching and temperature sensitivity in 42°C. This suggests that ModB and SepA may perform different functions despite having some similar characteristics. The absence of SepA and ModB doesn't seem to affect the polarity establishment or maintenance but it does affect the septum formation.

The double mutant of $\Delta mesA \Delta modB$ show the phenotype of both parents of restrictive growth and dichotomous branching

To further explore the role ModB in polarity establishment we generated a double mutant by crossing and PCR verification was used to show absence of ModB (Fig 4A). The crossed strains were then compared to both parents $\Delta mesA$ and $\Delta modB$ by growing in 42°C on MAGUU plates to test their temperature sensitivity. The plate analysis shows the double mutants had restricted growth in 42°C (Fig 4B). Further microscopic analysis and staining with Calcofluor showed $\Delta mesA$ to have a restrictive growth phenotype but $\Delta modB \Delta mesA$

showed an increase in dichotomous branching of the hyphae and restricted growth (Figure 4C). Although, previous research showed both MesA and SepA are required for the stabilization and establishment of polarity axes of the hyphae as the double mutant $\Delta sepA \Delta mesA$ is unable form a stable polarity axis and hyphae. The double mutant of $\Delta modB \Delta mesA$ form a stable polar axis even when the growth is restricted. This further shows that ModB and SepA may have different functions.

The double mutant of $\Delta cdc42 \Delta modB$ were inviable

Cdc42 plays a central role in most organisms to establish polarity. To further explore role of ModB in polarity establishment we attempted to generate a double mutant of $\Delta cdc42 \Delta modB$ but this cross yielded only wildtype phenotype on minimal media and even in rich media the segregants were either wildtype or either of the parents. The segregants were verified through PCR and noted that nearly all of the segregants had been wildtype as they contained both ModB and Cdc42. Only a few were a deletion of either $\Delta modB$ or $\Delta cdc42$ parents when the segregants were tried to be revived on MAG and MAGUU plates but most were wildtypes. This shows that either ModB or Cdc42 are required for polarity establishment. This also shows that they both may be required to form cleistothecia (sexual spore) therefore unable to form the double mutants.

The double mutant of $\Delta racA \Delta modB$ phenotype show hyper- and dichotomous branching.

In *A. nidulans* Cdc42 and RacA have overlapping functions as in the absence of Cdc42 or RacA the hyphae can still establish and maintain polarity, but during the absences of both it is lethal. To explore the role of ModB we generated double mutants of $\Delta racA \Delta modB$ and the segregants were verified through PCR. The verified double mutants were then analyzed

through BF microscopy. The double mutants displayed the phenotype of hyper branching and dichotomous branching. The *ΔracA* mutant displays reduced growth and the hyphae remain similar to wildtype but *ΔmodB* showed the dichotomous branching phenotype. This shows the presence of RacA and ModB are required for proper formation of hyphae as the absence of both leads to hyper-branching and dichotomous branching in some hyphae (Figure 5) (Virag et al.2007). This shows that ModB may share some function with RacA.

Discussion

The Rho related GTPases are crucial in the polarity establishment of animal and fungal cells. Although this process is not fully understood in filamentous fungi yet the yeast molecular mechanisms have acted as a model system. However, in yeast cells a functional Cdc42 is required to establish polarity. In filamentous fungi such as, *A. nidulans*, either RacA or Cdc42 is adequate to establish or maintain polarity in cells, even though Cdc42 has a major role in hyphal morphogenesis. Cdc42 also interacts with several effectors including formin, SepA, a component of the Polarisome that plays an important role in establishing and maintaining polarity. Another fungal protein that is crucial to establish polarity is MesA as it recruits and stabilizes SepA to polarized sites. The initial analysis of searching for homologues for polarisome components lead to the gene ModB that showed some genetic similarity in the coiled coil domain of SepA (Harris unpublished). In an effort to understand the role and function of ModB, we deleted *ΔmodB* and constructed ModB::GFP. The comparison between *ΔmodB* and *ΔsepA* displayed a similar phenotype of dichotomous branching. The phenotypes displayed also differed as the phenotype of dichotomous branching in *ΔmodB* did not occur in all hyphal tips but only in ~40% of the hyphae. This is different from the *ΔsepA* phenotype as the dichotomous branching occurs

in all hyphal tips. Other difference that was displayed was that *ΔmodB* could form a septa similar to wildtype whereas, *ΔsepA* could not form a septa. The comparison between ModB::GFP and SepA::GFP showed similar localization pattern at the septa and at the crescent of hyphal tip. However, there were some differences in ModB::GFP localization as the initial localization was at the hyphal tips and at the septa but overtime the localization remained only at the crescent of the hyphal tip. The localization of SepA::GFP was present in 100% of hyphal tips but the localization in ModB::GFP was only present in ~40% hyphal tips (Sharpless et al. 2002). This indicated that ModB and SepA may share similar roles. Further analysis was done to understand the role the ModB by creating double mutants of *ΔmodB: ΔsepA*, *ΔmesA*, *Δcdc42* and *ΔracA*. The double mutants of *ΔsepA ΔmodB* showed the same phenotype of *ΔsepA* mutant where the mutants had restricted growth and in temperature sensitive conditions in 42°C, could not form a septa and branched dichotomously. These phenotypes indicated that SepA and ModB may function in different pathways. Further analysis of the double mutant of *ΔmesA ΔmodB* showed restricted growth of colonies and hyphae in 42°C and also showed the phenotype of dichotomous branching but the polarity was established and maintained. This was different from the double mutant of *ΔsepAΔmesA* as they were unable to establish a proper polarity axis (Pearson et al. 2004). So far the results indicated that ModB functions in a different pathway from SepA.

To further explore the role of ModB in polarity establishment the generation of double mutant of *Δcdc42ΔmodB* was attempted and noted to be inviable as most of the outcrosses were wildtype. This leads to show that ModB could have a more important role in establishment of polarity and may play a role in both actin and microtubule organization

of the establishment within hyphae. Previous research shows that in the absence of Cdc42 the function of microtubule to establish and maintain a polarity axis becomes important. It was observed that when $\Delta cdc42$ mutant was exposed to microtubule depolymerizing agent benomyl, there was a delay in polarity establishment. Also the spores fail to polarize in $\Delta sepA$ mutant as well as in the double mutant of $\Delta cdc42\Delta sepA$ when exposed benomyl (Virag et al. 2007). To further understand the role ModB in polarity establishment the double mutant of $\Delta racA\Delta modB$ was generated and showed similar phenotype of dichotomous branching present only in $\Delta modB$. The $\Delta racA$ exhibited delay in hyphal growth by formed wildtype hyphae. The $\Delta modB\Delta racA$ also displayed hyphae that were hyper branching as they form significantly wider hyphae different from both parents. This shows that RacA and ModB may have a related role in polarity establishment (Virag et al. 2007).

Future Directions

Further studies can be done to understand ModB's role in microtubule organization by exposing $\Delta modB$ and the double mutants of $\Delta modB$: $\Delta sepA$, $\Delta mesA$, and $\Delta racA$ to benomyl. This could show what role ModB plays in microtubule organization and how this affects the polarity establishment and maintenance. More analysis could be done to explore the role of ModB in the conidiophore and sexual development to understand what causes the inviability of the double mutant $\Delta cdc42\Delta modB$. Further analysis can also be done to the role of ModB in endocytosis and exocytosis by crossing $\Delta modB$ to SynA::GFP (v-snare that binds to SPK and plays a role in exocytosis) and SlaB::GFP (component that couples with the endocytic vesicle formation to actin polymerization). These crosses can give us

more insight in the role ModB in endocytosis and exocytosis of polarized growth of the *A. nidulans* hyphae (Penalva et al. 2012).

Tables and Figures

Table 1

Name	Strain name	Relevant genotype	Source
wildtype	A4		FGSC
wildtype	TNO2A3	<i>pyrG89; argB2 ; pyroA 4 nkuA ::argB</i>	FGSC
modB	T15	<i>pyrG89 ΔmodB::pyr-4 wA3 pyroA4</i>	Lab stock
ModB::GFP	T17	<i>pyrG89 modB::gfp::pyr-4 wA3 pyroA4</i>	Lab stock
cdc42	AAV 128	<i>pyrG89; argB2; pyroA4ΔmodA::pyroA Δnku::argB</i>	Lab stock
sepA	ASH 630	<i>pyrG89 wA3 sepA1</i>	Lab stock
mesA	DD8 A2	<i>mesA, pyrG89;paba</i>	Lab stock
racA	AAV 129	<i>pyrG89; argB2 ΔracA::pyroA;pyroA4 Δnku::argB</i>	Lab stock

Figure A: The gene replacement of *nkuA* was replaced with *argB* and was fused with PCR fusion and transformed into the genome of *A. nidulans*. The same phenomenon was used for gene replacement of *modB* with *pyrG* (amplified with pFNO3) and use fusion PCR to make the transforming fragment and then transformed into the genome of *A. nidulans* (Nayak et al. 2006).

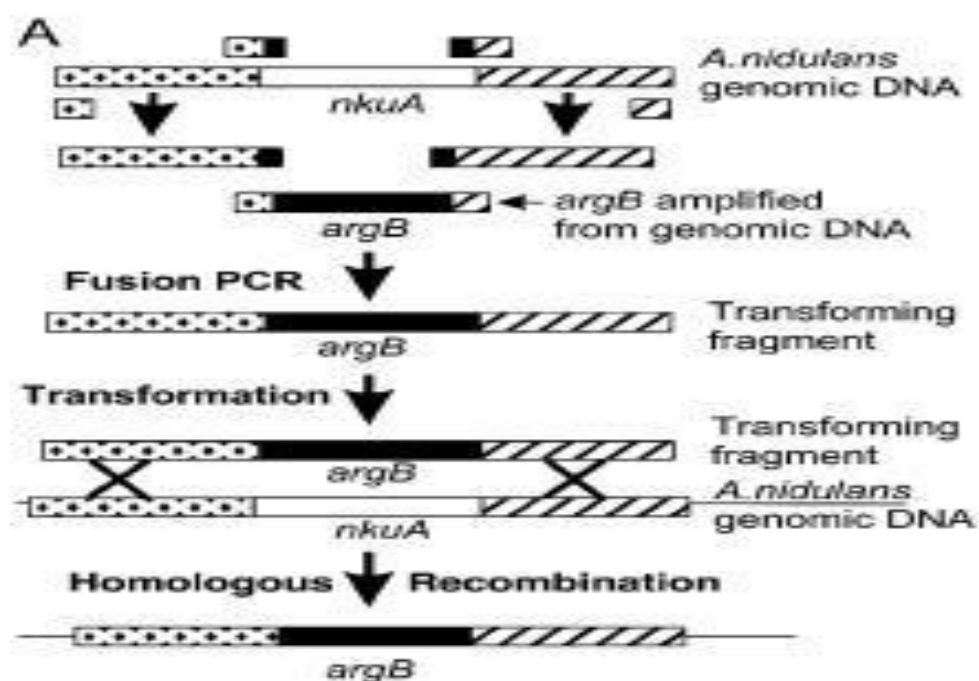


Figure: 1 a) The phenotype of $\Delta modB$ shows dichotomous branching indicated by red arrows, b) The phenotype of wildtype strain A4 shows normal branching of the hyphal tip. C) The phenotype of $\Delta sepA$ shows dichotomous branching indicated by red arrows. The $\Delta modB$ and $\Delta sepA$ also displays the frequency of the phenotype of dichotomous branching as the phenotype is more prevalent in $\Delta sepA$ than in $\Delta modB$.

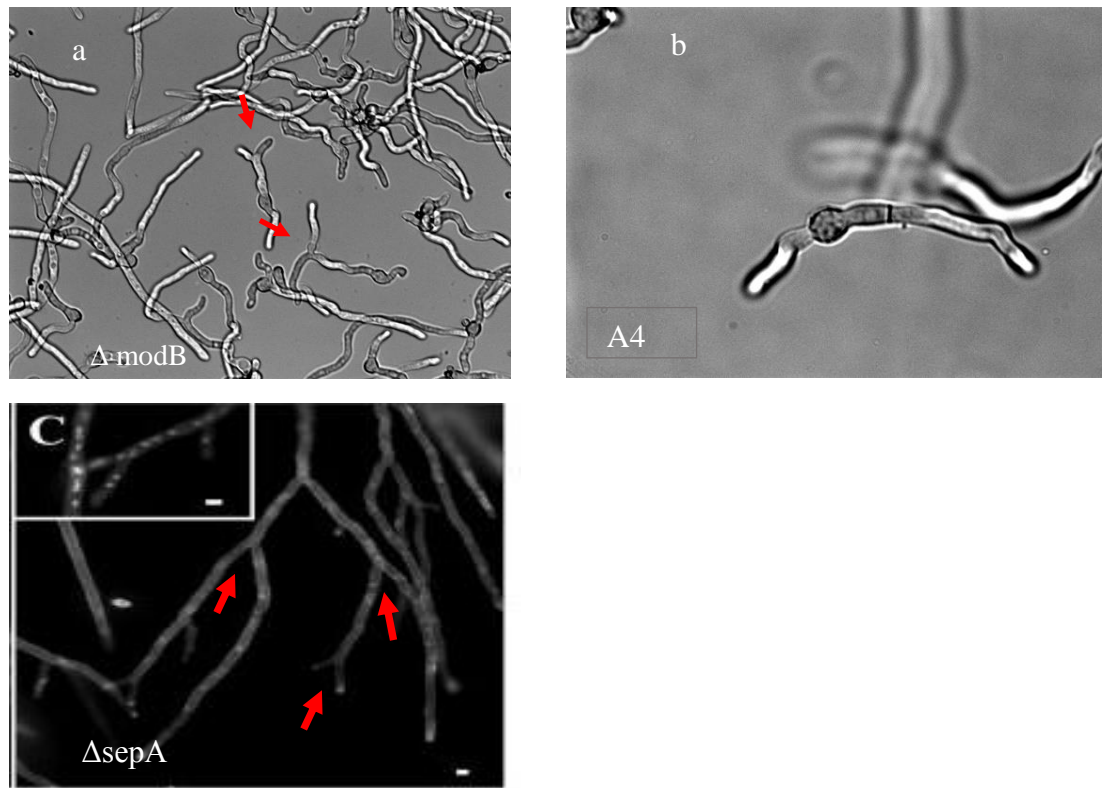
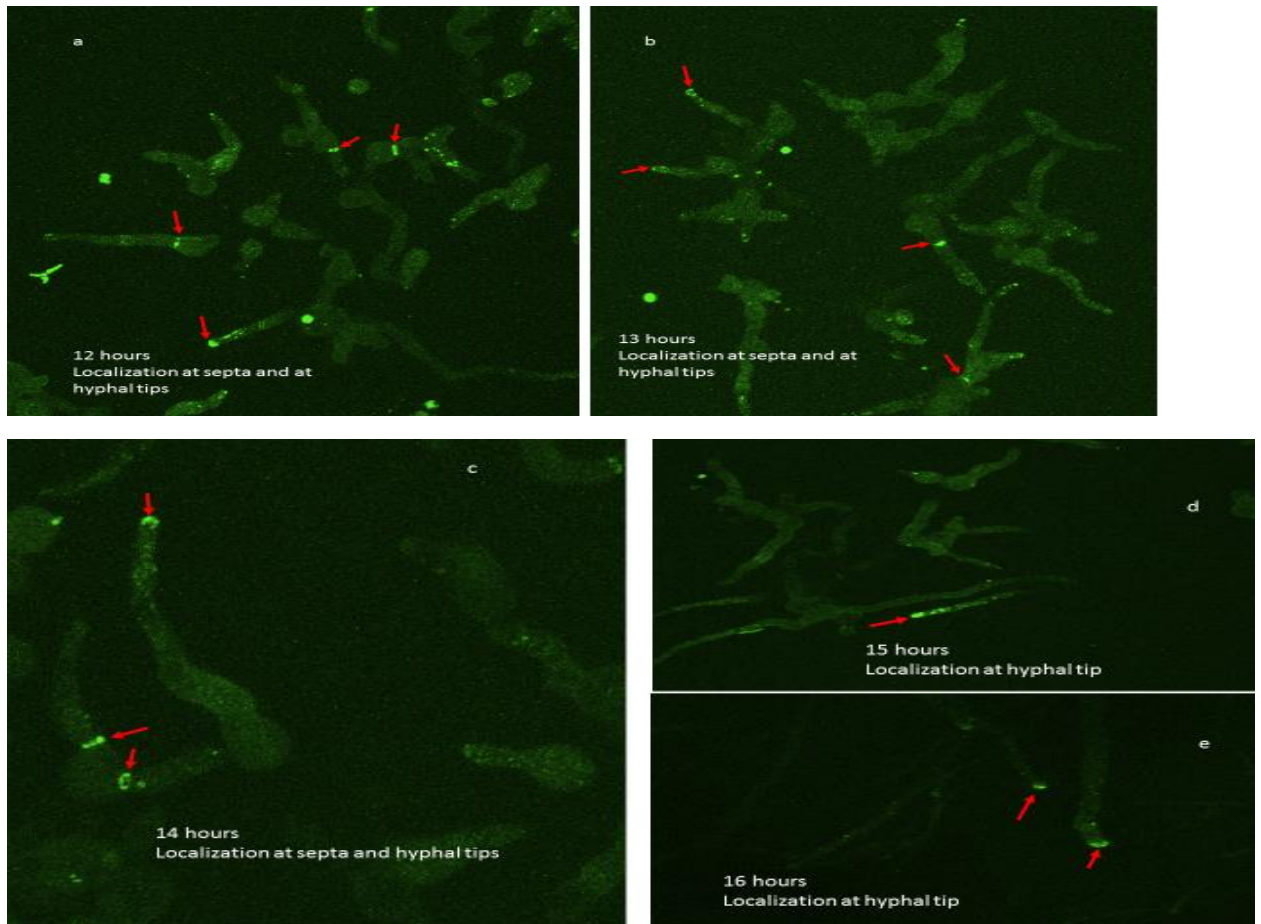


Figure 2 (a-e): ModB::GFP localization analyzed in a time course from 12 hours to 16 hours in YGV media at 28°C. The red arrows show the GFP localization at the septa and the hyphal tips.



Overview Figure 9: SepA::GFP localization in *A. nidulans* is at the septa and at the hyphal tips (Sharpless and Harris.2002)

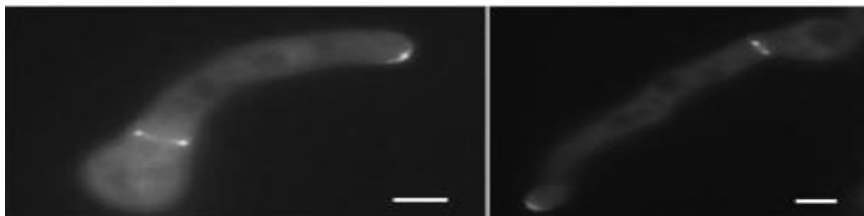


Figure 3A: The PCR verification was performed to check the presence of ModB in the segregants from the crosses of $\Delta sepA$ and $\Delta modB$. Then a gel electrophoresis was done to visualize the results of PCR. The gel image shows the TN (wildtype) and the double mutants of $\Delta sepA\Delta modB$ (10, R, W and Y). The gel image indicates the presence of ModB in TN but not in the other strains.

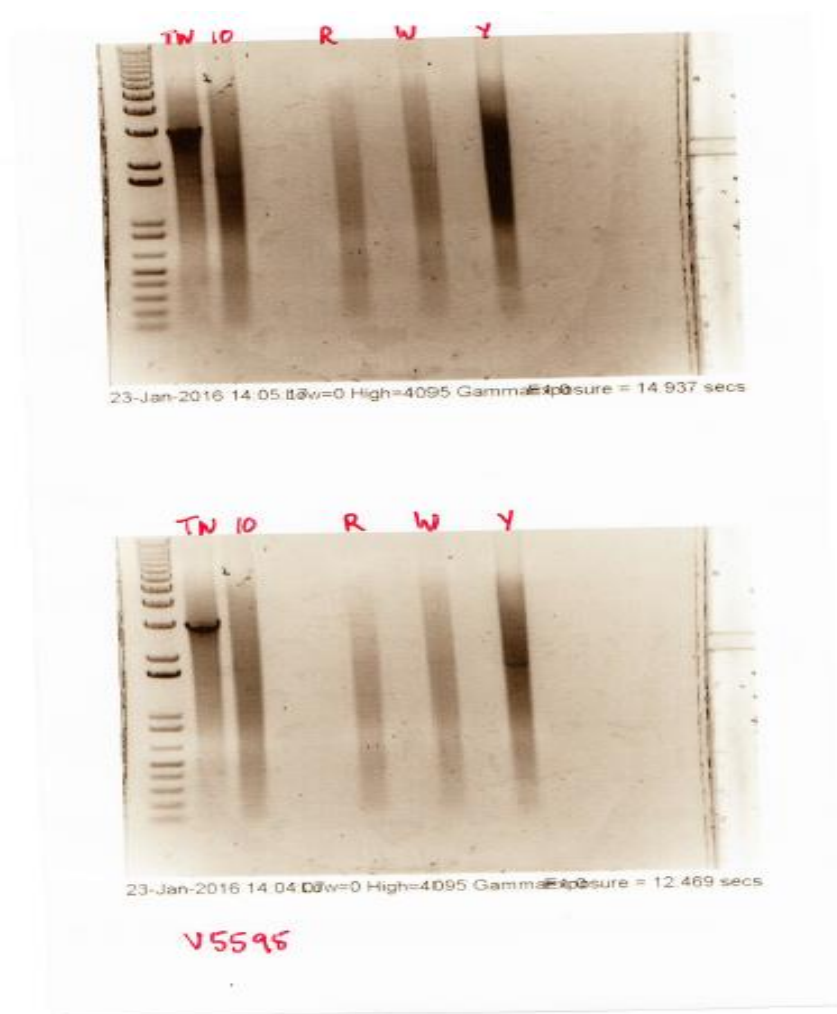


Figure 3B: The phenotype of $\Delta modB\Delta sepA$ double mutants shows the same phenotype as $\Delta sepA$. The phenotype of $\Delta modB$ shows dichotomous branching indicated by red arrow. The phenotype of $\Delta sepA$ show a restricted growth and dichotomous branching phenotype indicated by the red arrow. The double mutant of $\Delta modB\Delta sepA$ shows the dichotomous branching phenotype and restricted growth similar to $\Delta sepA$. The phenotype of TN (wildtype) shows normal branching. All strains were grown in YGVUU for 11 hours in 42°C a) $\Delta modB$ b) $\Delta sepA$ c) $\Delta modB\Delta sepA$ d) TN (wildtype).

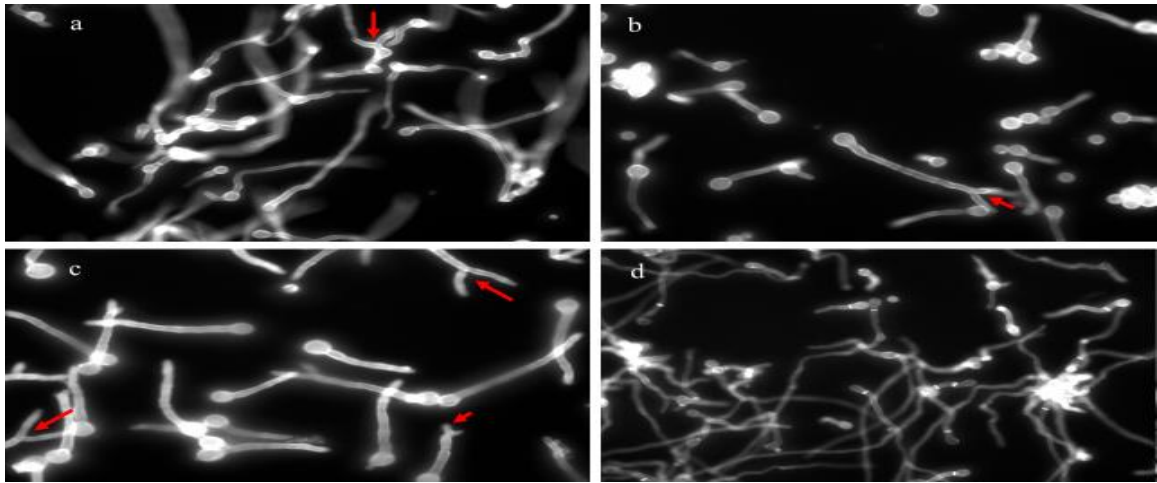


Figure 3C: The MAGUU plates shows the phenotypic growth of all strains in 42°C. The growth of $\Delta modB$ is restricted compared to TN. The growth of $\Delta sepA$ shows restricted growth and the same colony phenotype is found in the double mutants of $\Delta modB\Delta sepA$. Row1 shows $\Delta modB$ and $\Delta sepA$. Row2 shows all the double mutants $\Delta modB\Delta sepA$ strains and row 3 shows TN (wildtype).



Figure 4A: The PCR verification was performed to check the presence of ModB on the segregants from the crosses of *ΔmesA* and *ΔmodB*. Then a gel electrophoresis was done to visualize the results of PCR. The gel image shows the TN labeled as E and C (wildtype) and the double mutants of *ΔmesAΔmodB* (1, 2, 3, 6, 7 and 8). The gel image indicates the presence of ModB in E and C but not in the other strains.

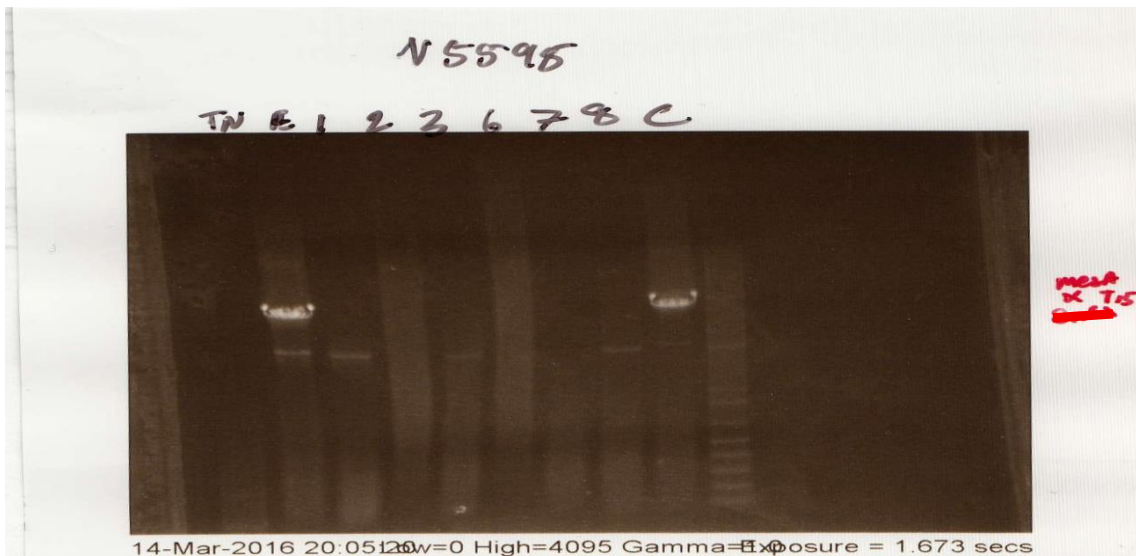


Figure 4B: The MAGUU plates shows the phenotypic growth of all strains in 42°C. The growths of *ΔmodB* and *ΔmesA* is restricted compared to TN. The colony phenotype found in the double mutant of *ΔmodBΔmesA* shows a more restricted growth compared to *ΔmodB* and *ΔmesA*. Row1 shows *ΔmodB*, *ΔmodBΔsepA*, and *ΔmesA* strains. Row 2 shows TN (wildtype).



Figure 4C: The phenotype of $\Delta modB\Delta mesA$ double mutants displays the same phenotype as $\Delta modB$ and $\Delta mesA$. The phenotype of $\Delta modB$ shows dichotomous branching indicated by red arrow. The phenotype of $\Delta mesA$ show a restricted growth of the hyphae. The double mutant of $\Delta modB\Delta mesA$ shows the dichotomous branching phenotype and restricted growth similar to both $\Delta modB$ and $\Delta mesA$. The phenotype of TN (wildtype) shows normal branching. All strains were grown in YGVUU for 12 hours in 42°C a) $\Delta modB$ b) $\Delta mesA$ c) $\Delta modB\Delta mesA$ d) TN (wildtype).

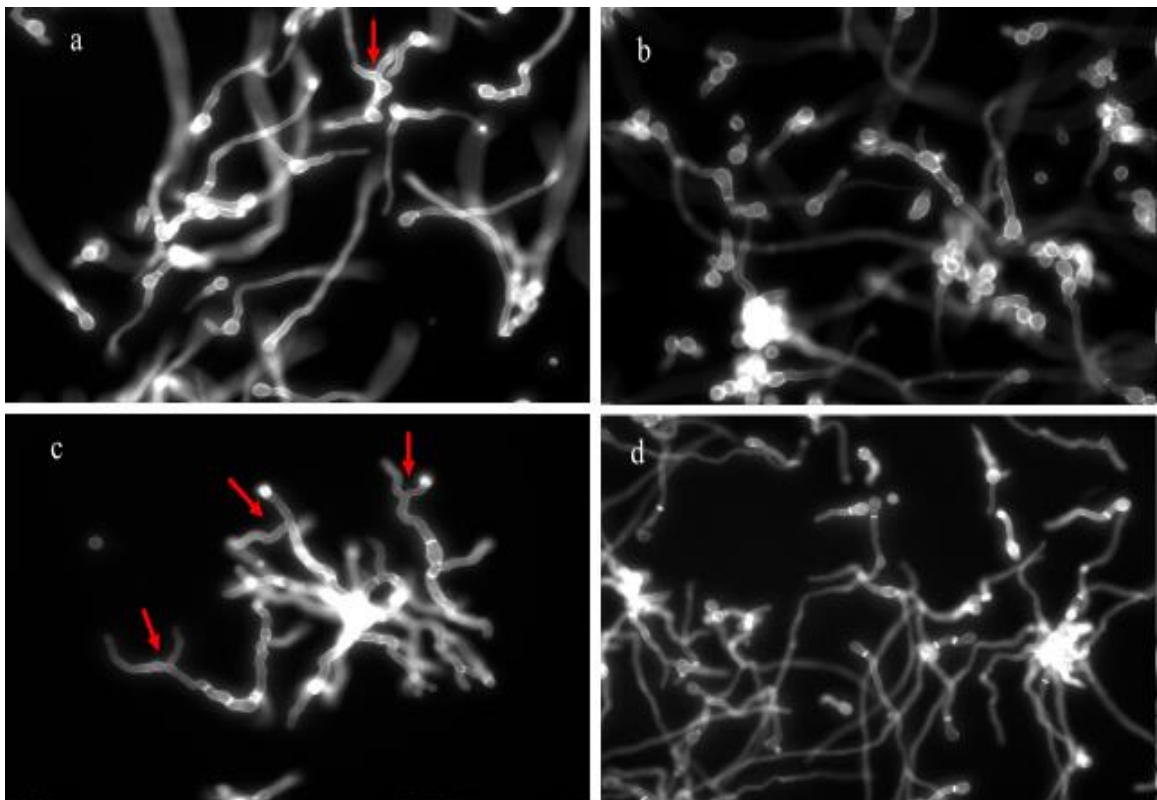
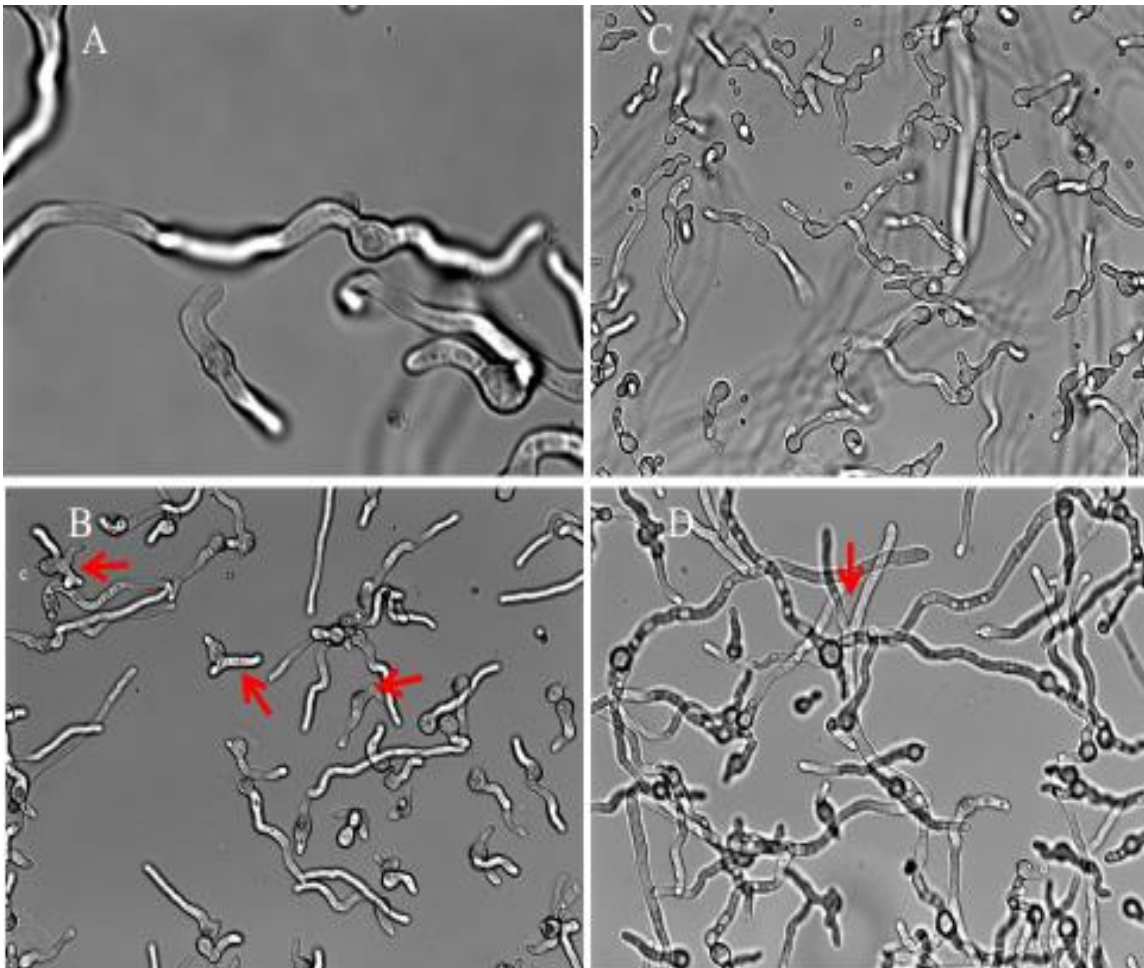


Figure 5: The phenotype of $\Delta modB \Delta racA$ double mutant shows hyper- and dichotomous branching as indicated by the red arrows. The $\Delta modB$ mutant shows dichotomous branching indicated by the red arrows. The $\Delta racA$ mutant displays slower growth but hyphae look similar to A4 (wildtype). All strains were grown in YGV for 12 hours at 28°C.
A) A4 (wildtype) B) $\Delta modB$, C) $\Delta racA$ D) $\Delta modB \Delta racA$.



Chapter 2

Introduction

Reproduction in *Aspergillus nidulans* produces both conidia (asexual spores) and ascospores (sexual spores) that are vital for survival and dispersal in any environment. Spore dispersal and germination is essential for pathogenicity and growth in the environment. Dormant conidia can be viable for years until appropriate conditions are detected for germination, including water, salt, carbon and nitrogen sources. Germination can be described in two morphological phases: isotropic growth (swelling of the spore) and the germ tube emergence. Germination also involves the detection of external nutrients to initiate the primary metabolism to energy yielding reactions to not only initiate the cell cycle but also the biosynthesis of cellular components and differentiation of growth morphology (Assis, 2015).

A.nidulans can germinate and sustain growth on a diverse range of simple and complex carbon sources, including saccharides, alcohols, proteins and lipids. This metabolic flexibility has enabled *A.nidulans* to adjust metabolism and nutrient uptake to fit its environment (Assis, 2015).

The primary trigger for germination in *A.nidulans* appears to be glucose. Glucose is sensed both intracellularly and extracellularly in addition to glucose transport which occurs through facilitated diffusion (Fernanda dos Reis. 2013).

Intracellularly, the presence of glucose is sensed by a G protein-coupled receptor (GPCR), since this $G\alpha$ protein (GanB) is constitutively active (GTP bound) so germination can be activated even in the absence of a carbon source. A downstream effector of GanB is CyaA, an adenylate cyclase, is required for cyclic AMP (cAMP) production. cAMP acts as a secondary messenger that binds to regulatory subunit of protein kinase A (PkaA) and

activates the catalytic subunit. In *A.nidulans* both CyaA and PkaA are required for germination (Fernanda dos Reis. 2013). An additional intracellular signaling pathway that controls vegetative growth or switch to asexual development is through another G-protein/cAMP/PkaA signaling pathway. This involves FlbA, a RGS (regulator of G-protein signaling) protein that negatively regulates another G α subunit, FadA, similar to GanB. When FadA is GTP bound it is active and leads to the activation of cAMP/PkaA pathway which stimulates vegetative growth in formation of vegetative hyphae. FlbA suppress the function of FadA by converting FadA into an inactive state by FadA being bound to GDP. The Δ flbA leads to constitutively active state of FadA and PkaA (Krijgsheld et al. 2013). Both of these cAMP/PkaA signaling pathway lead to vegetative growth.

When glucose is available, the synthesis of enzymes specific for the use of alternative less preferred carbon sources such as xylose and carboxymethylcellulose sodium (CMC), is repressed by a mechanism termed as carbon catabolite repression (CCR) (Lockington et al. 2001). CreA is a transcriptional repressor in *A.nidulans* that is central to CCR. This process is beneficial for two major reasons: firstly, the most favorable carbon source is used and secondly no energy is wasted in synthesizing the other catabolic systems (Orejas, 1999). Extracellularly glucose is sensed by glucose transporters that have yet to be fully defined in *A.nidulans*. Budding yeast has been used as a model system for the study of hexose sensing and transport. In *Saccharomyces cerevisiae* extracellular glucose is sensed by two specific transmembrane proteins that act as sensors, Rgt2 and Snf3 and also show similarity to hexose transporters (HXT proteins). These sensors however are unable to transport glucose. In the presence of extracellular glucose the transcriptional repressor complex Rgt1, Std1 and Mth1 are bound to the promoter regions of HXT genes and inhibiting

transcription. In the absence of extracellular glucose Std1 and Mth1 are phosphorylated by Yck1 and Yck2 kinases and targeted to the SCF Grr1 E2/E3 complex for degradation. This process then results in PkaA hyperphosphorylating Rgt1 and is released from the promoter region of HXT genes. Hxt proteins are part of sugar porter family within the Major Facilitator Superfamily (MFS) group. In *S.cerevisiae* twenty proteins have been classified as hexose transporters and these classifications are based on their different substrate affinities or specificities such as low-affinity, moderate affinity and high affinity. Differences in individual HXT gene expression is based on not just the availability of glucose but also the osmotic pressure, starvation, and the physiological state of the cell. Even though significant progress has been made in how *S.cerevisiae* senses glucose not much has been known about filamentous fungi. In *A.nidulans* hxtA is characterized as high affinity glucose transporter and In *A. niger* mstE genes is characterized as low affinity glucose transporter. Recent research revealed four homologues HxtB- HxtE for hexose transporter and were characterized based on their ability to transport glucose. All four of these genes were classified as glucose transporters (Fernanda dos Reis, 2013). The mechanism for the transport of glucose still needs to be defined therefore HxtB::GFP strain. The construction of the HxtB Strain can be found in Fernanda dos Reis et al. 2013.

CCR has become fairly important as most fungi in nature and in the bioprocess industry experience limitation or even starvation which leads to morphological and/or physiological changes. This can be detrimental in some processes where it could lead to decreased production of a product or limits growth. Many studies have indicated that carbon starvation has morphological changes which include fragmentation due to cell wall degradation or physiological changes such as increased expression of hydrolytic enzymes,

increased vacuolation. Most of these studies show the increase in cellular degradation activity. However we don't have a complete picture of how the starvation effects filamentous fungi. This is mainly due to the fact that most studies have measured the population-average behavior which does not capture the spatial and temporal changes in individual mycelium (Bhargava et al. 2005).

To capture the morphological and physiological changes submerged cultures were used and strains of A4, $\Delta pkaA$, $\Delta schA$ (a protein kinase involved in cAMP- dependent signaling during germination and has overlapping functions with PkaA), $\Delta flbA$ (negative regulator of G-protein signaling promoting conidiophore development) and HxtB::GFP were exposed to brief periods of glucose rich conditions during germination and then switched to glucose limiting conditions with different carbon sources (xylose, CMC, 1% glucose, 0.1% glucose) as well as with no carbon source (NCS). The morphology of these shift was seen within an hour in most old and newer hyphae as they would switch growth form wider to narrow hyphae in all strains. Some strains like $\Delta pkaA$, $\Delta schA$ and $\Delta flbA$ showed a lag time (where the switch from wider to narrow hyphae was slower for about three hours) in non-glucose conditions and in $\Delta flbA$ strain there was slow or no growth after the switch. In HxtB::GFP the localization during these shifts was seen primarily in the nuclear membrane and overtime localization was reduced. This derepression studies would help us predict how the morphology and physiology of a single hyphae would change from carbon rich to carbon limiting or starvation conditions.

Material and Methods

Strains, media and growth conditions

The strain used in study HxtB-GFP strain was acquired from Goldman lab (Fernanda dos Reis. 2013). The following strains were made in Harris lab: *ΔpkaA* (CEA 198), *ΔschA* (CEA 182) and *ΔflbA* (RJH 046). Strains used in this study are also listed in Table 2.

The glucose rich media and supplements was prepared as previously described in Harris et al.1994. The minimal media was prepared as previously described in Kafer.1997. All medias used in this study were liquid media (no agar). YGV (0.5 % yeast extract, 1% dextrose and vitamins), MNV (minimal media with 1% glucose and vitamins), MNV (0.1%) (minimal media with 0.1% glucose and vitamins) CMCV (1% Carboxymethylcellulose sodium salt in minimal media and vitamins), NCS (no carbon source, minimal media with only nitrate salts) and XV (1% xylose in minimal media and vitamins). All the strains were grown in 28°C unless indicated otherwise. For septation and hyphal growth studies showed conidia were grown at 28°C for 12 hours on coverslips. During shift experiments after 12 hours of growth in YGV media the coverslips were then washed with sterilized ddH₂O in stain jars and then placed into the shifting media (NCS, CMCV, MNV and MNV (0.1%)). The coverslips were then grown in shifted media for 4 to 6 hours and analyzed each hour.

Microscopy methods and staining

The microscopy was done by using the Metamorph software. The microscopic methods used in this study were Bright Field, Calcofluor stain (a non-specific fluorochrome that binds with cellulose and chitin which is contained in the cell walls of fungi), Wheat Germ Agglutinin (an agglutinin protein that binds to N-acetyl-D- glucosamine found in chitin of the cell membrane and acts as a marker for growth before the coverslips were switched

from YGV to MN to different carbon sources) and Hoechst stain (blue fluorescent stain specific for DNA such as nuclei of eukaryotic cell).

Bright Field (BF)

The spores of strains were collected from fresh plates. 15mL and/or 50 mL YGV was added into falcon tubes depending on the number of coverslips being used. Sterile glass coverslips (22X22mm) were flamed to remove lint and laid on the bottom of a clean Petri dish. For small Petri dish (60 cm) use 10mL of media and 10 μ L of spores were used. For large Petri dish (100 cm) 20mL of media and 20 μ L of spores were used. Media and spores were mixed in the Falcon tube then poured into the Petri dish with coverslips. Gentle tapping was used to eliminate air bubbles between the coverslips and the bottom of the Petri dishes, which were then put in the incubator 28°C or 42°C (when ts strains were used) for 12- 14 hours.

Calcofluor

Samples were set up as it was done in BF. After the 12-14 hour incubation time the coverslips were fixed with ethanol for 2 min. They were then treated with Calcofluor (40mL of water with 17 μ L Calcofluor (10mg/mL) and mixed well) for 5 min. The final wash was with sterile water. Then mount solution was added onto the slide and the stained coverslip was added to the slide and finally analyzed on the microscope.

Wheat Germ Agglutinin (WGA) Stain

Sample were set up as it was done in BF. After the 12-14 hour incubation time the coverslips stained in YGV media containing WGA for 20 min (20 μ L of wheat germ agglutinin in 20mL of YGV media). Then washed with fresh YGV media without wheat

germ agglutinin twice and then with sterile water in staining jars. The samples were then switched to fresh minimal media and incubated and analyzed after every hour.

Hoechst/Calcofluor stain and fix

HxtB::GFP was set up as it was done in BF. After the 12-14 hour incubation time the coverslips were fixed in fix solutions (5mL of 1M pipes pH 6.7, 10mL of 0.25 EGTA pH7.0, 5mL of DMSO and 10mL formaldehyde 10%) for 5 min and then into Hoechst/Calcofluor stain (1 μ L Hoechst to 9 μ L water in a 0.5 μ L centrifuge tube. In a 50mL falcon add 40mL water, 10 μ L concofluor and 4 μ L Hoest with water) for 20 min. After staining the coverslips were washed with sterile water. Mount solution was added onto the slide before the stained coverslip was added.

Strains in microscopy

The analysis with Harris lab strains was done using BF, Calcofluor staining and wheat germ agglutinin. The analysis of HxtB::GFP was done using BF, Hoechst/concofluor stain. All strains were first grown in YGV and then switched to MNV (1% glucose), MNV (0.1% glucose), CMCV, NCS and XV. Confocal microscope at the Microscopy Core Facility was used for GFP images.

Results

For visualizing A4, Δ pkaA, Δ schA and Δ flbA shift from glucose rich to glucose minimal shows immediate change in the hyphal growth except for Δ flbA which forms a pointed hyphal tip. During derepression of hyphae when A4, Δ pkaA, Δ schA and Δ flbA are moved from glucose rich to alternate minimal carbon sources shows Δ pkaA and Δ schA share a lag time whereas Δ flbA shows no change in growth.

During the microscopic studies of A4, *ΔpkaA*, *ΔschA* and *ΔflbA* were used for shift experiments from rich to minimal media. We noted the same change in morphology when A4, *ΔschA*, *ΔpkaA* were switched from YGV (rich) media to MNV (minimal with 1% glucose) and stained with WGA. The hyphae was seen to be narrowing in MNV media within an hour and showed no difference between the strains (Fig1a). The morphology of *ΔflbA* on the other hand did not show any changes and there was no growth after the switch until 24 hours but the morphology of the hyphal tip was changed from a crescent shape to pointed (Fig 1b). There is a change in adaption when A4, *ΔpkaA*, *ΔschA* and *ΔflbA* are switched from YGV to minimal media without glucose (xylose or CMC). A4 shows no difference between glucose and CMC switch the hyphae went from broad hyphae to thinning within an hour as in MNV (Fig 1c). We noted that there is a lag time of about three hours when *ΔpkaA* is switched from YGV to CMC (Fig 1d), however with *ΔschA* there is a shorter lag time of about two hours (Fig 1e). The morphology of *ΔflbA* is quite different as there is not switch to thinner hyphae but the tips of hyphae seemed normal and there was no growth after 24 hours (Fig 1f). This derepression study showed some of the players that might be involved in helping a hyphae transition between different carbon sources. PkaA and SchA seem to have similar function conforming the results from previous research that PkaA and SchA have parallel functions as they both reacted the same way in the switch experiments. FlbA is known to work independently as it negatively regulates that FadA, a Gα-protein that promotes vegetative growth and suppresses asexual and sexual development through PkaA. But the absence of *ΔflbA* appears to affect its ability to respond different nutrient conditions.

HxtB::GFP localization is seen at the hyphal tips and septa when grown in different carbon sources. The derepression of HxtB::GFP from glucose rich media to different carbon sources shows it localizes at the septa, the vacuolar membrane and in xylose at the hyphal tips.

HxtB::GFP has been characterized as a high affinity glucose transporter as there is no GFP expression in high glucose environments as seen in YGV (Fernanda dos Reis. 2013) (Fig 2). The localization of GFP is seen in MNV (1% and 0.1% glucose), CMCV, NCS and XV the expression was noted at the septum and in vacuoles along the hyphae in all media (Fig 2).

When HxtB::GFP was grown in YGV and switched to MNV (1% and 0.1% glucose), CMCV, NCS and XV showed no lag time and the GFP expression was seen from the first hour of the switch. We also noted that the HxtB::GFP localization after the switch experiments was in vacuoles which we later indicated to be the nuclear membrane by the Hoechst/Calcofluor stain. The intensity of GFP expression also differed in different media as it was the localization was more visible in NCS, Xylose, MNV (0.1% glucose) and CMC. But the localization was barely visible in MNV (1% glucose) (Fig 2a).

Hoest/Concoflour stain was performed to determine the vacuoles as nuclei. We noted that most of the nuclei stained by Hoest/Concoflour were in same position as the vacuoles seen expressing GFP and therefore showing that HxtB::GFP is expressed in the nuclei (Fig 3). The localization was mainly seen in the membrane of the nucleus as the localization was seen as rings formed along the hyphae (Fig 2b).

Discussion

The study of morphology and physiology of hyphae in different nutrient stresses is important to study as many filamentous fungi play important roles in environment and in bio industries for producing important compounds. One of the ways to characterize the molecular mechanics of how a hyphae reacts in different nutrient environments is by either deletion of important genes or by tagging these genes to GFP. The deletion strains used in this study were $\Delta pkaA$, $\Delta schA$ and $\Delta flbA$ have shown that they play important roles when the environment changes from glucose rich conditions to minimal conditions and from glucose rich conditions to different carbon or no carbon conditions. This was displayed when $\Delta pkaA$ and $\Delta schA$ exhibited a slight delay in the morphological shift, when these strains were shifted from glucose rich to minimal media with CMC. Whereas, the $\Delta flbA$ strain did not exhibit any changes even after 24 hours. In the presence of glucose the shift from glucose rich to glucose minimal the morphology was similar to wildtype in $\Delta pkaA$ and $\Delta schA$ as there was no lag time. The $\Delta flbA$ strain exhibited a unique hyphal morphology when glucose was present as the hyphal tip went from crescent to pointed hyphal tips after 24 hours. The delay in PkaA and SchA could attributed to the fact that the change in glucose rich levels and could delay the activation cAMP and thereby delaying the activation of PkaA and SchA. The FlbA signaling however has been interesting as previous research only notes the FlbA works independently from FluG signaling pathway to controls the hyphal and conidiophore development. In *A. nidulans* the deletion of FlbA has resulted in fluffy-autolytic colony that lacks sexual/asexual sporulation and has also shown to increase secondary metabolites (Yu and Keller. 2005). In *A. fumigatus* deletion of $\Delta flbA$ negatively affects cellular response associated with detoxification of reactive oxygen species and exogenous gliotoxin. In *A. niger*, the deletion of $\Delta flbA$ resulted in spatial changes in

secretion and a more complex secretome as the mutant has thinner cell wall components allowing it to release proteins efficiently (Shin et al. 2013, Lee et al. 1995, Krijghsheld et al 2013).

The localization of HxtB::GFP shows it is a high affinity glucose transporter as it shows no localization in YGV but when grown in different carbon source media and in no carbon source it shows GFP expression in what looks like vacuoles. The same localization pattern was seen when HxtB::GFP is switched from YGV to (CMC, MNV (0.1%), Xylose and NCS). After Hoechst staining we noted most of the localized pattern of GFP matches with Hoechst staining of the nuclei. This shows that HxtB::GFP primarily localizes in the nuclear membrane. During the shift experiments it was also noted that the initial switch showed a higher expression of GFP compared to the later hours of the switch. Although further analysis of mRNA expression needs to be measured to analyze the full function HxtB::GFP after the switch but judging from the current data it can be said that the expression over time might have decreased.

Future Directions

The future directions for this study would be to expand to other glucose transports and analyze the localization and to understand if different glucose affinity transporters have the same localization. It would also be informative to see if mRNA expression of HxtB during the switch experiments to show conclusively that HxtB expression is reduced overtime after the switch. Crossing HxtB::GFP to *ΔpkaA*, *ΔschA* and *ΔflbA* would not only help visualize the glucose transport with the hyphae but also help in understanding what could cause the delay when the deletion strains are shifted from glucose rich conditions to limiting or no glucose conditions. Other directions would also to be analyze regulator genes

in other pathway such as TOR and MAPK to understand how they affect the morphology and physiology of the hyphae during nutrient stress. Further analysis of the switch experiment could be done to see if *ΔfadA* and double mutant of *ΔflbA ΔfadA*, if viable, would have any effect on physiological and morphological patterns.

Tables and Figures

Table 2

Name	Strain	Relevant genotype	Source
Wildtype	A4		FGSC
pkaA	CEA 198	<i>pyrG89; wA3; argB2; ΔpkaA::pyrG</i>	Lab stock
schA	CEA 182	<i>pyrG89; wA3; argB2; ΔschA::pyrG</i>	Lab stock
flbA	RJH 046	<i>ΔflbA, pyro A4, biA</i>	Lab stock
HxtB::GFP	HxtB	<i>pyroA4 pyrG89; HxtB::GFP::pyrG</i>	Gastavo lab

Figure 1: To visualize the morphological changes when a single hyphae are moved from glucose rich to glucose minimal conditions. We also used gene deletions of know carbon sensing regulators such as: $\Delta pkaA$, $\Delta schA$ and A4 (wildtype) to understand their roles in morphological shifts. We grew all strains in YGV on coverslips for 13 hours in 28°C and these coverslips were switched to MNV after staining the coverslips with WGA (wheat germ agglutinin). We noted that all strains transition from thick to thin hyphae within the first hour.

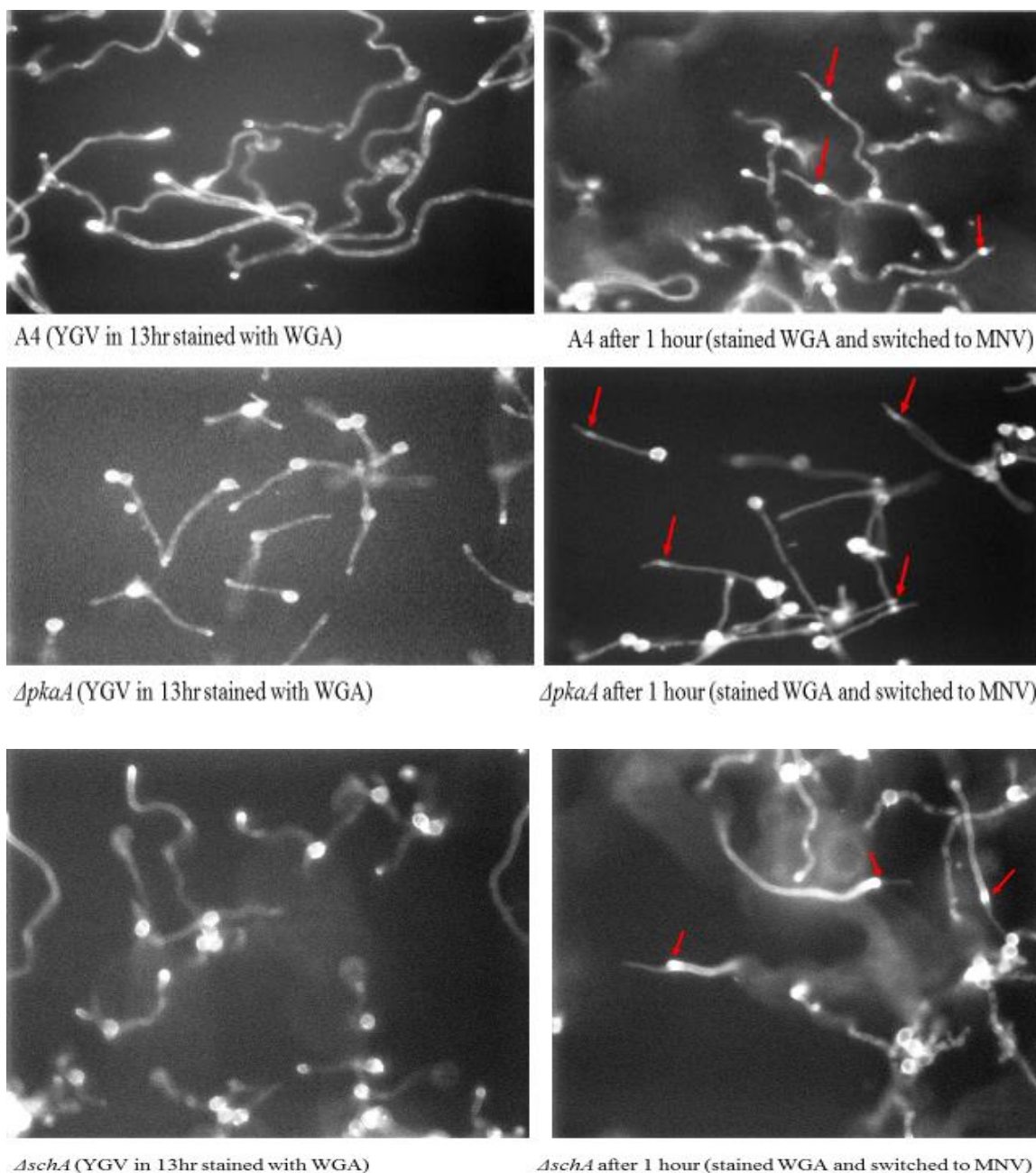
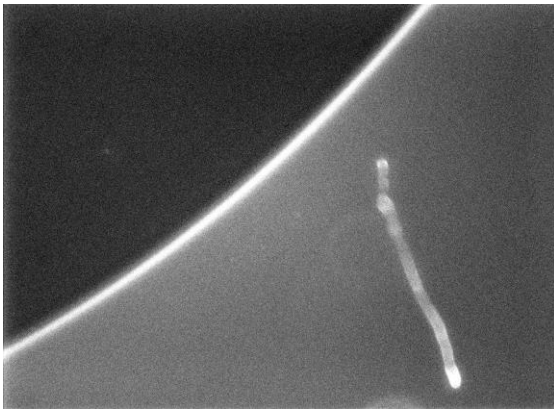
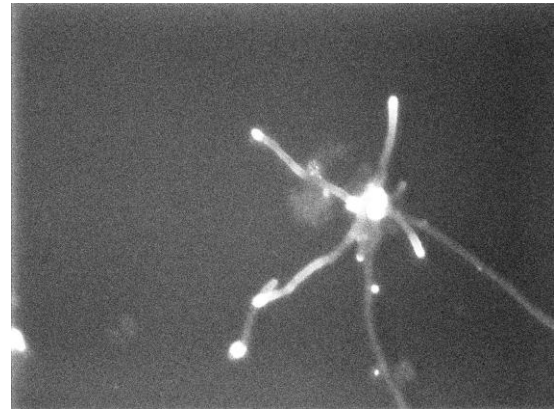


Figure 1b: In the process of visualizing the morphological changes when hyphae are moved from glucose rich to glucose minimal conditions, we also noted $\Delta flbA$ switch did not occur at the same time as wildtype, which was within an hour but $\Delta flbA$ took about 24 hours to change. We grew $\Delta flbA$ in YGV on coverslips for 13 hours in 28°C and these coverslips were switched to MNV after staining the coverslips with WGA (wheat germ agglutinin). The $\Delta flbA$ transition from thick to thin hyphae did not take place however, the hyphal tip shape had switched from a crescent shape to a pointer hyphal tip and this transition took about 24 hours .



$\Delta flbA$ (YGV in 13 hours stained with WGA)



$\Delta flbA$ after 1 hour (stained WGA, and switched to MNV)



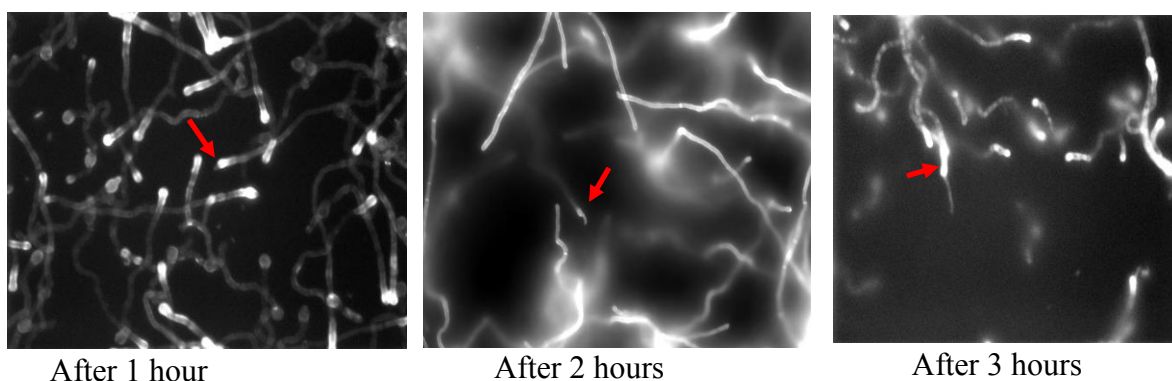
YGV to MNV after 24 hours stained with WGA



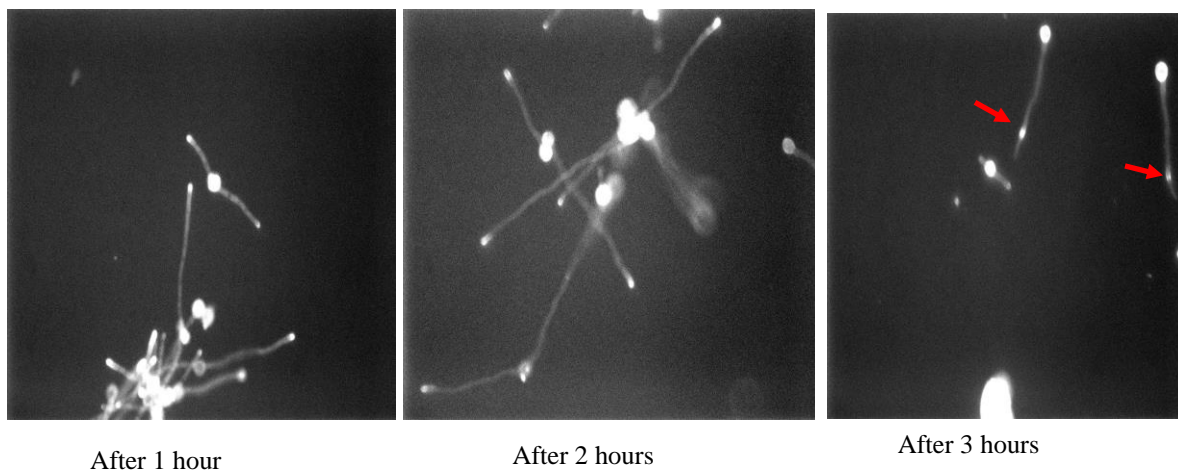
Switched from YGV to MNV after 24 hours

Figure 1c: To visualize morphological changes in carbon derepression in central regulators such as $\Delta pkaA$, $\Delta schA$, and A4 (wildtype) which control carbon signaling respond to change in carbon source from glucose to cellulose. All strains were grown on coverslips in YGV and the coverslips were then switched to CMC after being stained with WGA.

A4 switched from YGV to CMC after being stained with WGA shows the morphological shift occurs immediately after the switch. The change in morphology is indicated by red arrows. This phenotype is similar to the switch from glucose rich to glucose minimal condition.



$\Delta pkaA$ switched from YGV to CMCV after being stained with WGA shows morphological shift occurs after a delay of 3 hours. The change in morphology is indicated by red arrows. This phenotype is different from glucose rich to glucose minimal conditions.



ΔschA switched from YGV to CMCV after being stained with WGA shows morphological shift occurs after a delay of 2 hours. The change in morphology is indicated by red arrows. This phenotype is different from glucose rich to glucose minimal conditions.

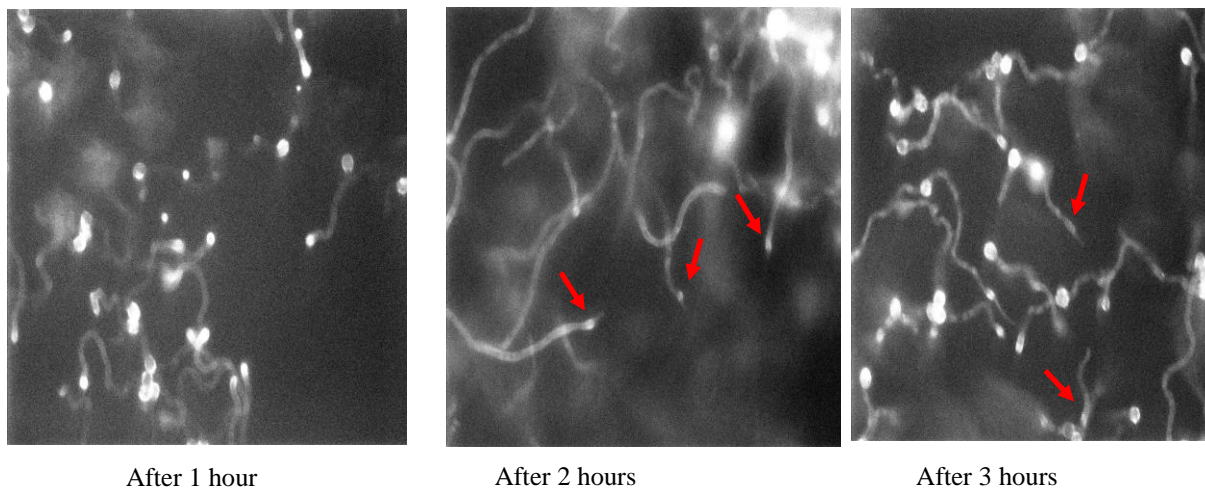


Figure 1d: To visualize morphological changes in carbon derepression in *ΔflbA* switched from YGV to CMCV after being stained with WGA shows no morphological change even after 24 hours. This phenotype is different from wildtype and for glucose rich to glucose minimal conditions.

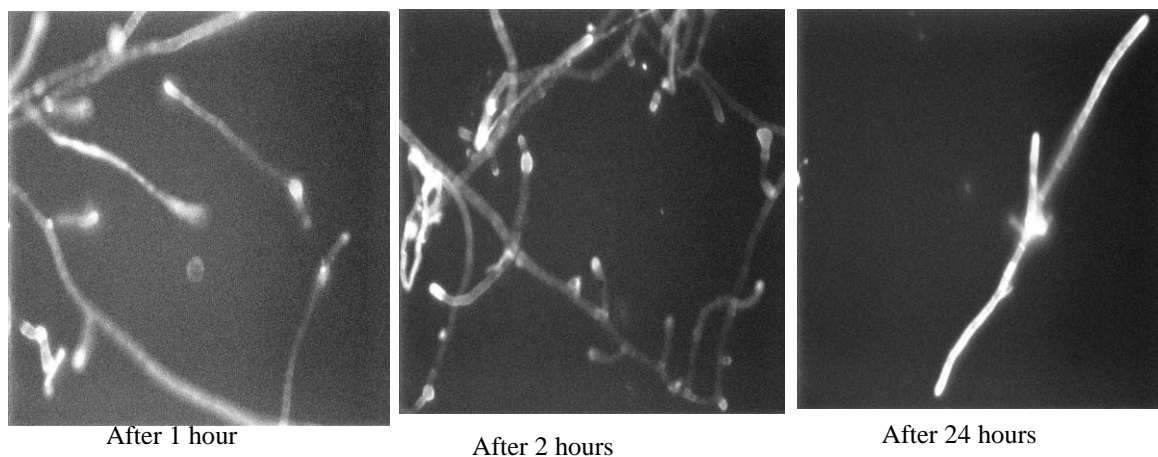
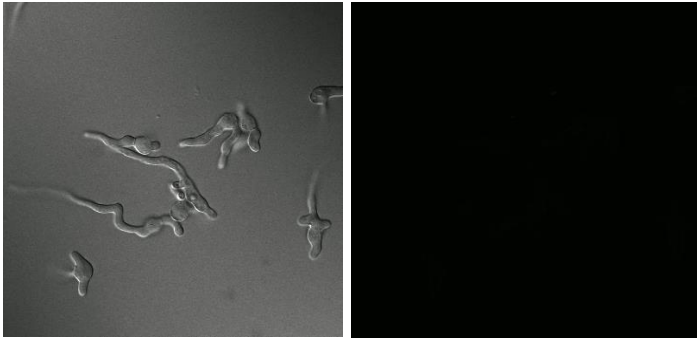
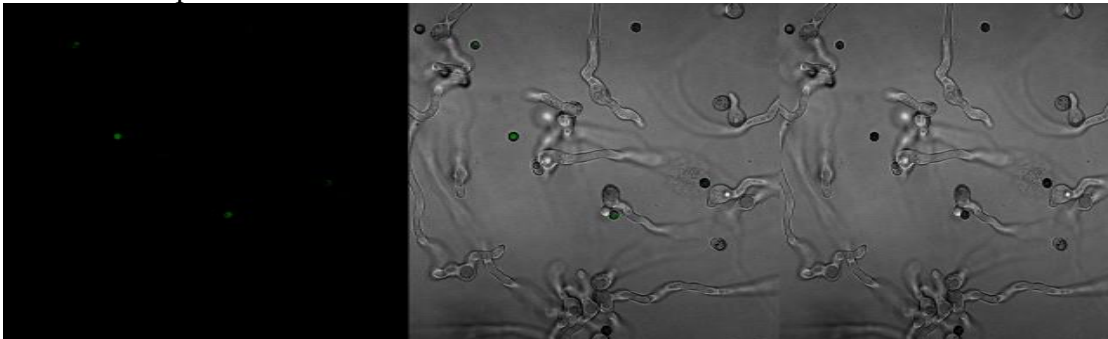


Figure 2: HxtB::GFP used to visualize the carbon transport and sensing occurs within the hyphae. HxtB::GFP was first grown in different carbon sources for 16 hours in 28°C. No GFP localization was seen in YGV and MNV (1% glucose). GFP localization was displayed in vacuoles and septa in NCS, CMC and MNV (0.1% glucose).

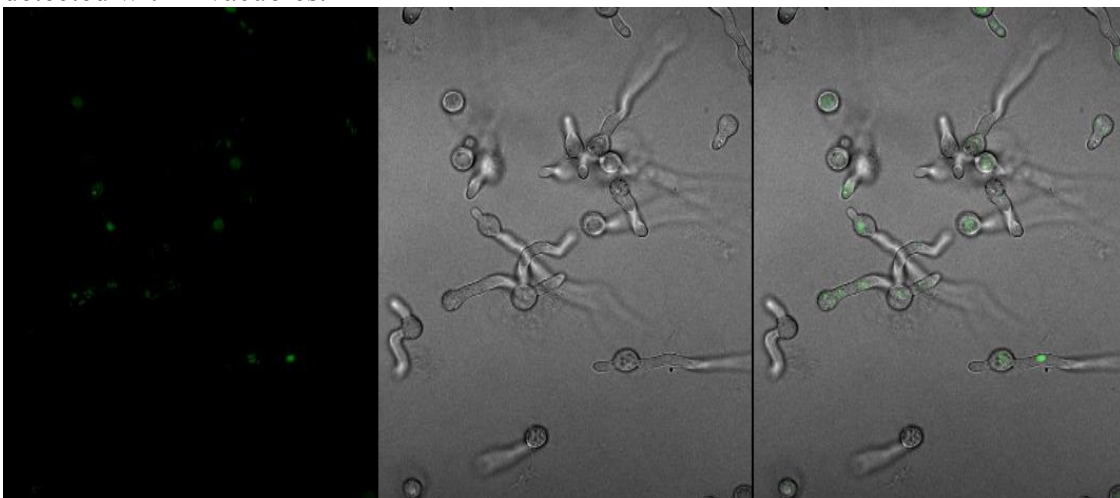
HxtB::GFP was grown in YGV for 16 hours and there was no GFP localization detected.



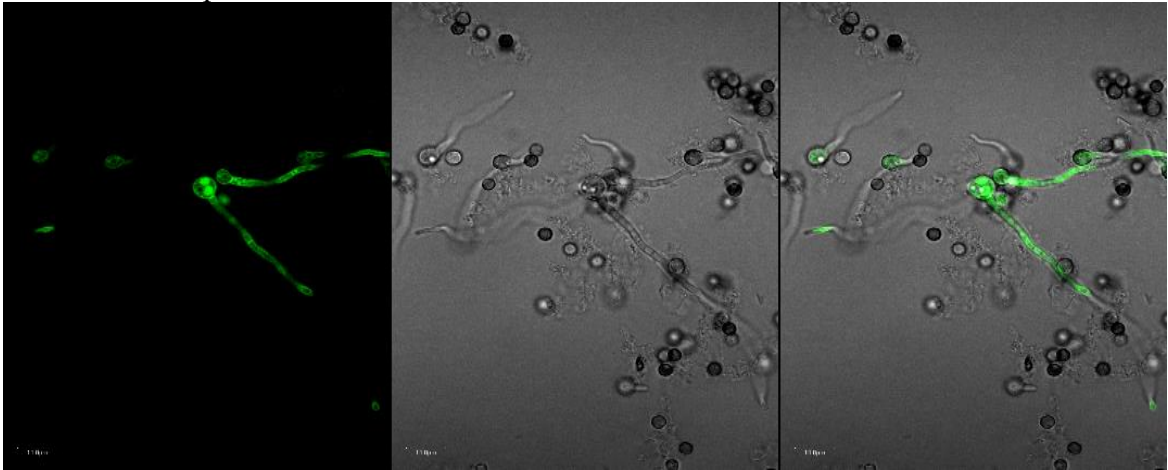
HxtB::GFP was grown in MNV (1% glucose) for 16 hours and no GFP localization was detected except auto-fluorescence.



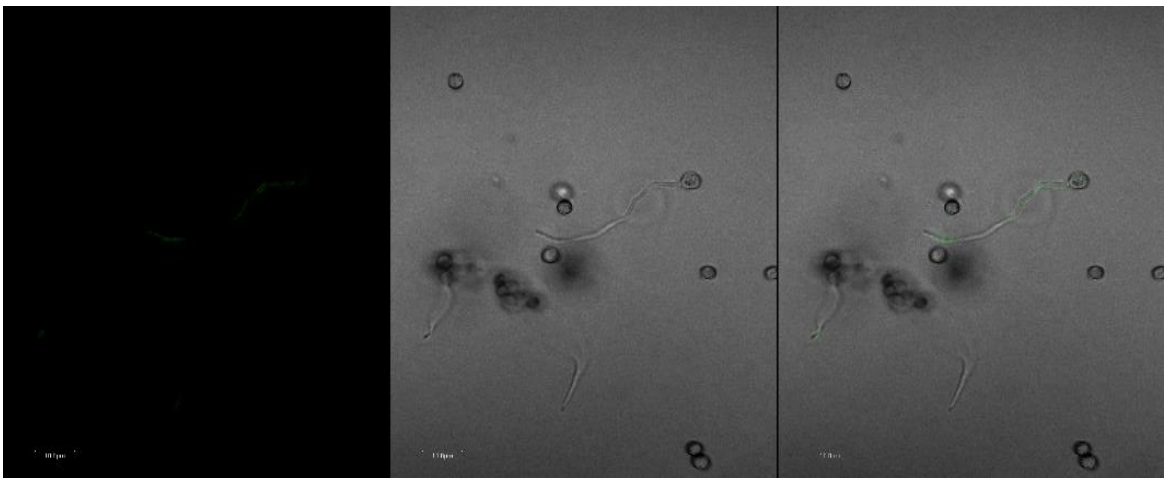
HxtB::GFP was grown in MNV (0.1% glucose) for 16 hours and GFP localization was detected within vacuoles.



HxtB::GFP was grown in NCS for 16 hours and GFP localization was detected within vacuoles and septa.



HxtB::GFP was grown in CMC for 16 hours and GFP localization was detected within vacuoles.



HxtB::GFP was grown in Xylose for 16 hours and GFP localization was detected within vacuoles.

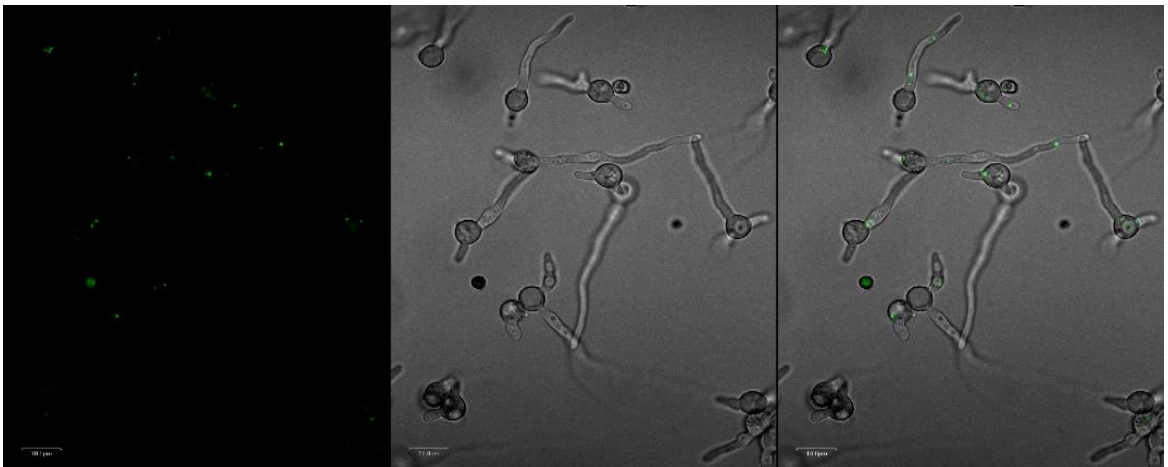
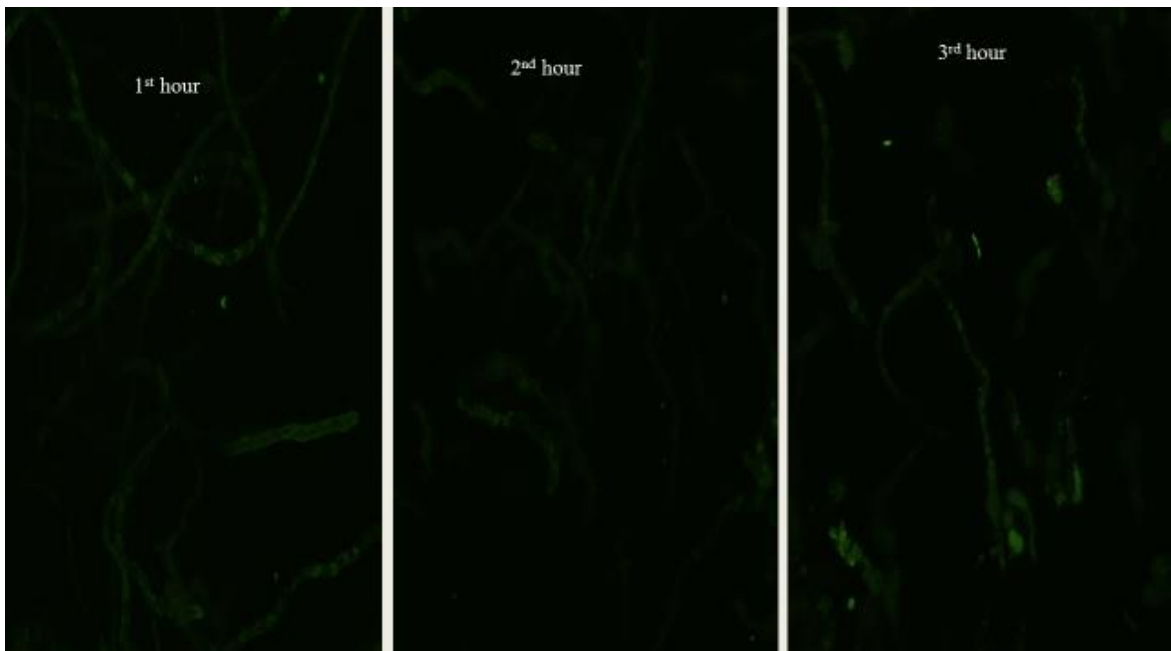
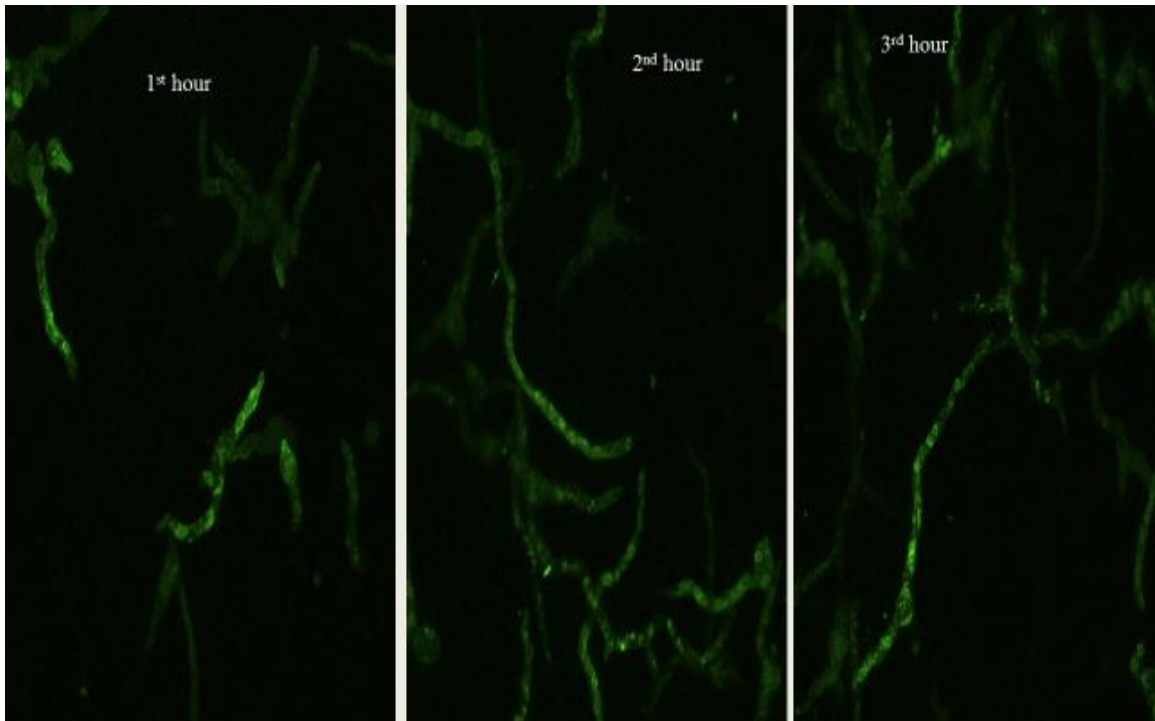


Figure 2a): To explore the localization of HxtB::GFP in carbon derepression conditions was explored by growing HxtB in YGV and shifting them into different carbon source media. This yield similar results to grown HxtB in different media. The localization was seen within an hour at the septa and around the vacuolar membrane, making it look like rings within the hyphae.

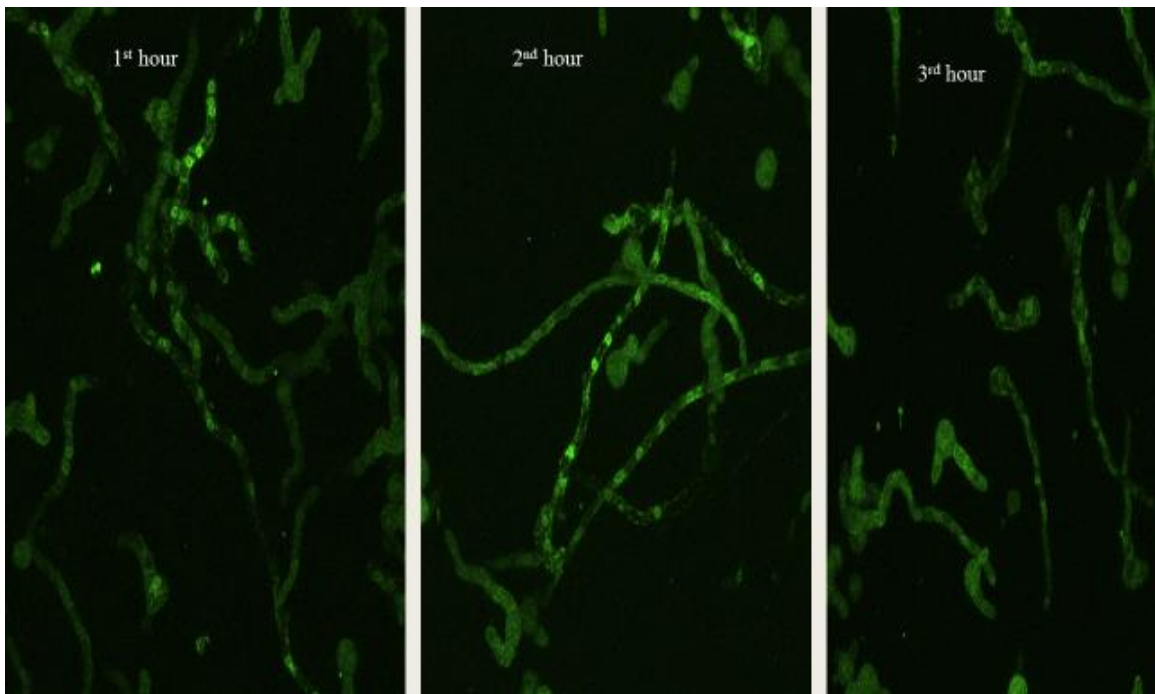
HxtB::GFP switched from YGV to MNV (1% glucose) shows little or no localization



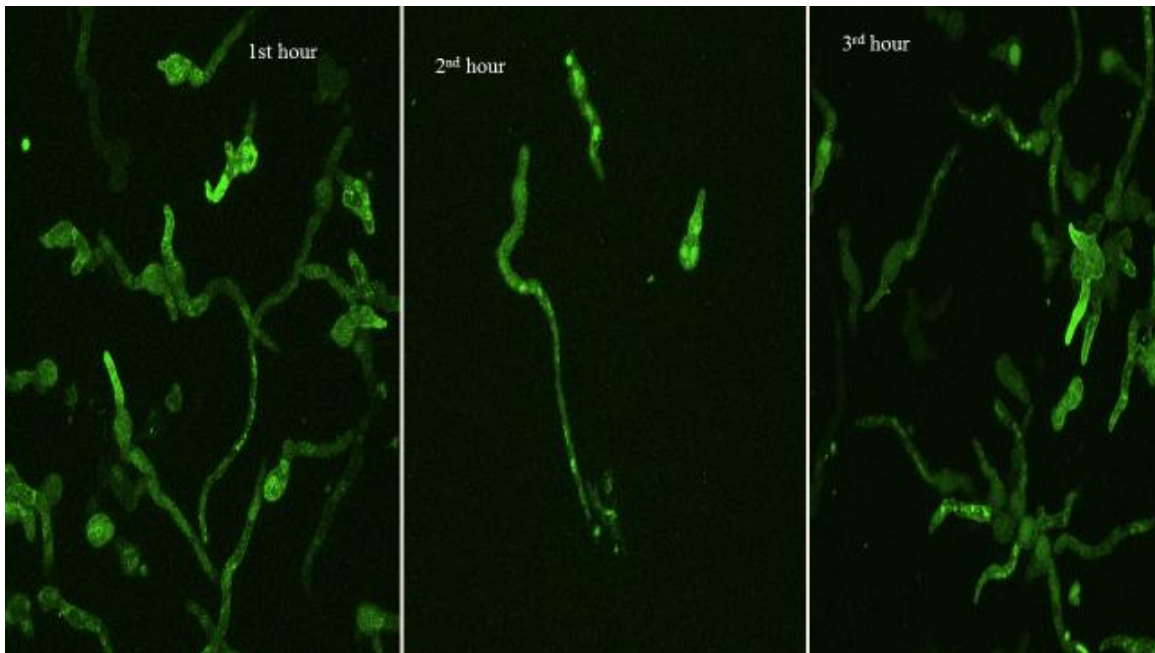
HxtB::GFP switched from YGV to MNV (0.1% glucose) shows localization at the vacuolar membrane



HxtB::GFP switched from YGV to NCS shows localization at the vacuolar membrane and septa.



HxtB::GFP switched from YGV to Xylose shows localization at the hyphal tips, within the vacuoles and around the vacuolar membrane and at the septa.



HxtB::GFP switched from YGV to CMCV shows localization at the vacuolar membrane and septa.

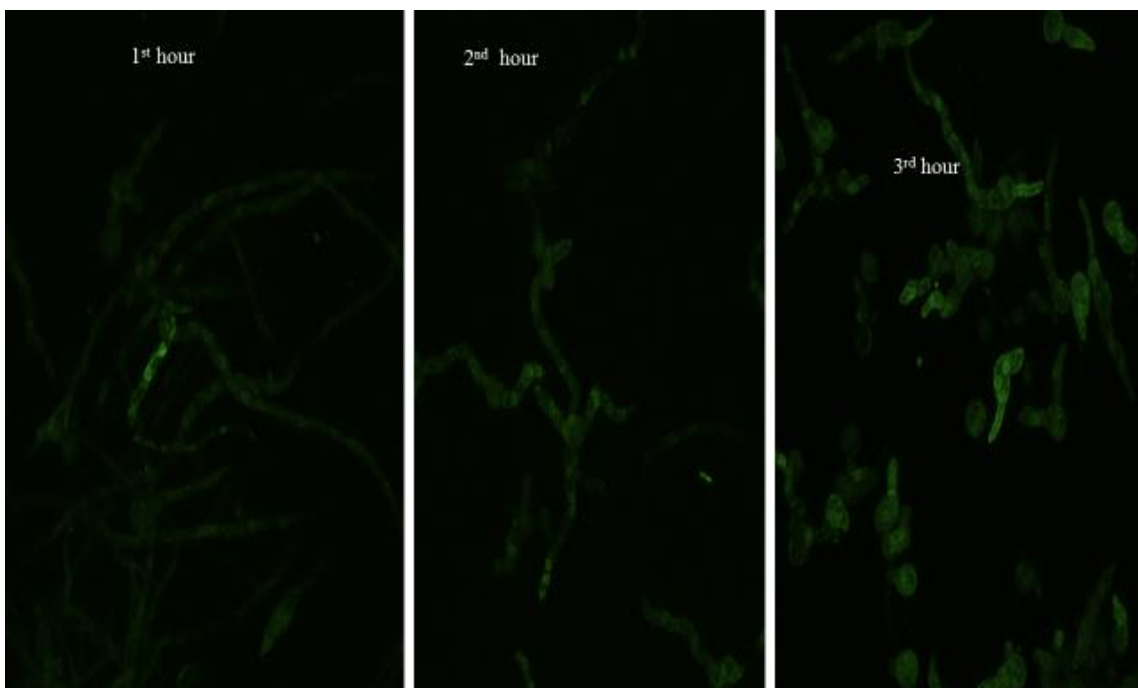


Figure 2b: Taking a closer look at the HxtB::GFP localization after it has been switched from YGV to CMC after 3 hours. Localization is seen as rings along the hyphae indicated by the red arrows and the yellow arrows showing the localization at the septa.

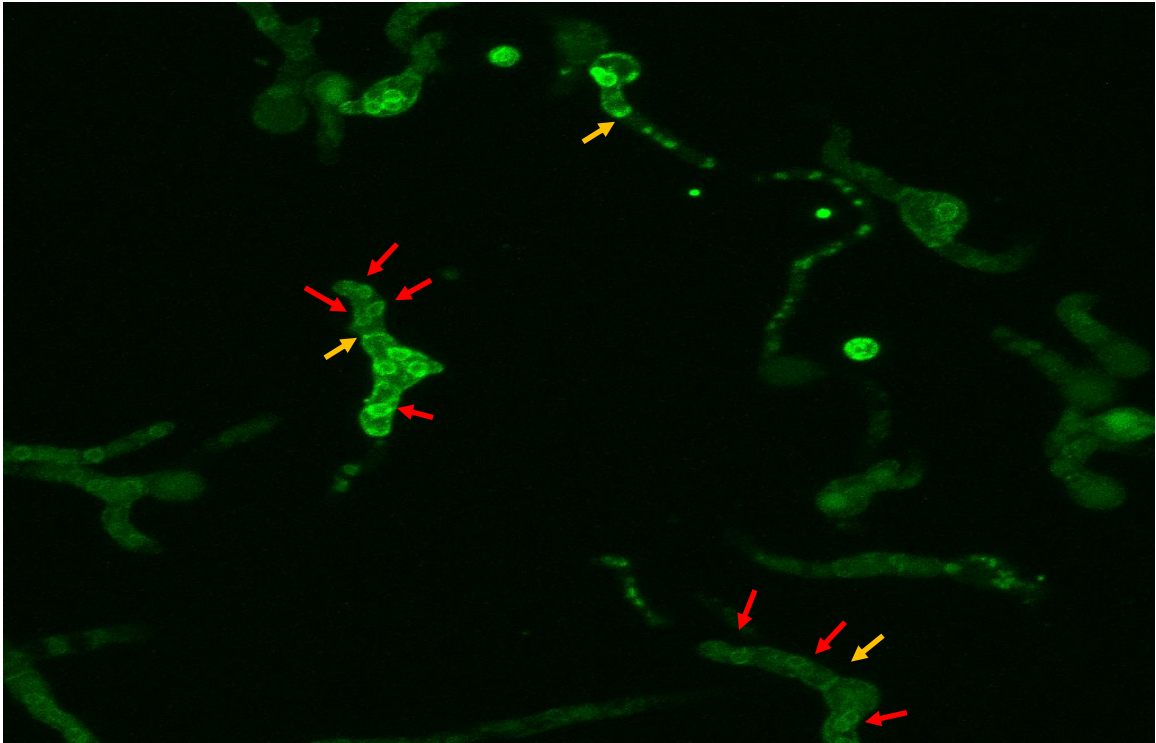
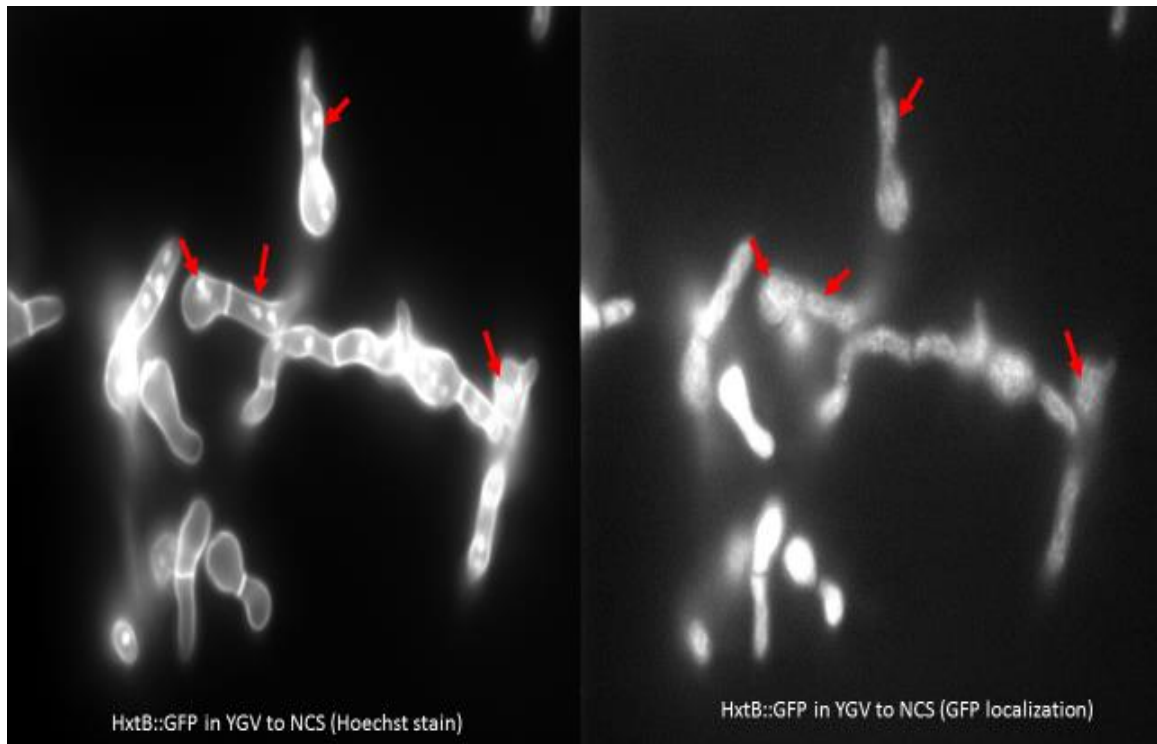


Figure 3: Comparing the GFP localization and nuclei stained by Hoechst/Calcofluor stain in HxtB::GFP. As indicated by the red arrows the localization of nuclei is in the same location as the GFP localization. The GFP localization is present at the membrane around the nucleus.



Chapter 3

Introduction

The plant cell wall is a complex structure composed mainly of polysaccharides which are the most abundant organic compounds found in nature. They make about 90% of the plant cell wall which can be divided into three groups: Cellulose, Hemicellulose and Pectin. The use of plant biomass (largely cell wall material) in food, agriculture, fabric, timber, biofuel and biocomposite industries makes it essential to understand the structure and development of plant cell wall. The bioconversion of converting cellulose to glucose requires multienzyme system of cellulases, xylanases and other accessory enzymes. The enzymatic hydrolysis of cellulose includes three types of cellulases: cellobiohydrolases, endoglucanases and β -glucosidases (BglA) which work in synergy. Endoglucanases and cellobiohydrolases act directly on cellulose fiber whereas BglA hydrolysis oligosaccharides and cellobiose into glucose. The end product of hydrolysis of cellulose fibers is cellobiose which acts as an inhibitor for converting cellulose to glucose so it can be further utilized by yeast and other organisms. This makes BglA activity crucial to the process of cellulose degradation. Most filamentous fungi such as *Trichoderma* and *Aspergillus* produce these cellulases, although not sufficient enough for biomass conversion. Also BglA is known to be inhibited in the presence of high concentration of glucose. Therefore the need to understand the secretion and to improve the yield of BglA has become of great interest (Pettolino et al. 2012, Vries et al. 2001, Ketudant et al. 2010, Baraldo et al. 2014 and Chauve et al. 2010).

Filamentous fungi have high protein secretion capacity. Hence, they have been a lot of interest in turning filamentous fungi into hosts for producing industrially relevant enzymes and other biopharmaceutical compounds. Producing naturally secreting fungal enzymes has been more fruitful compared to producing proteins of non-fungal origin or recombinant proteins, which has been disappointingly low and not cost effective. This is due to the fact that fungal secretory pathway is poorly understood. Previous research has shown the limitations occur at the post-translational level with blockages due to compartmentalization or during the stages in processing of the proteins for secretion (Schalen et al. 2015). Another aspect of the limiting factors of how different environment and nutrient stresses affect the production of different fungal proteins still needs to be investigated. Pulse feeding and limiting carbon sources during pulse fed fermentation has been noted to improve the productivity of enzyme production in *Aspergillus oryzae* by helping to produce smaller mycelia, lower broth viscosity and control dissolved oxygen concentration (Bhargava et al. 2003).

Protein secretion undergoes two main tasks: 1) performing proper folding and post translation modifications such as glycosylation and sulfation and 2) sorting cargo proteins to their functional states and final cellular localizations. Secretory proteins start their journey by entering the endoplasmic reticulum (ER). The ER proteins are folded and undergo distinct modifications such as glycosylation, disulfide bridge formation, phosphorylation and subunit assembly. Proteins then leave ER packed in transport vesicle and move to Golgi for further modifications such as glycosylation and peptide processing. Eventually the protein packed secretory vesicles are directed to the plasma membrane from where they are secreted (Liu et al.2014, Conesa et al. 2001).

Usually studies to understand secretion pathway in filamentous fungi have involved the deletion of genes or fusion of fluorescent proteins to secreted native proteins to characterize the function of the gene and how the protein is secreted (Schalen et al. 2015). Using BglA::GFP a strain acquired from Gastavo's lab and using it cross different genes that are important to the hyphal development (*ΔsepA* and *ΔmesA*) will shed light to the process of how the secretory process of BglA is taking place in *Aspergillus nidulans* specifically. BglA::GFP was noted to be have no GFP localization and the growth was slower compared to wildtype in YGV (glucose). There was GFP localization however when BglA::GFP was grown in CMC, NCS, xylose, MNV (01%) and MNV. To study the effects of carbon limitation in shift experiments were performed from YGV to: CMC, MNV (1% glucose), MNV (0.1% glucose) and NCS. The results were consistent with increased expression of GFP in CMC, MNV (0.1% glucose) and NCS but not in MNV (1% glucose). The localization pattern also matched in the crosses of BglA with *ΔsepA* and BglA with *ΔmesA*. The localization was also similar to the localization of HxtB::GFP but the expression of BglA increased after the switch compared to the HxtB::GFP localization.

Materials and Methods

Strains, media and growth conditions

The strains used in this study Sng10 (BglA::GFP) and HxtB::GFP were acquired from Goldman lab (Ishitsuka et al. 2015 and Fernanda dos Reis et al. 2013) The following strains were made in Harris lab *ΔsepA* (ASH 630) and *ΔmesA* (DD8 A2) (Sharpless et al. 2002 and Pearson et al. 2004). The glucose rich media and supplements was prepared as previously described in Harris et al.1994. The minimal media was prepared as previously described in Kafer.1997. Liquid media (without agar) was used as YGV (0.5 % yeast

extract, 1% dextrose and vitamins), MNV (minimal media with 1% glucose and vitamins), MNV (0.1%) (minimal media with 0.1% glucose and vitamins) CMCV (1% Carboxymethylcellulose sodium salt in minimal media and vitamins), NCS (no carbon source, minimal media with only nitrate salts) and XV (1% xylose in minimal media and vitamins). All the strains were grown in 28°C unless indicated otherwise. For septation and hyphal growth studies conidia are grown at 28°C for 12 hours on coverslips. During shift experiments after 12 hours of growth in YGV media the coverslips were then washed with sterilized ddH₂O in stain jars and then placed into the shifting media (NCS, CMCV, MNV and MNV (0.1%)). The coverslips were then grown in shifted media for 4 to 6 hours and analyzed after each hour.

For crosses the BglA::GFP with *ΔsepA* and *ΔmesA* strains were grown on solid media (~2% agar) of MAG (2% Malt extract, 2% dextrose with vitamin), and in MAGUU (with Uridine and Uracil). The parent strains were streaked on MAGUU plates and then crossed sections were plated on MN plates. Once the cleistothecia had matured, they were dissected on water agar plates. The dissected spores were diluted with water and spread on MN plates. Selected segregants (a selection that includes all phenotypes) were then plated on MAG plates to perform DNA extraction (Mio-Bio Powersoil kit) and then PCR verified (Invitrogen, native/ recombinant Taq polymerase). Once the segregants were verified the spores were stored at -80°C and imaged using both BF and Confocal microscopy.

DNA Extraction

DNA was extracted using the Mo Bio Powersoil DNA isolation kit (Catalog No. 12888-100). The protocol followed instructions provided by the vendor. This kit has been used in

many studies and has been used to extract DNA from a variety of yeast, bacterial and filamentous fungi.

PCR

After DNA extraction, sequences were amplified by PCR. The PCR reaction used in this study was native polymerase (Invitrogen, Carlsbad, CA). The native Taq polymerase was used for PCR verification on all sequences that were not used in transformations. PCR reaction was set up: 5 μ L of buffer, 2.5 mM MgCl₂, 200 μ M dNTP, 100ng of DNA template, 400nM of downstream and upstream primers (each), 0.5 units of Taq polymerase and double distilled water to bring the final solution to 50 μ L.

The PCR Conditions

The simplest protocol was PCR verification, where the thermocycler, (Biorad MJ mini gradient thermocycler) lid was set for 105°C and the block was set to reach 94°C (the DNA denaturing temperature). The block was then held 94°C and polymerase was added to each reaction. After polymerase was added, there was a 90 second 94°C denaturing step. The annealing temperature was specific for each primer set, usually 50-60°C, for 30 seconds. The elongation temperature was 72°C with the time dependent on the length of the product. In this study, for every 1kb, 1 minute was added to the elongation time. This cycle was repeated 30 times. The final step was 72°C for 7 minutes to finish up all of the elongations. The PCR reaction was then held at 4°C to stabilize the sequence after the run.

Electrophoresis

The gels used for electrophoresis in this study was made of 0.8% purified agar in 1xTAE and 1 μ L of ethidium bromide. To determine the size of the band, 1+KB ladder

(Invitrogen) was used. To determine the mass of the bands, the High Mass Ladder (Invitrogen) was added to the gel in two different quantities of 2 μ L and 4 μ L.

Microscopy (Bright Field (BF) and fluorescent GFP filter)

The microscopy was done by using the Metamorph software. The microscopic methods used in this study used Bright Field and GFP was analyzed with GFP filter. Confocal microscope at the Microscopy Core Facility was used for some GFP images.

Results

BglA::GFP localization in various carbon sources occurs at the hyphal tips, septa and in secretory vesicles. The carbon derepression studies show similar localization except in NCS and CMC where the localization was also around the nuclear membrane.

BglA::GFP does not show any localization when grown in YGV except some autofluorescence (Fig1a). When BglA::GFP is grown in different carbon sources (MNV (0.1% glucose), Xylose, CMC and NCS) the localization was seen at hyphal tips, septa and secretory vesicles. But when BglA::GFP is grown in MNV (1% glucose) there was no GFP expression which is consistent with the fact that BglA expression is inhibited in the presence of high glucose concentrations (Chauve et al. 2010).

Shift experiment was conducted from YGV to: MNV (1% glucose), MNV (0.1% glucose), NCS, Xylose and CMC. The localization was noted after four hours mainly at hyphal tips, secretory vesicles and septa (Fig 1c and Fig 1d). However, in CMC and NCS the localization also matched the localization of HxtB::GFP. The localization was also displayed around the nuclear membrane as it was displayed in HxtB::GFP and this localization was noted only in the CMC and NCS. The secretory vesicular movement was

not seen in HxtB::GFP indicating that nuclear localization could involve different function compared to the secretory pathway.

The localization of $\Delta sepA$ BglA::GFP strain localizes in the same locations as BglA::GFP, at the hyphal tips, septa, in secretory vesicles and around the nuclear membrane.

Actin is an important player in the polarity establishment. To visualize how the absence of actin affects the secretion pathway we generated the cross of $\Delta sepA$ BglA::GFP. The segregants were verified through PCR and used brightfield to visualize the $\Delta sepA$ BglA::GFP in carbon derepression. After $\Delta sepA$ BglA::GFP was grown in YGV and shifted into CMC media, the localization pattern was displayed to be in similar to BglA::GFP localization (Fig 2). The phenotype of the hyphae resembled $\Delta sepA$ as the growth was restricted as they were grown in 42°C. This however did not hinder the expression of BglA::GFP and it was similar to the expression in BglA::GFP. We noted the same vesicular and nuclear localization pattern in the BglA::GFP $\Delta sepA$ strains as it was displayed previously in the shift experiments from YGV to CMC in BglA::GFP. This indicated that absence of actin does not hinder the expression of BglA::GFP.

The localization of $\Delta mesA$ BglA::GFP strain shows similar localization pattern as BglA::GFP but there was an absence of localization around the nuclear membrane.

MesA a predicted cell surface protein that promotes the localized assembly of actin cables at polarized sites and is required for recruitment of SepA. To further explore the role of actin's function in the secretory pathway we generated the strain $\Delta mesA$ BglA::GFP and verified the strain through PCR. The phenotype of the $\Delta mesA$ BglA::GFP strain is similar to the phenotype of $\Delta mesA$. The shift experiment of $\Delta mesA$ BglA::GFP showed similar

localization pattern as BglA::GFP as it localizes at the secretory vesicles, hyphal tip and at the septa. But the nuclear localization was not visible (Fig 3). This may indicate that MesA is important for nuclear localization.

HxtB::GFP and BglA::GFP localizations compared during a time course of five hours are initially different but after four hours both show localization around the nuclear membrane.

To further explore how HxtB::GFP and BglA::GFP localize we compared both strains in carbon derepressed conditions over a time course of five hours. We noted the localization of HxtB and BglA is slightly similar, as they both localize at the septa and sometimes at the hyphal tips (HxtB in xylose). The localization pattern over time also differs as HxtB localizes primarily in the nuclear membrane and BglA primarily localizes at hyphal tips, septa and secretory vesicles. This localization displays the movement from the spore head to the hyphal tip in indistinct vesicles. BglA localization in the nucleus does not appear until after three hours in the shift experiment YGV to CMC (Fig 4) whereas the HxtB localization appears in the nucleus within the first hour of the shift. Over the time course it can be seen that HxtB and BglA localization not only differ in localization patterns but also in the protein expression overtime. HxtB::GFP expression could be reduced but BglA::GFP expression seems to increase overtime because of the intensity of expression seen in microscopy (Fig 4). This shows that over time BglA and HxtB may share some common function.

Discussions

The bioconversion of cellulose to glucose requires multienzyme system of cellulases which include the final hydrolyzing enzyme BglA which breaks down cellobiose into glucose. Most filamentous fungi such as *A. nidulans* already secrete this enzyme in small amounts. The need to improve our understanding in the secretory pathway has become a major importance as most filamentous fungi have high protein secretion capacity. This ability makes them an appealing host to secrete relevant enzymes and other biopharmaceutical compounds. Although producing naturally secreting enzymes has been shown to be more cost effective to secrete than non-fungal proteins. While the secretion in filamentous fungi has been of interest, the pathway for secretion is not fully understood. Recent research revealed that in carbon limiting conditions improve the secretion of enzymes in *A. oryzae* (Bhargava et al. 2003). Using BglA::GFP we looked for the localization patterns when BglA is grown in different carbon sources and when switched from carbon rich to carbon limiting conditions. It was also noted that BglA is inhibited in high glucose concentration (Chauve et al. 2010). Our findings were consistent with previous research where the different carbon sources mainly CMC, Xylose and NCS showed an increase in GFP expression compared to MNV in different glucose amounts (1% and 0.1%). All were seen to localize at the septa and at hyphal tip and secretory vesicles. Shift experiments from YGV to MNV (1%), MNV (0.1%), CMC, xylose and NCS showed the localization at the hyphal tip, septa and secretory vesicles. But only CMC and NCS were shown to also localize in nuclear membrane similar to the localization pattern of HxtB::GFP. Further analysis needs to be done to understand the importance of localization in the nuclear membrane as both HxtB::GFP and BglA::GFP have this same localization. This process may improve or deter the secretion process.

Further analysis was done by crossing BglA::GFP to deletions of genes that play a role in establishing hyphal polarity, *ΔsepA* and *ΔmesA*. In both instances the shift experiments were performed when moving mutants from YGV to CMC and we found in the case of *ΔsepA* the phenotype of both parents was maintained. The strains were grown in 42°C as *ΔsepA* is a temperature sensitive mutant and the localization of *ΔsepA* BglA::GFP matches that of BglA::GFP as there was localization at the tip, septa, and the secretory vesicles but the localization was also seen around the nuclear membrane. The *ΔmesA* BglA::GFP however had similar localization patterns and at the tip, secretory vesicles and septa but there didn't seem to be any nuclear localization. This could be due to the fact that it could need more time to localize in the nuclear membrane or MesA is required for nuclear localization.

The comparison between HxtB::GFP and BglA::GFP showed some similar localization patterns but were mostly quite different. HxtB localizes primarily in the nuclear membrane and BglA showed distinct pattern of moving from the spore head to the hyphal tip using vesicles that are part of the protein secretion pathway. Over time the HxtB expression also seemed to display reduced GFP expression whereas the BglA expression was intensified showing a reverse pattern, while HxtB::GFP secretion is reduced BglA::GFP secretion is increased.

Future directions

Using BglA::GFP can be used to define the secretory pathway by crossing it to deletion of genes that play a part in hyphal morphogenesis (Cdc42, RacA) but also to genes that control the carbon catabolite repression like CreA, PkaA and SchA. These crosses could help us understand what genes play a role in secretion pathway and could help us improve the

production of not just the fungal enzymes but also of the recombinant proteins. It would also be beneficial to measure the RNA levels of HxtB and BglA during shift experiments to further show what conditions are beneficial for the secretion and if the nuclear localization would improve or deter the secretory process.

Figures

Figure 1a: BglA::GFP grown in YGV for 17 hours showed no GFP localization as imaged in Brightfield and Confocal microscopic images.

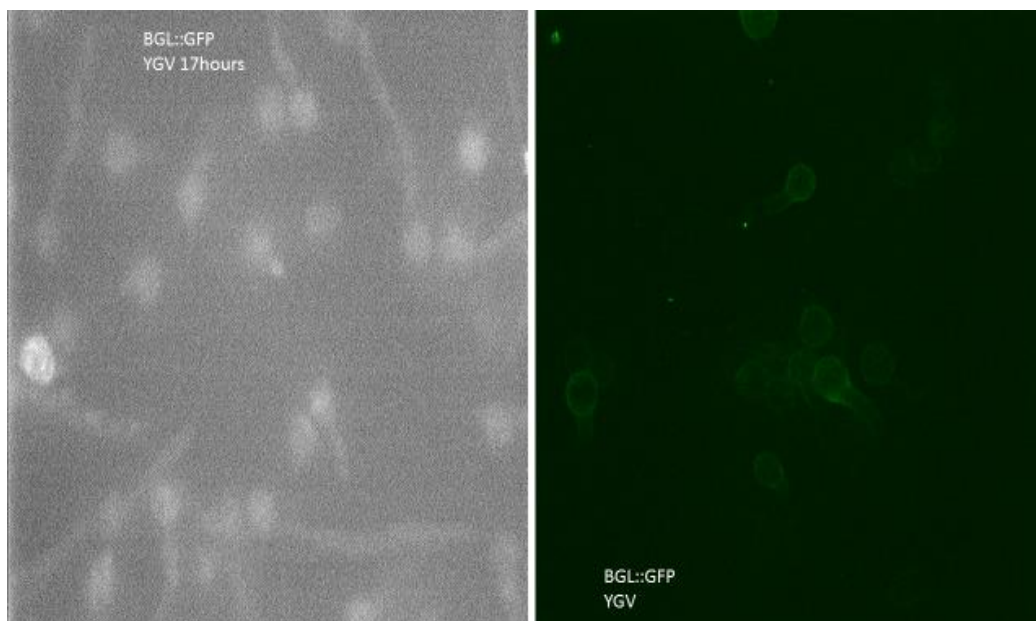


Figure 1b: BglA::GFP was grown in different carbon source minimal media (MNV (0.1% and 1% glucose), CMC, Xylose and NCS for 17 hours showed localization at the hyphal tips, secretory vesicles and at the septa. There was no localization in MNV (1% glucose).

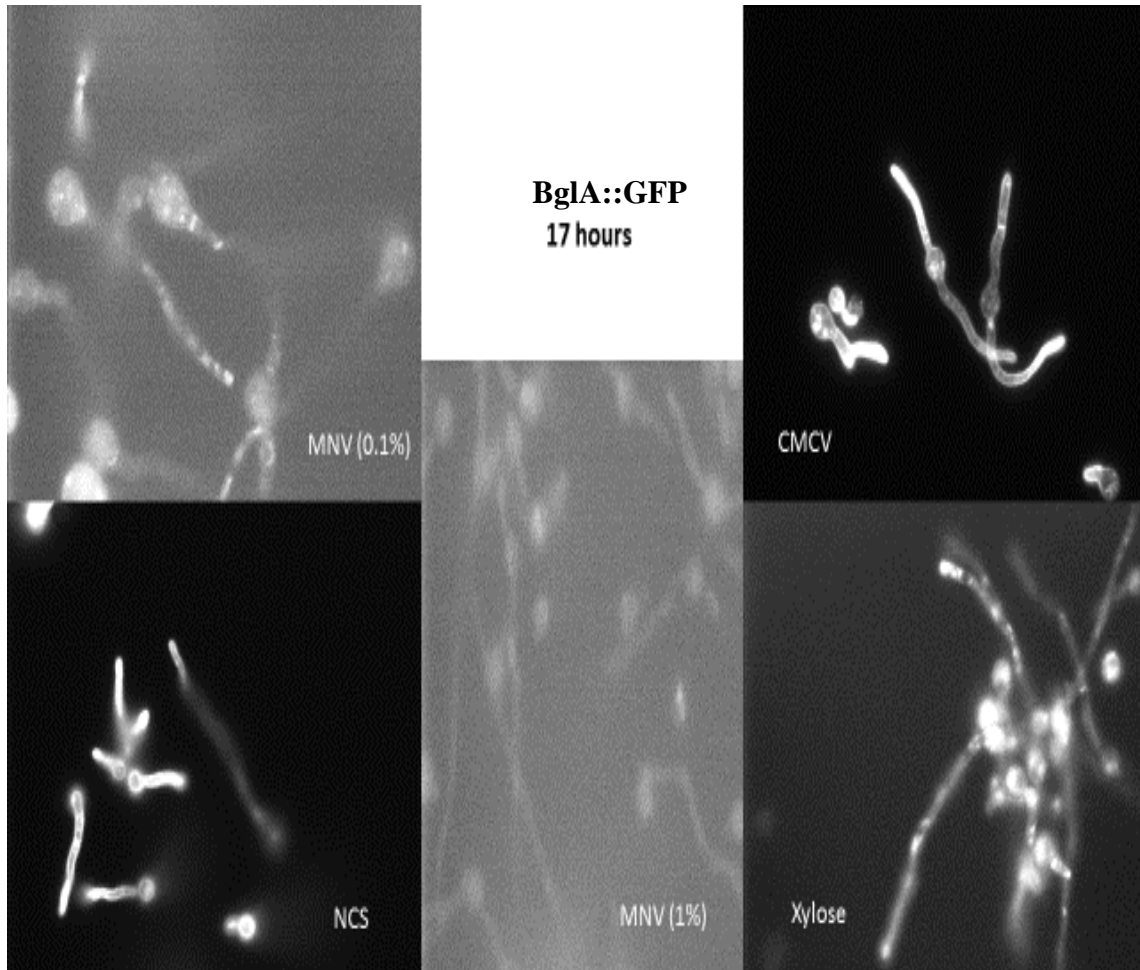


Figure 1c: BglA::GFP grown in YGV for 12 hours and shifted to different carbon source minimal media (CMC, NCS, MNV (0.1% and 1% glucose)) and captured after 4 hours. The GFP localization was seen at the hyphal tips, septa and secretory vesicles along the hyphae. The localization in NCS and CMC also shows nuclear membrane similar to HxtB localization.

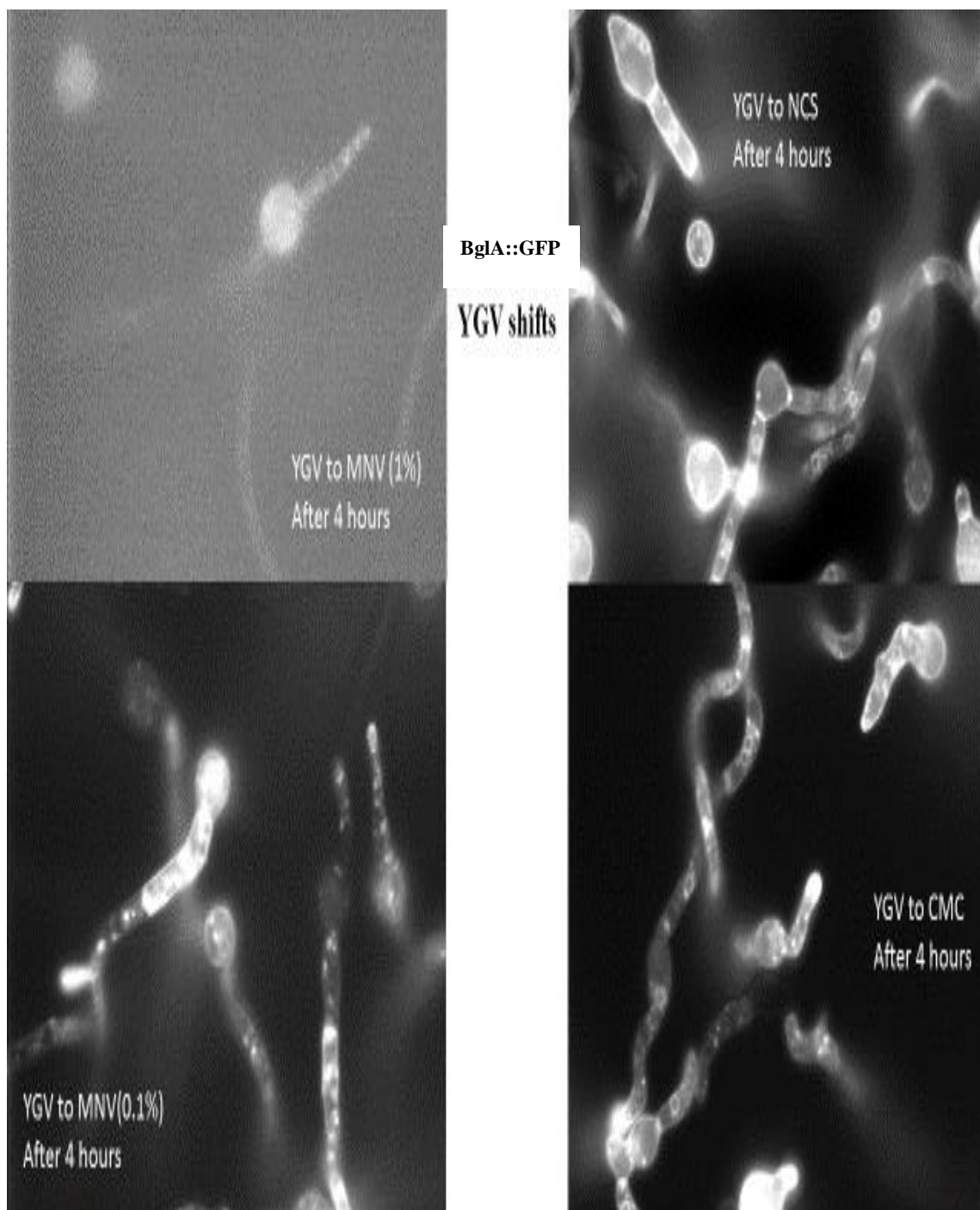


Figure 1d: BglA::GFP grown in YGV for 12 hours and shifted to different carbon source minimal media (Xylose) and captured after 4 hours. The GFP localization was seen at the hyphal tips, septa and secretory vesicles along the hyphae.

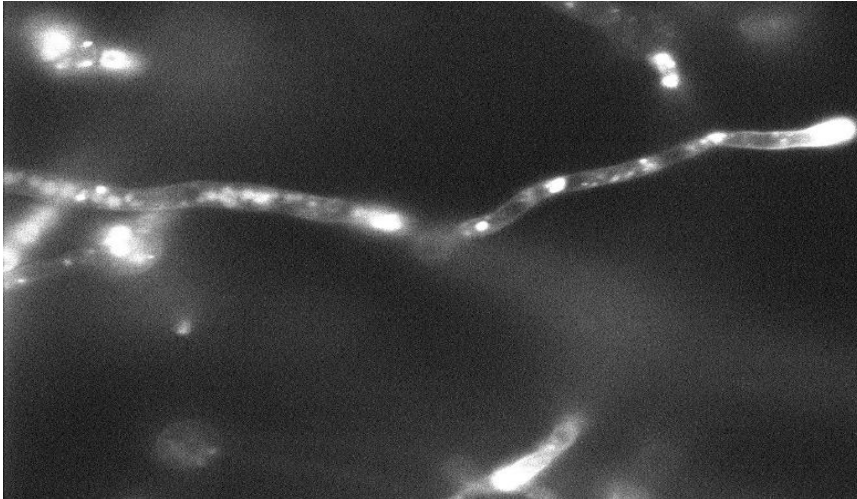


Figure 2: BglA::GFP Δ sepA mutant strain was grown in YGV for 12 hours and switched to CMC minimal media and imaged after 4 hours. The localization was seen in hyphal tips, septa, in secretory vesicles and also at the nuclear membrane as HxtB localization.

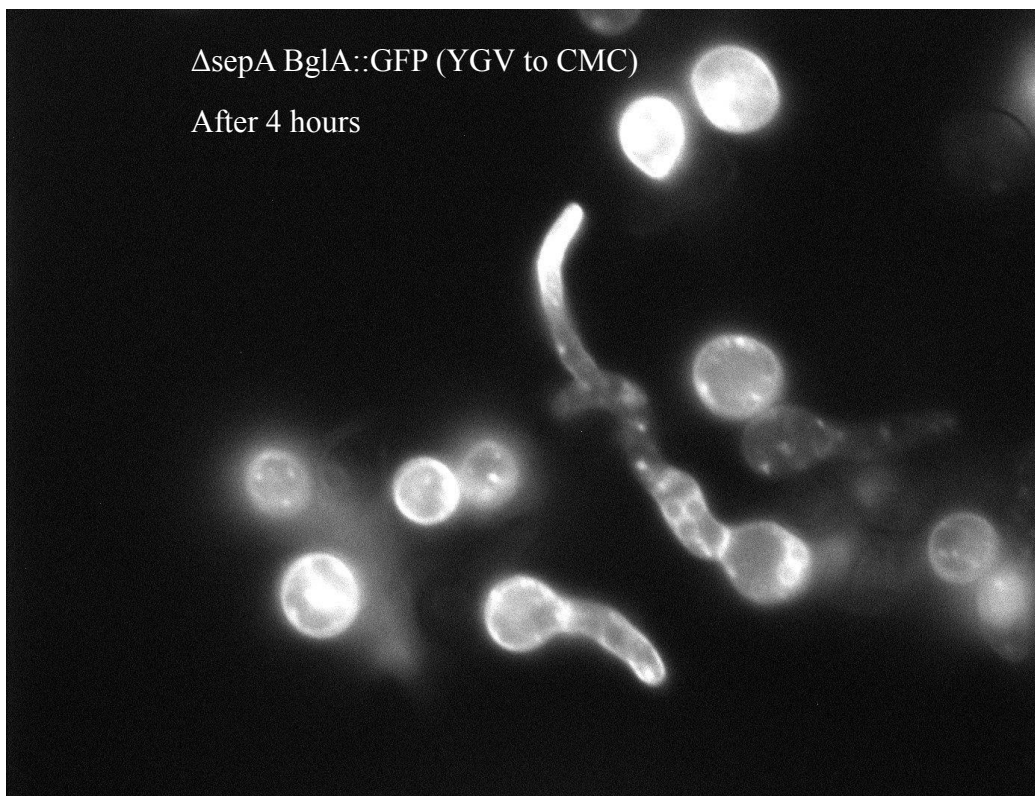


Figure 3: BglA::GFP $\Delta mesA$ grown in mutant strain was grown in YGV for 12 hours and switched to CMC minimal media and imaged after 4 hours. The localization was seen in hyphal tips, septa and secretory vesicles.

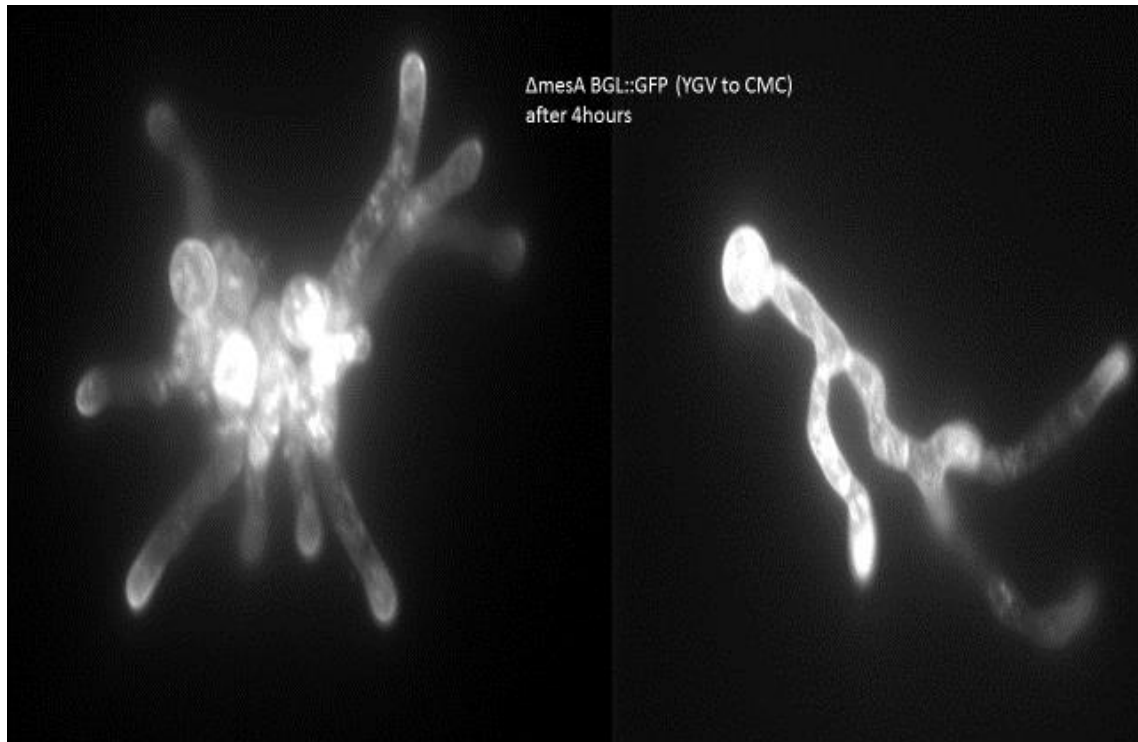
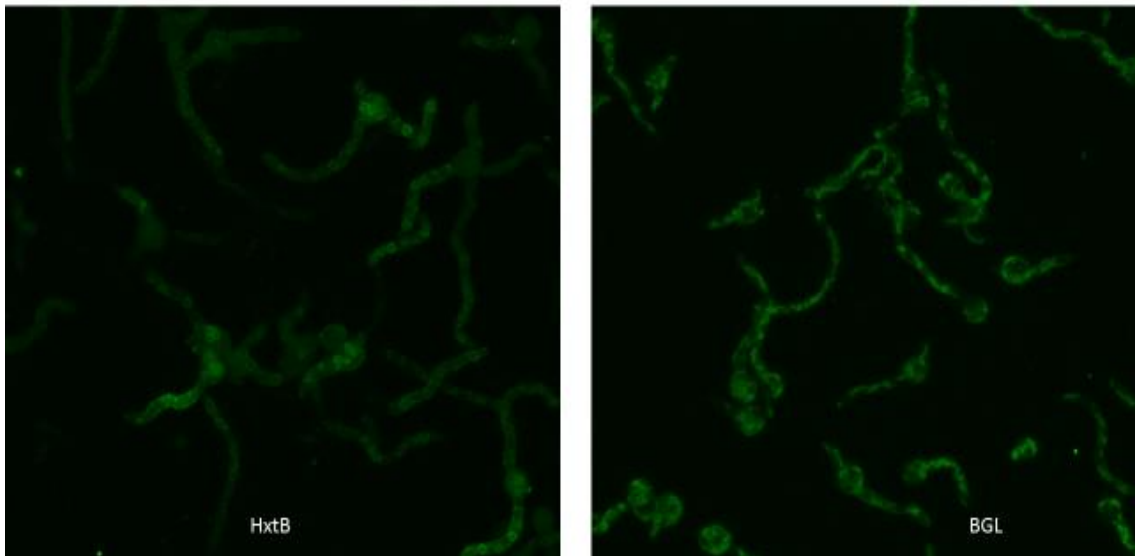
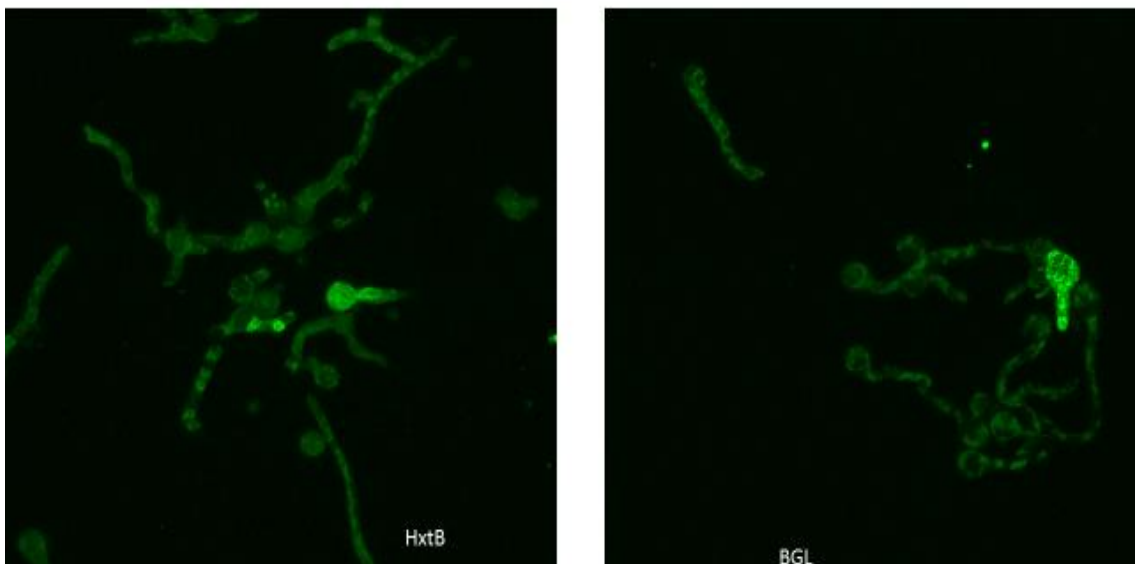


Figure 4: Comparing the confocal microscopic images of BglA::GFP (BGL) and HxtB::GFP grown in YGV for 12 hours and switched to CMC and imaged after every hour for 5 hours. The localization was initially different as HxtB showed localization around the nuclear membrane and BGL shows localization at the hyphal tips, septa and in the secretory vesicles. But around the 5th hour shows some localization around the nuclear membrane can be seen and is indicated by the red arrow.

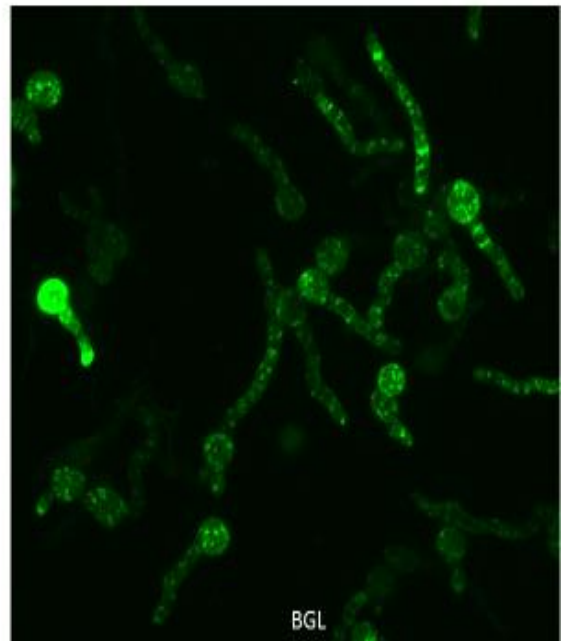
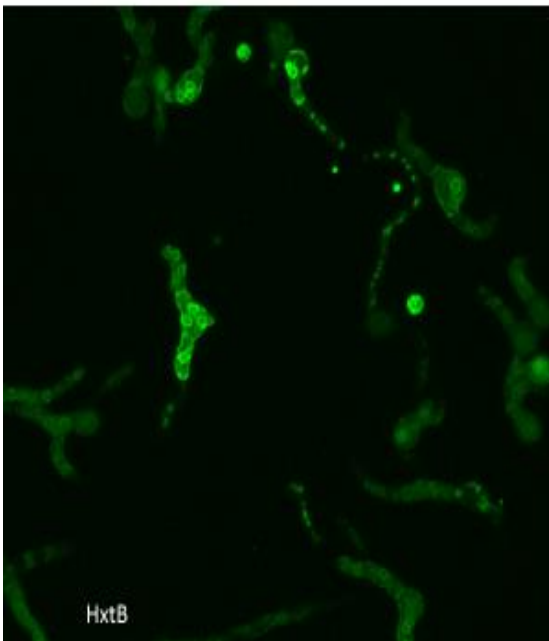
1st hour (YGV- CMC)



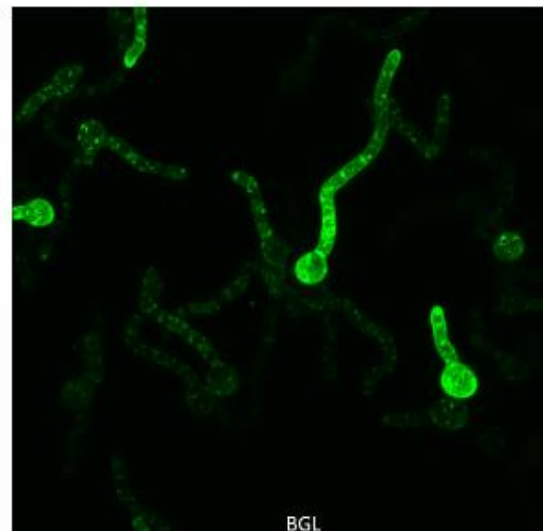
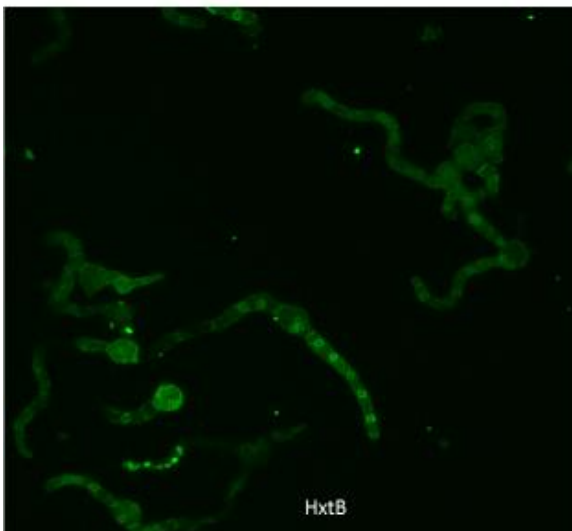
2nd hour (YGV-CMC)



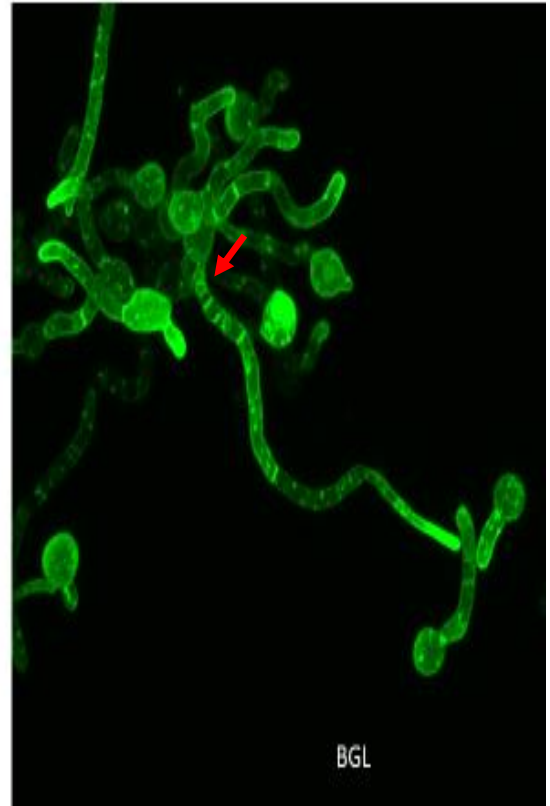
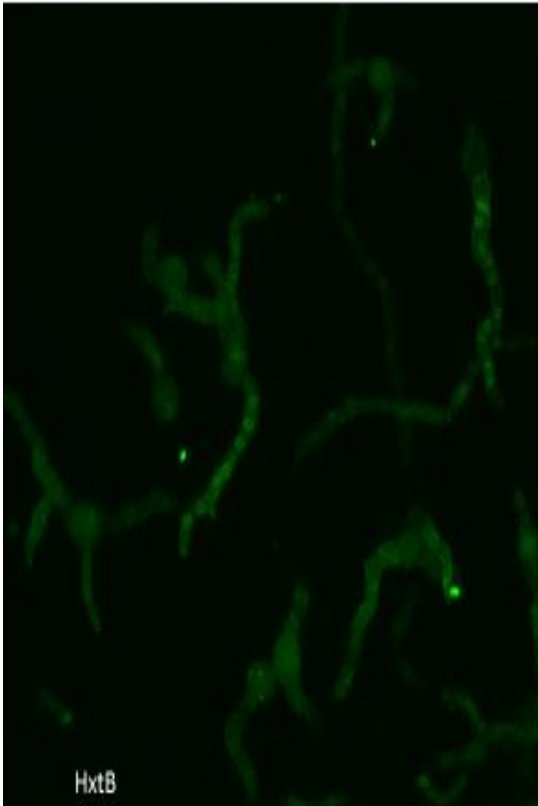
3rd hour (YGV-CMC)



4th hour (YGV-CMC)



5th hour (YGV- CMC)



References

- Adama, T. H., Wieser, J. K., & Yu, J.-H. (1998). Asexual sporulation in *Aspergillus nidulans*. *Microbiology and Molecular Biology Reviews*, 35-54.
- Adamson P, M. C. (1992). Post-translational modifications of p21rho proteins. *J. Biol. Chem*, 267, 20033-38.
- Aleksandra Virag, M. P. (2007). Regulation of hyphal morphogenesis by *cdc42* and *rac1* homologues in *Aspergillus nidulans*. *Molecular Microbiology* 66(6), 1579-1596.
- Araujo-Bazan, L. P. (2008). Preferential localization of the endocytic internalization machinery to hyphal tips underlies polarization of the actin cytoskeleton in *Aspergillus nidulans*. *Molecular Microbiology*, 67(4), 891-905.
- Baraldo. Jr.A, B. D. (2014). Characterization of beta-Glucosidase produced by *Aspergillus niger* under Solid-State Fermentation and Partially Purified using Manne- Agarose. *Biotechnology Research International*, vol. 2014, 8.
- Bender A, P. J. (1989). Multicopy suppression of the *cdc24* budding defect in yeast by *CDC42* and three newly identified genes including the ras-related gene *RSR1*. *Natl.Acad.Sci. USA*, 86, 9976-80.
- Bhargava. S, N. M. (2003). Pulsed feeding during fed-batch fungal fermentation leads to reduced viscosity without detrimentally affecting protein expression. *Biotechnology and Bioengineering*, 81, 341-7.
- Bhargava. S, W. K. (2003). Pulsed addition of limiting carbon during *Aspergillus oryzae* fermentation leads to improved productivity of a recombinant enzyme. *Biotechnology and Bioengineering*, 82 (1), 111-7.
- Bhargava. S, W. K. (2005). Effect of cycle time on fungal morphology, broth rheology, and recombinant enzyme production during pulsed addition of limiting carbon source. *Biotechnology and Bioengineering*; 89(5), 524-9.
- Boyce, K. S. (2009). In vivo yeast cell morphogenesis is regulated by a p21- activated kinase in the human pathogen *Penicillium marneffeii*. *Plos Pathogens*, 5(11), e1000678.
- Brown JL, J. M.-t. (1997). Novel *Cdc42*- binding proteins *Gic1* and *Gic2* control cell polarity in yeast. *Genes and Development*, 11, 2972-82.
- Cerione RA, Z. Y. (1996). The *Dbl* family of oncogenes. *Current Opinion Cell Biology*, 8, 216-22.
- Chant J and Herskowitz, I. (1991). Genetic control of bud site selection in yeast by a set of gene products that constitute a morpho- genetic pathway. *Cell*, 65, 1203-12.
- Chauve. M, M. H. (2010). Comparative Kinetic Analysis of Two Fungal beta-Glucosidases. *Biotechnology for Biofuels*, 3:3.
- Chen, C. M. (1997). Geometric control of cell life and death. *Science*, 276(5317), 1425-8.

- Chen, L. L. N.-H. (2012). A glucose-tolerant beta-glucosidase from *Prunus domestica* seeds: Purification and Characterization. *Process Biochemistry*, 47(1), 127-132.
- Chenevert, J. (1994). Cell polarization directed by extracellular cues in yeast. *Molecular Biology of Cell*, 5, 1169-75.
- Cheng J, P. T.-S. (2001). Cell cycle progression and cell polarity require sphingolipid biosynthesis in *Aspergillus nidulans*. *Molecular Cell Biology*, 21, 6198-6209.
- Claire L. Pearson, K. X. (2004). MesA, a Novel Fungal Protein Required for the Stabilization of Polarity Axes in *Aspergillus nidulans*. *Molecular Biology of the Cell* 15(8), 3658-3672.
- Collard, S. I. (n.d.). Crosstalk between small GTPases and polarity proteins in cell polarization.
- Conesa, A, P. P. (2001). The Secretion Pathway in Filamentous Fungi A Biotechnological View. *Fungal genetics and Biology*, 33, 155-171.
- Cvrckova F, D. V. (1995). Ste20- like protein kinases are required for normal localization of cell growth and for cytokinesis in budding yeast. *Genes Development*, 9, 1817-30.
- de Vries, R. F. (2003). Glycerol dehydrogenase encoded by *gldB* is essential for osmotolerance in *Aspergillus nidulans*. *Molecular Microbiology*, 49(1), 131-41.
- D'Enfert, C. a. (1997). Molecular characterization of the *Aspergillus nidulans* *treA* gene encoding an acid trehalase required for growth on trehalose. *Molecular Microbiology*, 24(1), 203-16.
- D'Enfert, C. B. (1999). Neutral trehalases catalyse intracellular trehalose breakdown in the filamentous fungi *Aspergillus nidulans* and *Neurospora crassa*. *Molecular Microbiology*, 32(3), 471-83.
- Downs, B. (2012). Characterization of the Rho-Like GTPase Effector PakB in *Aspergillus nidulans*. *Thesis*, 1-56.
- Egan. M.J, M. M.-P. (2012). Microtubule- based transport in filamentous fungi. *Current Opinion Microbiology* 15(6), 637-645.
- Elmouelhi, N., & Yarema, K. (2008). Building on What Nature Gave Us: Engineering Cell Glycosylation Pathways. In W. Flynn, *Biotechnology and Bioengineering* (pp. 37-73). New York: Nova Science Publishers, Inc.
- Esen,A, K. J. (2010). Beta-Glucosidases. *Cellular and Molecular Life Sciences, Vol: 67*, 3389-3405.
- Etxebeste, O. G. (2010). *Aspergillus nidulans* asexual development: making the most of cellular modules. *Trends in Microbiology*, 18(12), 569-576.
- Evangelista, M. B. (1997). Bnip, a yeast formin linking *cdc42p* and the actin cytoskeleton during polarized morphogenesis. *Science*, 276(5309), 118-22.
- Fernanda dos Reis, T. M. (2013). Identification of Glucose Transporters in *Aspergillus nidulans*. *Plos One*, 8(11) e81412.

- Fillinger, S. C. (2001). Trehalose is required for the acquisition of tolerance to a variety of stresses in the filamentous fungus *Aspergillus nidulans*. *Microbiology*, *147*(Pt7), 1851-62.
- Fillinger, S. C. (2002). cAMP and ras signalling independently control spore germination in the filamentous fungus *Aspergillus nidulans*. *Molecular Microbiology*, *44*(4), 1001–1016.
- Fillinger, S., Chaverroche, M.-K., Shimizu, K., & Keller, N. a. (2002). cAMP and ras signalling independently control spore germination in the filamentous fungus *Aspergillus nidulans*. *Molecular Microbiology*, *Vol 44*(4), 1001-1016.
- Fillinger, S, C. M. (2002). cAMP and ras signalling independently control spore germination in filamentous fungus *Aspergillus nidulans*. *Molecular Microbiology Vol.44* (4).
- Gladfelter AS, B. I. (2002). Septin ring assembly involves cycles of GTP loading and hydrolysis by Cdc42p. *Journal of Cell Biology*, *156*(2), 315-26.
- Gladfelter, A. (2006). Control of filamentous fungal cell shape by septins and formins. *Nature Reviews Microbiology*, *Vol.4*.
- Goto, M. (2007). Protein O-Glycosylation in Fungi: Diverse Structures and Multiple Functions. *Bioscience, Biotechnology, Biochemistry*; *71*(6), 1415-1427.
- Harris, A. V. (2006). Functional Characterization of *Aspergillus nidulans* Homologues of *Saccharomyces cerevisiae* Spa2 and Bud6. *Eukaryotic Cell* *5*(6), 881-895.
- Harris, S. (1997). The duplication cycle in *Aspergillus nidulans*. *Fungal Genetics and Biology*, *22*(1), 1-12.
- Harris, S. (2013). Golgi organization and the apical extension of fungal hyphae: an essential relationship. *Molecular Microbiology* *89*(2), 212-215.
- Harris, S. (2015, January 30). *Regulation of morphogenesis and development in Aspergillus nidulans*. Retrieved from United States Department of Agriculture, Research, Education and Economics Information System:
<http://www.reeis.usda.gov/web/crisprojectpages/0222307-regulation-of-morphogenesis-and-development-in-aspergillus-nidulans.html>
- J, V. R. (2001). *Aspergillus* enzymes involved in degradation of plant cell wall polysaccharides. *Microbiology and Molecular Biology Reviews*. *Vol. 65*(4), 497-522.
- Johnson, D. a. (1990). Molecular Characterization of Cdc42, a *Saccharomyces cerevisiae* gene involved in the development of cell polarity. *Journal of Cell Biology*, *111*, 143-52.
- Kafer, E. (1977). Meiotic and mitotic recombination in *Aspergillus* and its chromosomal aberration. *Advanced Genetics*, *19*, 33-131.
- Katayama, M. K. (1991). The posttranslationally modified C-terminal structure of bovine aortic smooth muscle rhoA p21. *Journal of Biological Chemistry*, *266*(19), 12639-45.

- Kato, N. B. (2003). The Expression of Sterigmatocystin and Penicillin Genes in *Aspergillus nidulans* Is Controlled by veA, a Gene Required for Sexual Development. *Eukaryotic Cell*, 2(6), 1178-1186.
- Knechtle, P., Dietrich, F., & Philippsen, P. (2003). Maximal polar growth potential depends on the polarisome components AgSpa2 in filamentous fungus *Ashbya gossypii*. *Molecular Biology of the Cell*, 14(10): 4140-4154.
- Krijghsheld, P. N. P. (2013). Deletion of flbA results in increased secretome complexity and reduced secretion heterogeneity in colonies of *Aspergillus niger*. *Journal of Proteome Research* 12(4), 1808-19.
- Lamson, R. W. (2002). Cdc42 regulation of kinase activity and signaling by the yeast p21-activated kinase Ste20. *Molecular and Cell Biology*, 22(9), 2939-51.
- Lee, B. a. (1995). fluG and flbA function interdependently to initiate conidiophore development in *Aspergillus nidulans* through brlA β activation. *The EMBO Journal Vol.15 (2)*, 299-309.
- Li, X., Ferro-Novick, S., & Novick, P. (2013). Different polarisome components play distinct roles in Slr2p- regulated cortical ER inheritance in *Saccharomyces cerevisiae*. *Molecular Biology of the Cell*, Vol 24.
- Lichius, A., Yanez-Gutierrez, M., Read, N., & Castro-Longoria, E. (2012). Comparative live-cell imaging analyses of Spa-2, Bud-6 and Bni-1 in *Neurospora crassa* reveal novel features of the filamentous fungal polarisome. *Plos One*, 7(1).
- Liu, Lifang, F. A. (2014). Genome-scale analysis of the high efficient protein secretion of *Aspergillus oryzae*. *Bio Med Central Systems Biology* 8:73.
- Lockington, R. a. (2001). Carbon catabolite repression in *Aspergillus nidulans* involves deubiquitination. *Molecular Microbiology* 40(6), 1311-21.
- M.R, M. V. (2004). In silico reconstruction of nutrient-sensing signal transduction pathways in *Aspergillus nidulans*. *In Silico Biology* (4).
- Miguel A. Penalva, A. G.-P. (2012). Searching for gold beyond mitosis Mining intracellular membrane traffic in *Aspergillus nidulans*. *Cellular logistics* 2(1), 2-14.
- Momany, M. (2002). Polarity in filamentous fungi: establishment, maintenance and new axes. *Current Opinion in Microbiology*, 5, 580-585.
- Moskow, J. A. (2000). Role of Cdc42p in pheromone-stimulated signal transduction in *Saccharomyces cerevisiae*. *Molecular Cell Biology*, 20, 7559-7571.
- Nathan W Gross, B. D. (2013). Functional Characterization of *Aspergillus nidulans* ANID_0.5595.1: a possible homologue of polarisome components Pea2. *Fungal Genetic Conference Abstracts*.
- Nayak, T. S. (2006). A Versatile and Efficient Gene-Targeting System for *Aspergillus nidulans*. *Genetics*, 172(3), 1557-1566.

- Oakley, T. H. (2005). The Role of Microtubules in Rapid Hyphal Tip Growth of *Aspergillus nidulans*. *Molecular Biology of the Cell* 16(2), 918-926.
- Perez, P. a. (2010). Rho GTPases: regulation of cell polarity and growth in yeasts. *Biochemical Journal*, 426(3), 243-253.
- Pettolino. F.A, W. C. (2012). Determining the polysaccharide composition of plant cell walls. *Nature Protocols* 7, 1590-1607.
- Quilliam LA, K.-F. R. (1995). Guanine nucleotide exchange factors: activators of the Ras superfamily of proteins. *BioEssays*, 17, 395-404.
- Riquelme, M., Yarden, O., Bartnicki-Garcia, S., Bowman, B., Castro-Longoria, E., Free, S., . . . Richthammer, C. (2011). Architecture and development of the *Neurospora crassa* hypha- a model cell for polarized growth. *Fungal Biology* , (115) 446-474.
- Rittenour WR, C. M. (2011). Control of glucosylceramide production and morphogenesis by the Bar1 ceramide synthase in *Fusarium graminearum*. *PLoS One* 6: e19385.
- Rittenour, W. S. (2009). Hyphal Morphogenesis in *Aspergillus nidulans*. *Fungal Biology Reviews* , 23 (20-29).
- Schalen. M, W. M. (2015). Monitoring and Control of Protein Production in Fungi. *Technical University of Denmark (PhD Thesis)*.
- Schmidt, A. M. (1998). Signaling to the actin cytoskeleton. *Annual Reviews Cell Developmental Biology*, 14, 305-338.
- Sharpless, K. H. (2002). Functional Characterization and Localization of the *Aspergillus nidulans* Formin SEPA. *Molecular Biology of the Cell*, 13(2) 469-479.
- Si, H. (2010). Regulation of morphogenesis in filamentous fungi. *Thesis*.
- Si, H. R. (2016). Roles of *Aspergillus nidulans* Cdc42/Rho GTPase regulators in hyphal morphogenesis and development. *Mycologia*.
- Sloat BF, A. A. (1981). Roles of the CDC24 gene product in cellular morphogenesis during the *Saccharomyces cerevisiae* cell cycle. *Journal of Cell Biology*, 89, 395-405.
- Snyder.M, B. S. (2004). Regulation of polarized growth initiation and termination cycles by polarisome and Cdc42 regulators. *Journal of Cell Biology* 164(2), 207-218.
- Song, Q., Johnson, C., & Wilson, T. E. (2014). Pooled segregant sequencing reveals genetic determinants of yeast pseudohyphal growth. *Plos Genetics*, Aug 21.
- Sudbery, P. (2011). Growth of *Candida albicans* hyphae. *Nature Reviews Microbiology*, 9, 737-748.
- Taheri-Talesh, N. H.-B. (2008). The Tip Growth Apparatus of *Aspergillus nidulans*. *Molecular Biology of the Cell*, 19, 143901449.
- Takai Y, S. T. (1995). Rho as a regulator of the cytoskeleton. *Trends Biochem. Sci*, 20, 227-31.

- Takeshita, N. H. (2007). Apical sterol-rich membranes are essential for localization cell end markers that determine growth directionality in the filamentous fungus *Aspergillus nidulans*. *Molecular Biology of the Cell*, 19(1), 339-51.
- Tazebay, U. S. (1995). Post-transcriptional control and kinetics characterization of proline transport in germinating conidiospore of *Aspergillus nidulans*. *FEMS Microbiology Letters*, 132, 27-37.
- Tazebay, U. S. (1997). The gene encoding the major proline transporter of *Aspergillus nidulans* is upregulated during conidiospore germination and in response to proline induction and amino acid starvation. *Molecular Microbiology* 24(1), 105-17.
- Thompson, D. C. (2011). Coevolution of Morphology and Virulence in *Candida* Species. *Eukaryotic Cell*, 10(9), 1173-1182.
- Timberlake, W. (1990). Molecular genetics of *Aspergillus* development . *Annual Review Genetics*, 24, 5-36.
- Upadhyay, S. a. (2008). The role of actin, fimbrin and endocytosis in growth of hyphae in *Aspergillus nidulans*. *Molecular Microbiology*, 68(3), 690-705.
- Valtz, N., & Herskowitz, I. (1996). Pea2 protein yeast is localized to sites of polarized growth and is required for efficient mating and bipolar budding. *The Journal of Cell Biology* , Vol 135.
- Virag, A. H. (2006). The Spitzenkorper: a molecular perspective. *Mycological Research* , 110(1), 4-13.
- Watanabe, T, S. T. (1992). Purification and properties of *Aspergillus niger* beta-glucosidase. *European Journal of Biochemistry*. 209, 651-659.
- Whitehead IP, C. S. (1997). Dbl family proteins. *Biochim. Bio-phys. Acta* 1332, F1-23.
- Xiaorong Lin, J. A. (2015). Fungal Morphogenesis . *Cold Spring Harbor Laboratory Press* .
- Yu, J.-H. a. (2005). Regulation of Secondary Metabolism in Filamentous Fungi. *Annual Review of Phytopathology*, Vol: 43, 437-458.
- Zheng Y, B. A. (1995). Interactions among proteins involved in bud-site selection and bud-site assembly in *Saccha romyces cerevisiae*. *J. Biol. Chem*, 270(2), 626-30.
- Ziman M, P. D. (1993). Subcellular localization of Cdc42p, a *Saccharomyces cerevisiae* GTP-binding protein involved in the control of cell polarity. *Molecular Biology of Cell*, 4, 1307-16.

